AD-A099 906 SYRACUSE UNIV NY DEPT OF ELECTRICAL AND COMPUTER EN--ETC F/G 20/14
ELECTROMAGNETIC TRANSMISSION THROUGH A ROTATIONALLY SYMMETRIC H--ETC(U)
JUN 81 C CHA, R F HARRINGTON N00014-76-C-0225
UNCLASSIFIED TR-81-2 NL

10

TR-81-2

ELECTROMAGNETIC TRANSMISSION THROUGH A ROTATIONALLY SYMMETRIC HOLE IN A THICK SCREEN

by

Chung-Chi Cha
Roger F. Harrington

Department of
Electrical and Computer Engineering
Syracuse University
Syracuse, New York 13210

Technical Report No. 13

June 1981

Contract No. N00014-76-C-0225

Approved for public release; distribution unlimited

Prepared for

DEPARTMENT OF THE NAVY
OFFICE OF NAVAL RESEARCH
ARLINGTON, VIRGINIA 22217

UNCLASSIFIED

SECURITY CLASSIFICATION OF THIS PAGE (When Data Entered)

REPORT DOCUMENTATION PAGE		READ INSTRUCTIONS BEFORE COMPLETING FORM
1. REPORT NUMBER 14 TR-81-2, TR-13	2. GOVT ACCESSION NO. AD-A099	3. RECIPIENT'S CATALOG NUMBER 906
4. TITLE (and Subtitle) (6) ELECTROMAGNETIC TRANSMISSION THROUGH A ROTATIONALLY SYMMETRIC HOLE IN A THICK SCREEN		5. TYPE OF REPORT & PERIOD COVERED 9 Technical Report, No. 13
		6. PERFORMING ORG. REPORT NUMBER
7. AUTHOR(s) 10 Chung-Chi Cha Roger F. Harrington		8. CONTRACT OR GRANT NUMBER(s) 15 N00014-76-C-0225
9. PERFORMING ORGANIZATION NAME AND ADDRESS Dept. of Electrical & Computer Engineering Syracuse University Syracuse, New York 13210		10. PROGRAM ELEMENT, PROJECT, TASK AREA & WORK UNIT NUMBERS 12
11. CONTROLLING OFFICE NAME AND ADDRESS Department of the Navy Office of Naval Research Arlington, Virginia 22217		12. REPORT DATE June 1981 13. NUMBER OF PAGES 105
14. MONITORING AGENCY NAME & ADDRESS(if different from Controlling Office)		15. SECURITY CLASS. (of this report) UNCLASSIFIED 15a. DECLASSIFICATION/DOWNGRADING SCHEDULE

16. DISTRIBUTION STATEMENT (of this Report)

Approved for public release; distribution unlimited.

17. DISTRIBUTION STATEMENT (of the abstract entered in Block 20, if different from Report)

18. SUPPLEMENTARY NOTES

19. KEY WORDS (Continue on reverse side if necessary and identify by block number)

Annular slot	Electromagnetic transmission
Aperture in thick conductor	Method of moments
Circular aperture	Narrow annular slot
Coaxial aperture	Rotationally symmetric aperture

20. ABSTRACT (Continue on reverse side if necessary and identify by block number)

Electromagnetic wave transmission through an aperture in a thick conducting screen is investigated. The aperture is assumed to be rotationally symmetric about an axis normal to the screen. The equivalence principle is used to divide the original problem into three regions. Fields in each region are expressed in terms of equivalent currents on the boundary, and integral equations for the unknown currents are established by enforcing proper boundary conditions. When the aperture region in the screen is a section of a →

DD FORM 1 JAN 73 1473 EDITION OF 1 NOV 65 IS OBSOLETE
S/N 0102-014-6601

UNCLASSIFIED
SECURITY CLASSIFICATION OF THIS PAGE (When Data Entered)

20. ABSTRACT (continued)

cylindrical or coaxial waveguide, the waveguide modes can be used to construct the operators in that region. In this case the boundary condition for the E-field on the waveguide walls is built into the operator. However, in a more general situation, operators in an unbounded medium are used and an extra integral equation is written for the aperture region, resulting in a larger system of equations. The moment method is used to solve the integral equations numerically and results are presented. An equivalent circuit is also developed for a narrow annular slot at low frequencies. Resonant behavior predicted from the circuit is supported by numerical results.

CONTENTS

Chapter 1

INTRODUCTION

Electromagnetic transmission through apertures in a conducting screen of finite thickness has been studied extensively by many investigators. The effect of screen thickness on the transmission is of interest in many cases. The simplest model of the problem is a two-dimensional one and is the focus of most investigations. Several solutions have been developed for the problem of electromagnetic penetration through an infinitely long slit in a thick screen [1]-[10]. Both TM and TE cases have been studied, and a variety of techniques are used. However, most investigators treat only the problem of a slit with rectangular cross section. Morita [3] and Auckland [10] developed solutions for two-dimensional slits with arbitrary cross sections. Uslenghi [28] also considered the problem of a two-dimensional gasket in a screen under several simplifying assumptions.

A three-dimensional problem is of greater complexity. Most of the related work has been done for the quasistatic case. Akhiezer [11] extended Bethe's [12] theory to the case of a circular aperture in a thick screen. Garb examined the problem of a narrow rectangular slot in a screen of finite but small thickness [13], and later studied the polarizability of small openings in a thick screen [14]. McDonald [15] considered the polarizabilities of small circular and rectangular apertures in a thick screen. The methods of solutions usually rely on the assumption that the aperture is electrically small, and also that the waveguide modes

are known for the aperture region inside the screen.

This report considers the more general problem for which an aperture in a thick screen is rotationally symmetric about an axis perpendicular to the screen. The method of solution, in general, does not depend on the size of the aperture. The formulation is not limited to the situation where the aperture region in the screen is a familiar waveguide section for which the characteristic modes are known. However, this case is also considered and investigated in detail.

In Chapter 2, we develop the basic formulation of the problem. The equivalence principle [16, Sec. 3-5] is used to separate the problem into different regions of interests by means of unknown boundary currents. Field operators and operator equations are then established for the currents. A modal formulation is used to treat the special case when the aperture region is a waveguide region (in our case a cylindrical or coaxial region). In the more general case a nonmodal formulation is used. Chapter 3 contains a moment method [17] approach to the solution of the simultaneous operator equations. Both modal and nonmodal formulations are given and the measurement matrix is discussed. A low frequency analysis is presented in Chapter 4 for a filled narrow annular slot. Resonant behavior of the power transmission is observed, and the transmission coefficient and the electric polarizability are discussed. Numerical results are presented in Chapter 5 for several examples. Emphasis is put on the electric and magnetic currents obtained. Modal and nonmodal results are compared when both formulations apply. Also,

numerical results and analytical predictions for low frequency power transmission are compared. A final discussion is presented together with some recommendations in Chapter 6.

Chapter 2

PROBLEM FORMULATION

2.1. Problem Specification

The problem to be considered is shown in Fig. 1, which shows a conducting screen of thickness d situated between the surfaces $z = 0$ and $z = d$. The regions $z \geq d$ (denoted region c) and $z \leq 0$ (denoted region a) are coupled through an aperture region (denoted region b) in the screen. The incident fields $\underline{E}_i$ and $\underline{H}_i$, generated in region a, penetrate through the aperture region and radiate into region c. $\underline{E}_i$ and $\underline{H}_i$ are the fields produced by the impressed sources $\underline{J}_i$ and $\underline{M}_i$ in unbounded space filled with the same material as in region a. The aperture region, region b, is bounded by the following three surfaces:

S_1: the interface between regions a and b which lies in the plane $z = 0$.

S_2: the interface between regions b and c which lies in the plane $z = d$.

S_3: the interface between region b and the conducting screen.

S_1, S_2 and S_3 are all assumed to be rotationally symmetric about the z-axis. The three regions are assumed to contain media characterized by their permittivities and permeabilities, (ε_a, μ_a), (ε_b, μ_b) and (ε_c, μ_c). For simplicity, all three regions are assumed lossless. A cross section of this situation is shown in Fig. 2(a).

For the special case where region b is a cylindrical waveguide

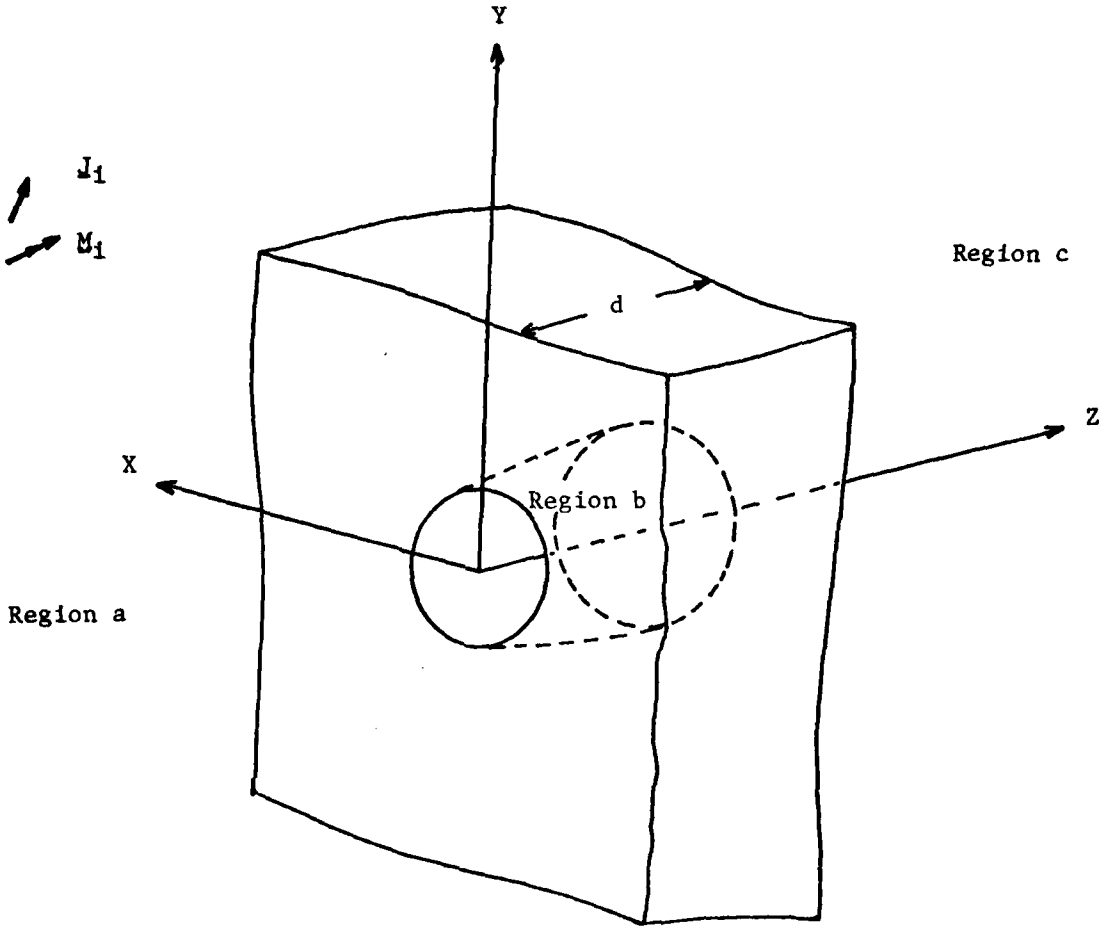

Fig. 1. Transmission through a rotationally symmetric aperture in a thick conducting screen.

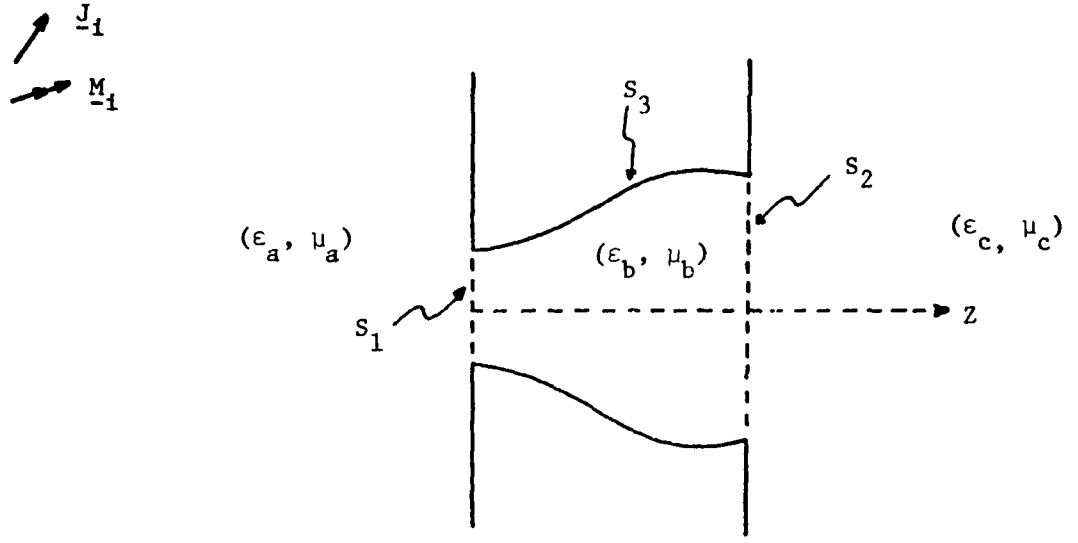

Fig. 2(a). Cross section in the y-z plane for a simply connected S_3.

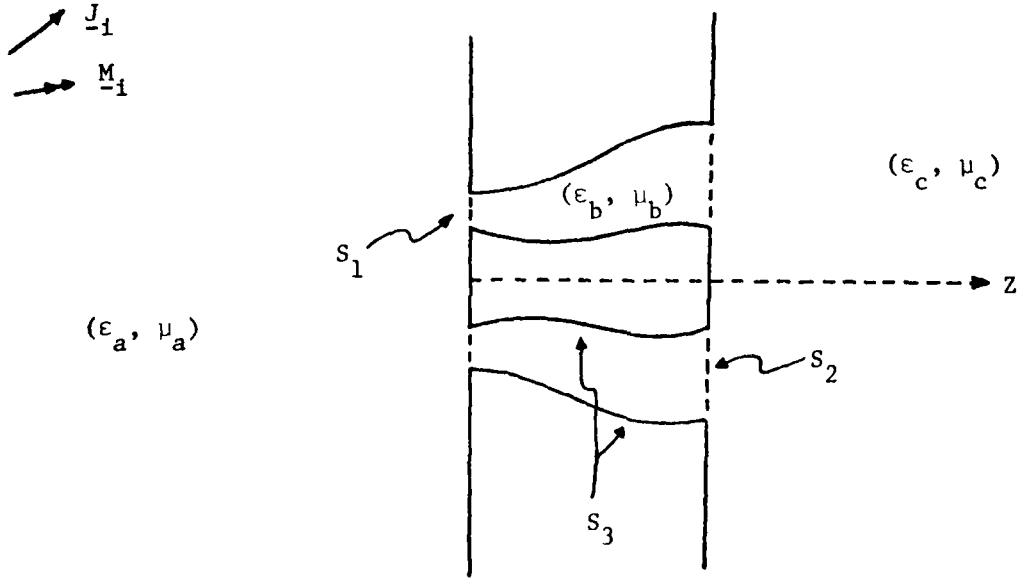

Fig. 2(b). Cross section in the y-z plane for a doubly connected S_3.

region, a conductor in the center of this region can support a TEM mode and thus increase the power transmission. Therefore, we generalize our problem of investigation to one for which the boundary surface S_3 can be either simply-connected (as shown in Fig. 2(a)) or doubly-connected (as shown in Fig. 2(b)). The boundary surfaces S_1 and S_2 are then either circular (when S_3 is simply-connected) or annualar (when S_3 is doubly-connected). Since S_1, S_2 and S_3 are all symmetric about the z-axis, their union, $S = S_1 \cup S_2 \cup S_3$, is also symmetric about the axis. In other words, S_1, S_2, S_3 and their union are all surfaces of revolution. A generating curve Γ, as well as its associated coordinate t, and unit tangent vector $\hat{\underline{t}}$, can be defined for S. Note that Γ is open with its end points on the z-axis when S_3 is simply-connected and closes upon itself when S_3 is doubly-connected. Γ is the union of the generating curves of S_1, S_2 and S_3, denoted Γ_1, Γ_2 and Γ_3. A unit normal vector is defined for every point on S as

$$\hat{\underline{n}} = \hat{\underline{\phi}} \times \hat{\underline{t}} \qquad (2\text{-}1).$$

Here $\hat{\underline{\phi}}$ is the conventional unit vector associated with the azimuth angle ϕ. The arrangement described above is illustrated in Figs. 3(a) and 3(b) for the two possible situations. Furthermore, each boundary surface can be approached from either of the two regions that the surface separates. We denote the side of each surface from which the normal vector $\hat{\underline{n}}$ points by the superscript "+", and the opposite side by the superscript "-". For example, according to the convention we use in this work, as shown in

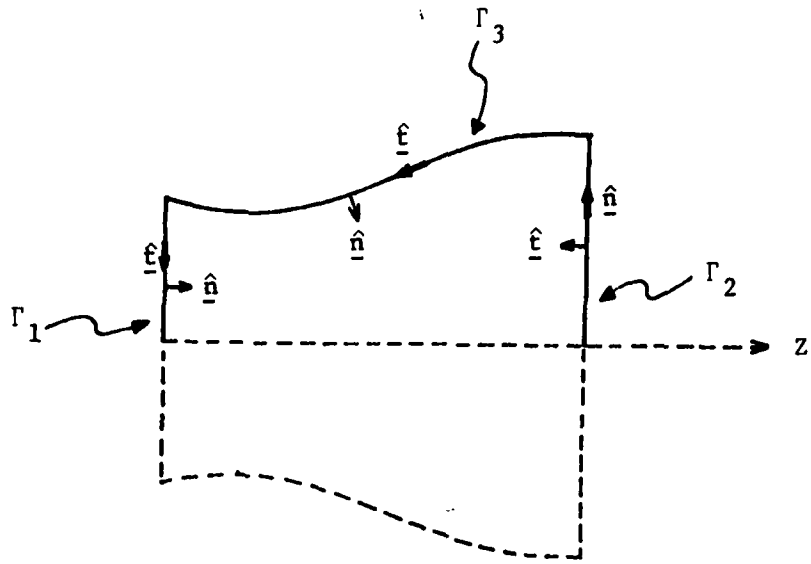

Fig. 3(a). Generating curves of S_1, S_2 and S_3 and the unit vectors, S_3 simply connected.

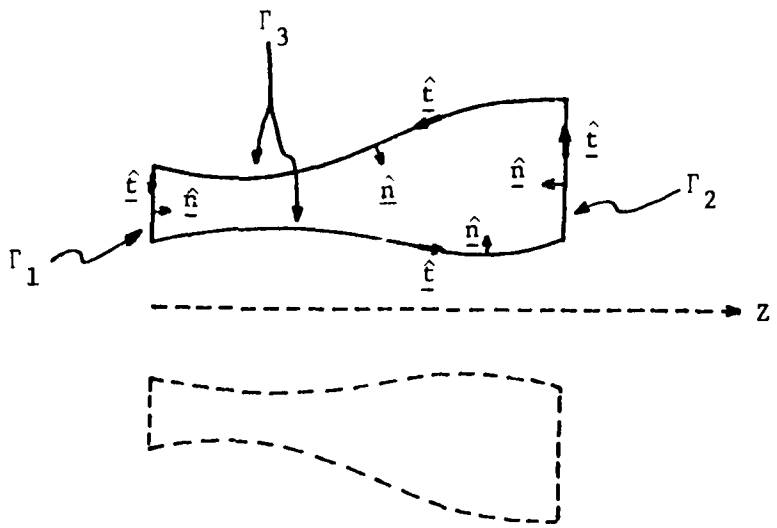

Fig. 3(b). Generating curves of S_1, S_2 and S_3 and the unit vectors, S_3 doubly connected.

Figs. 3(a) and 3(b), S_1^+ denotes the surface immediately next to S_1 just outside of region b.

2.2. Equivalent Problems

In this section, the equivalent principle [16, Sec. 3-5] is used to separate the original problem into three equivalent situations which exist in the three regions a, b, and c. For region a, a magnetic current sheet $\underline{M}_1$ is placed just inside the conducting plane at z = 0, with S_1 covered with conductor also. The equivalent magnetic current M_1 is defined as

$$\underline{M}_1 = \hat{z} \times \underline{E} \tag{2-2}$$

where $\underline{E}$ is the electric field over z = 0 in the original problem and is unknown on S_1. It has zero tangential (to the z = 0 plane) component elsewhere in the z = 0 plane. This magnetic current $\underline{M}_1$, and the impressed sources $\underline{J}_i$ and $\underline{M}_i$, radiate in the presence of the complete conducting screen over z = 0 to give the correct fields $\underline{E}_a$ and $\underline{H}_a$ in region a. This situation is shown in Fig. 4(a). Furthermore, image sources can be used to account for the effect of the infinite conducting plane as far as filled in region a are concerned. Therefore, we have the equivalent situation, shown in Fig. 4(b), established for region a. Here $\underline{J}_i$, $\underline{M}_i$, and $\underline{M}_1$, together with their images, radiate into unbounded space filled with a medium characterized by (ε_a, μ_a) to create the correct fields in region a. A similar equivalent situation can be developed for region c as shown in Fig. 5. Here the equivalent magnetic current $\underline{M}_2$ defined by

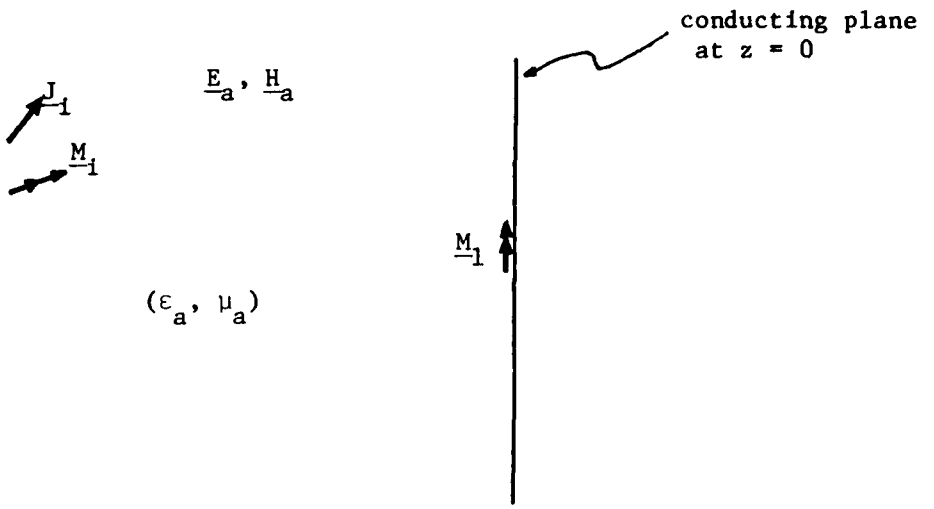

Fig. 4(a). Equivalent situation for region a.

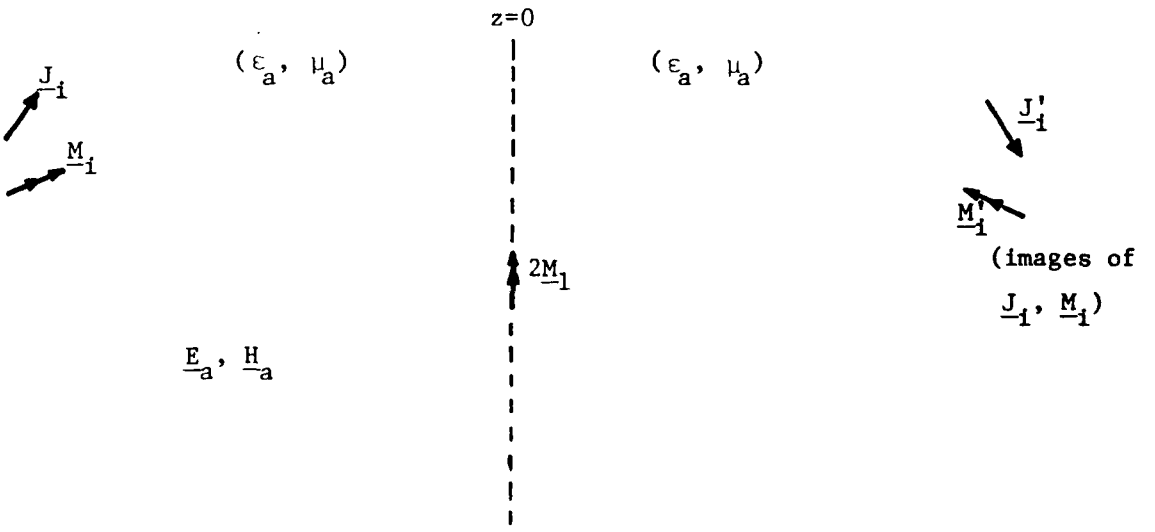

Fig. 4(b). Equivalent situation for region a, using images.

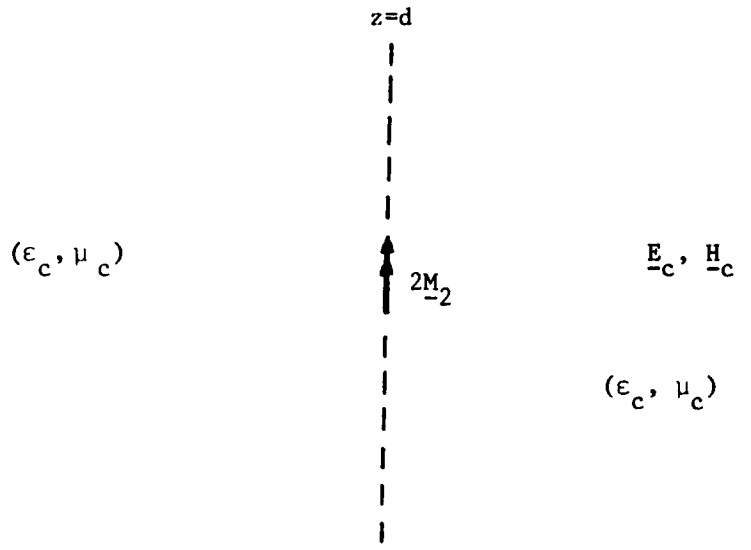

Fig. 5. Equivalent situation for region c.

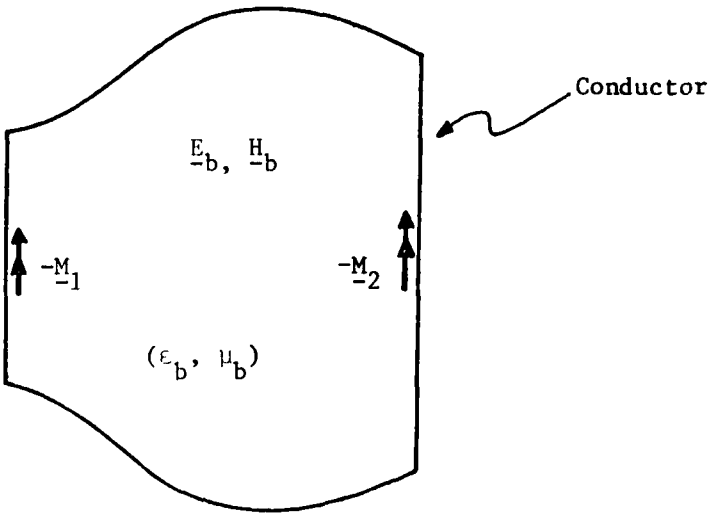

Fig. 6. Equivalent situation for region b.

$$\underline{M}_2 = \underline{E} \times \hat{z} \ , \tag{2-3}$$

together with its mirror image with respect to the plane z = d, exist on S_2 and radiate into unbounded space filled with the medium characterized by (ε_c, μ_c). These currents give the correct fields $\underline{E}_c$ and $\underline{H}_c$ in region c. Note that in the two equivalent situations for regions a and c, electromagnetic fields from the equivalent magnetic currents can be found using the field operators for unbounded space.

For region b, the entire closed boundary S is replaced by a perfect electric conductor, and equivalent magnetic current sheets $-\underline{M}_1$ and $-\underline{M}_2$ are placed just inside S_1 and S_2, respectively. This situation is shown in Fig. 6, where $-\underline{M}_1$ and $-\underline{M}_2$ radiate in the presence of the closed conductor to give the correct fields $\underline{E}_b$ and $\underline{H}_b$ in region b. Note that the use of $-\underline{M}_1$ and $-\underline{M}_2$ in this region ensures the continuity of tangential electric field across S_1 and S_2. In the special case where region b is a cylindrical or coaxial waveguide region, fields can be expressed in terms of $\underline{M}_1$ and $\underline{M}_2$ by means of the waveguide modes. However in a more general case, it is not possible to obtain the fields in region b directly from $\underline{M}_1$ and $\underline{M}_2$ alone. Therefore, for the general case, we replace the conducting surface S in Fig. 6 by the electric current, denoted $-\underline{J}$, induced on S by $-\underline{M}_1$ and $-\underline{M}_2$. This equivalent situation is shown in Fig. 7, where $-\underline{M}_1$, $-\underline{M}_2$, and $-\underline{J}$ radiate into unbounded space filled with a medium characterized by (ε_b, μ_b). They give zero fields just outside S and the correct fields $\underline{E}_b$ and $\underline{H}_b$ in region b. Note again that we have established an equivalent situation in which only the field operators for unbounded space are needed. To summarize, we have

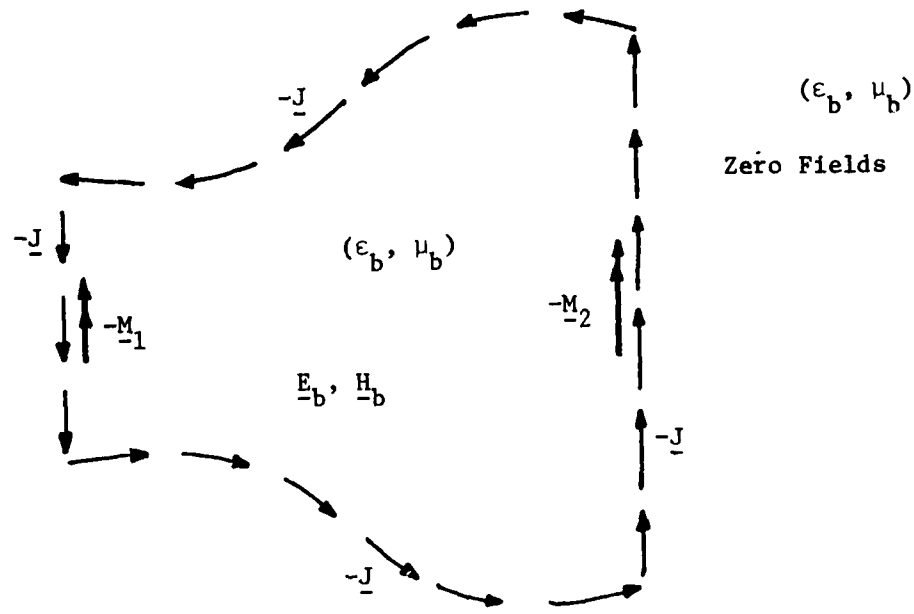

Fig. 7. Equivalent situation for region b.

developed equivalent situations shown in Figs. 4(b) and 5 for regions a and c respectively. The equivalent situation shown in Fig. 6 is intended for the special case where region b represents a waveguide region, while the equivalent situation shown in Fig. 7 is suited to the general case. In the special case where region b is a waveguide region, if waveguide modes are used for the field operators needed in the equivalent situation in Fig. 6, we call the formulation a modal formulation. If a general treatment corresponding to the equivalent situation in Fig. 7 is used, we call the formulation a nonmodal formulation.

2.3. Field Operators

From the discussion in the previous section, it is evident that two types of field operators are needed for our formulation. These are the potential integrals which give the electric field or magnetic field in an unbounded medium due to an electric or magnetic surface current distribution, and the modal representation which gives us the fields inside a waveguide region when the tangential electric field is specified at the two end surfaces. In the first case, although both the electric and magnetic types of currents and fields are considered, because of duality [16, Sec. 3-2], only the following two basic operators, L_α^e and L_α^h are needed:

$$L_\alpha^e(\underline{J}) = - jk_\alpha \int_A \frac{\underline{J}(\underline{r}')e^{-jk_\alpha R}}{4\pi R}\, da' + \frac{1}{jk_\alpha} \nabla \int_A \frac{(\nabla' \cdot \underline{J}(\underline{r}'))e^{-jk_\alpha R}}{4\pi R}\, da' \qquad (2\text{-}4)$$

and

$$L_\alpha^h(\underline{J}) = \nabla \times \int_A \frac{\underline{J}(\underline{r}')e^{-jk_\alpha R}}{4\pi R}\, da' \qquad (2\text{-}5)$$

The integrations in both (2-4) and (2-5) are over the surface A where the surface distribution $\underline{J}$ resides, and

$$R = |\underline{r} - \underline{r}'| = \sqrt{\rho^2 + \rho'^2 - 2\rho\rho' \cos(\phi' - \phi) + (z - z')^2} \tag{2-6}$$

$$k_\alpha = \sqrt{\omega^2 \mu_\alpha \varepsilon_\alpha} \tag{2-7}$$

If $\underline{r}$ approaches A from one side of the surface, and if the surface is assumed to be smooth there, then we can write [21]

$$L_\alpha^h(\underline{J}) = \frac{1}{2}\,\underline{J}(\underline{r}) \times \hat{\underline{n}}_o - \hat{\underline{n}}_o \times \int_A \frac{\hat{\underline{n}}_o \times \underline{J}(\underline{r}') \times (\underline{r}-\underline{r}')\,(1 + jk\,R)e^{-jk_\alpha R}}{4\pi R^3}\,da' + \hat{\underline{n}}_o[\hat{\underline{n}}_o \cdot L^h(\underline{J})] \tag{2-8}$$

where $\underline{n}_o$ is the unit normal vector of the surface at $\underline{r}$ which points toward the side of the surface from which $\underline{r}$ approaches A. Note that the component of $L_\alpha^h(\underline{J})$ that is normal to A is not written explicitly because it is not used in our operator equations. It follows that for a surface electric current distribution $\underline{J}$ and a surface magnetic current $\underline{M}$ in an unbounded medium characterized by $(\varepsilon_\alpha, \mu_\alpha)$, the electromagnetic fields $\underline{E}(\underline{J}, \underline{M})$ and $\underline{H}(\underline{J}, \underline{M})$ are given by

$$\underline{E}(\underline{J}, \underline{M}) = L_\alpha^e(\eta_\alpha \underline{J}) - L_\alpha^h(\underline{M}) \tag{2-9}$$

$$\underline{H}(\underline{J}, \underline{M}) = \frac{1}{\eta_\alpha}\,[L_\alpha^e(\underline{M}) + L^h(\eta_\alpha \underline{J})] \tag{2-10}$$

where

$$\eta_\alpha = \sqrt{\frac{\mu_\alpha}{\varepsilon_\alpha}} \tag{2-11}$$

Note that the linearity of the operators is used in (2-9) and (2-10).

To discuss the modal type of operators we consider the case in which we have a waveguide region b between z = 0 and z = d formed by two concentric cylindrical conductors, located at $\rho = R_{in}$ and $\rho = R_{out}$. The boundary conditions are, from (2-2), (2-3) and the equivalent situation shown in Fig. 6:

$$\hat{z} \times \underline{E}_b = \underline{M}_1 \qquad \text{at } z = 0 \tag{2-12}$$

and

$$\hat{z} \times \underline{E}_b = -\underline{M}_2 \qquad \text{at } z = d \tag{2-13}$$

Also we have the condition that the tangential electric field is zero on the waveguide walls. Note that when $R_{in} = 0$ the problem reduces to one in which S_3 is simply connected and the cylinder in the center is missing. To establish the operators in this case we first assume that the $\underline{E}_b$ and $\underline{H}_b$ are generated by two vector potentials, $\underline{A} = A_z\hat{z}$ and $\underline{F} = F_z\hat{z}$ [16, Sec. 3-12]. $\underline{A}$ is called the magnetic vector potential and $\underline{F}$ is called the electric vector potential. The electric and magnetic fields they generate are:

$$\underline{E}_b = -jk_b\eta_b\underline{A} + \frac{\eta_b}{jk_b}\nabla(\nabla\cdot\underline{A}) - \nabla\times\underline{F} \tag{2-14}$$

and

$$\underline{H}_b = -\frac{jk_b}{\eta_b}\underline{F} + \frac{1}{jk_b\eta_b}\nabla(\nabla\cdot\underline{F}) + \nabla\times\underline{A} \tag{2-15}$$

A_z and F_z satisfy the Helmholtz equations

$$\nabla^2 A_z + k_b^2 A_z = 0 \tag{2-16}$$

$$\nabla^2 F_z + k_b^2 F_z = 0 \tag{2-17}$$

and the fields they generate satisfy the boundary conditions on the waveguide walls. A_z can be expanded as a linear combination of the TEM modes, A^+_{TEM} and A^-_{TEM}, and a set of TM modes, $\{A^+_{nm}, A^-_{nm} \mid n=0,\pm1,\pm2,\ldots, m=1,2,3,\ldots\}$. F_z can be expanded as a linear combination of a set of TE modes, $\{F^+_{nm}, F^-_{nm} \mid n=0,\pm1,\pm2,\ldots, m=1,2,3,\ldots\}$. The waveguide modes are defined in the following:

$$A^{\pm}_{TEM} = \frac{\ln \rho}{\sqrt{\ln(R_{out}/R_{in})}} Z^{\pm}(k_b,z) \quad \text{(defined only for } R_{in} \neq 0) \tag{2-18}$$

$$A^{\pm}_{nm} = \psi^m_{nm}(\rho) e^{jn\phi} Z^{+}(k_{nm},z) \tag{2-19}$$

$$F^{+}_{nm} = \psi^e_{nm}(\rho) e^{jn\phi} Z^{\pm}(k'_{nm},z) \tag{2-20}$$

where

$$\psi^n_{nm}(\rho) = \begin{cases} \dfrac{N_n(x_{nm})J_n(\frac{\rho}{R_{out}}x_{nm}) - J_n(x_{nm})N_n(\frac{\rho}{R_{out}}x_{nm})}{\frac{1}{\pi}\sqrt{2\left(1 - \frac{J^2_n(x_{nm})}{J^2_n(\gamma x_{nm})}\right)}} & \text{if } R_{in} \neq 0 \\ \dfrac{\sqrt{2}\ J_n(\frac{\rho}{R_{out}}x_{nm})}{x_{nm}\lvert J_{n+1}(x_{nm})\rvert} & \text{if } R_{in} = 0 \end{cases} \tag{2-21}$$

$$\psi^e_{nm}(\rho) = \begin{cases} \dfrac{N'_n(x'_{nm})J_n(\frac{\rho}{R_{out}}x'_{nm}) - J'_n(x'_{nm})N_n(\frac{\rho}{R_{out}}x'_{nm})}{\frac{1}{\pi}\sqrt{2\left[1 - \frac{n^2}{x'^2_{nm}} - \left(1 - \frac{n^2}{\gamma^2 x'^2_{nm}}\right)\frac{J'^2_n(x'_{nm})}{J'^2_n(\gamma x'_{nm})}\right]}} & \text{if } R_{in} \neq 0 \\ \dfrac{\sqrt{2}\ J_n(\frac{\rho}{R_{out}}x'_{nm})}{\sqrt{(x'^2_{nm} - n^2)\ J^2_n(x'_{nm})}} & \text{if } R_{in} = 0 \end{cases} \tag{2-22}$$

$$Z^{\pm}(k,z) = e^{\pm jkz} \quad \text{if} \quad k \neq 0 \tag{2-23a}$$

$$Z^{+}(0,z) = z \tag{2-23b}$$

$$Z^{-}(0,z) = 1 \tag{2-23c}$$

and

$$\gamma = \frac{R_{in}}{R_{out}} \tag{2-24}$$

$$k_{nm} = \begin{cases} \sqrt{k_b^2 - \left(\frac{x_{nm}}{R_{out}}\right)^2} & \text{if } k_b R_{out} \geq x_{nm} \\ j\sqrt{\left(\frac{x_{nm}}{R_{out}}\right)^2 - k_b^2} & \text{if } k_n R_{out} < x_{nm} \end{cases} \tag{2-25}$$

$$k'_{nm} = \begin{cases} \sqrt{k_b^2 - \left(\frac{x'_{nm}}{R_{out}}\right)^2} & \text{if } k_b R_{out} \geq x'_{nm} \\ j\sqrt{\left(\frac{x'_{nm}}{R_{out}}\right)^2 - k_b^2} & \text{if } k_b R_{out} < x'_{nm} \end{cases}$$

J_n, N_n, J'_n, N'_n are the nth order Bessel functions of the first and second kind, and their respective derivatives. x_{nm} and x'_{nm} are the mth lowest positive real roots of the following equations:

$$\begin{cases} N_n(x_{nm})J_n(\gamma x_{nm}) - J_n(x_{nm})N_n(\gamma x_{nm}) = 0 \\ \\ N'_n(x'_{nm})J'_n(\gamma x'_{nm}) - J'_n(x'_{nm})N'_n(\gamma x'_{nm}) = 0 \end{cases} \quad \text{if } R_{in} \neq 0 \tag{2-26}$$

$$\begin{cases} J_n(x_{nm}) = 0 \\ \\ J'_n(x'_{nm}) = 0 \end{cases} \quad \text{if } R_{in} = 0 \tag{2-27}$$

Note that the TEM modes can only exist when $R_{in} \neq 0$. Now we examine the electric and magnetic fields associated with each of the modes. To compute the fields, we substitute $A^{\pm}_{TEM}\hat{z}$ and $A^{\pm}_{nm}\hat{z}$ in (2-14) and (2-15) for $\underline{A}$ to obtain their corresponding electric fields $\underline{E}^{TEM\pm}$ and $\underline{E}^{m\pm}_{nm}$, and their magnetic fields $\underline{H}^{TEM\pm}$ and $\underline{H}^{m\pm}_{nm}$. We substitute $F^{\pm}_{nm}\hat{z}$ into (2-14) and (2-15) for $\underline{F}$ to obtain the corresponding fields $E^{e\pm}_{nm}$ and $\underline{H}^{e\pm}_{nm}$. The results are the following:

$$\underline{E}^{TEM^{\pm}} \propto \underline{e}^{TEM}\, e^{\pm jk_b z} \tag{2-28a}$$

$$\underline{E}^{m\pm}_{nm} \propto \underline{e}^{m}_{nm}\, e^{jn\phi \pm jk_{nm}z} \mp \frac{Y_{nm}}{j\omega\varepsilon_b}\left(\frac{x_{nm}}{R_{out}}\right)^2 A^{\pm}_{nm}\hat{z} \quad \text{if } k_{nm} \neq 0 \tag{2-28b}$$

$$\left.\begin{aligned} \underline{E}^{m+}_{nm} &\propto \underline{e}^{m}_{nm}\, e^{jn\phi} + k_b^2 A^{+}_{nm}\hat{z} \\ \underline{E}^{m-}_{nm} &\propto A^{-}_{nm}\hat{z} \end{aligned}\right\} \quad \text{if } k_{nm} = 0 \tag{2-28c}$$

$$E^{e\pm}_{nm} \propto \underline{e}^{e}_{nm}\, e^{jn\phi}\, Z^{\pm}(k'_{nm}, z) \tag{2-28d}$$

$$\underline{H}^{TEM^{\pm}} = \mp \frac{1}{\eta_b}\hat{z} \times \underline{E}^{TEM^{\pm}} \tag{2-29a}$$

$$\underline{H}^{m\pm}_{nm} = \mp Y_{nm}\hat{z} \times \underline{E}^{m\pm}_{nm} \quad \text{if } k_{nm} \neq 0 \tag{2-29b}$$

$$\left.\begin{aligned} \underline{H}^{m+}_{nm} &= -j\frac{k_b z}{\eta_b}\hat{z} \times \underline{E}^{m+}_{nm} \\ \underline{H}^{m-}_{nm} &= -\hat{z} \times \underline{e}^{m}_{nm}\, e^{jn\phi} \end{aligned}\right\} \quad \text{if } k_{nm} = 0 \tag{2-29c}$$

$$\underline{H}^{e\pm}_{nm} = \mp Y'_{nm}\hat{z} \times E^{e\pm}_{nm} + \frac{1}{j\omega\mu_b}\left(\frac{x'_{nm}}{R_{out}}\right)^2 F_{nm}\hat{z} \quad \text{if } k'_{nm} \neq 0 \tag{2-29d}$$

$$\left.\begin{aligned} \underline{H}^{e+}_{nm} &= -\frac{1}{j\eta_b k_b z}\,\hat{z} \times \underline{E}^{e+}_{nm} - j\omega\varepsilon_b F^{+}_{nm}\hat{z} \\ \underline{H}^{e-}_{nm} &\propto F^{-}_{nm}\hat{z} \end{aligned}\right\} \text{ if } k'_{nm} = 0 \qquad (2\text{-}29e)$$

where

$$\underline{e}^{TEM} = \frac{1}{\sqrt{\ln(R_{out}/R_{in})}}\,\frac{\hat{\rho}}{\rho} \qquad (2\text{-}30)$$

$$\underline{e}^{m}_{nm} = \psi^{m'}_{nm}(\rho)\hat{\rho} + \frac{jn}{\rho}\,\psi^{m}_{nm}(\rho)\,\hat{\phi} \qquad (2\text{-}31)$$

$$\underline{e}^{e}_{nm} = -\frac{jn}{\rho}\,\psi^{e}_{nm}(\rho)\hat{\rho} + \psi^{e'}_{nm}(\rho)\hat{\phi} \qquad (2\text{-}32)$$

$$Y_{nm} = \begin{cases} \dfrac{1}{\eta_b\sqrt{1 - \left(\dfrac{x_{mn}}{k_b R_{out}}\right)^2}} & \text{if } x_{nm} \le k_b R_{out} \\ \dfrac{1}{j\eta_b\sqrt{\left(\dfrac{x_{nm}}{k_b R_{out}}\right)^2 - 1}} & \text{if } x_{nm} > k_b R_{out} \end{cases} \qquad (2\text{-}33)$$

$$Y'_{nm} = \begin{cases} \dfrac{\sqrt{1 - \left(\dfrac{x'_{nm}}{k_b R_{out}}\right)^2}}{\eta_b} & \text{if } x'_{nm} \le k_b R_{out} \\ \dfrac{j\sqrt{\left(\dfrac{x'_{nm}}{k_b R_{out}}\right)^2 - 1}}{\eta_b} & \text{if } x'_{nm} > k_b R_{out} \end{cases} \qquad (2\text{-}34)$$

The set of vectors $\{\underline{e}^{TEM}, \underline{e}^{m}_{nm}, \underline{e}^{e}_{nm} \mid m = 1,2,3,\ldots\}$ for a fixed n is an orthonormal set under the inner product:

$$(\underline{a}, \underline{b}) = \int_{R_{in}}^{R_{out}} \underline{a}^* \cdot \underline{b} \ \rho d\rho \tag{2-35}$$

We now write the electric field $\underline{E}_b$ in region b as a linear combination of all possible modes:

$$\begin{aligned}
\underline{E}_b = {} & (\underline{E}_b \cdot \hat{z})\hat{z} + (\alpha_o^+ e^{jk_b z} + \alpha_o^- e^{-jk_b z}) \ \underline{e}^{TEM} \\
& + \sum_{n=-\infty}^{\infty} \sum_{m=1}^{\infty} [\beta_{nm}^+ Z^+(k'_{nm}, z) + \beta_{nm}^- Z^-(k'_{nm}, z)] \ \underline{e}_{nm}^e \ e^{jn\phi} \\
& + \sum_{\substack{n=-\infty \\ k_{nm} \neq 0}}^{\infty} \sum_{m=1}^{\infty} (\alpha_{nm}^+ e^{jk_{nm} z} + \alpha_{nm}^- e^{-jk_{nm} z}) \ \underline{e}_{nm}^m \ e^{jn\phi} \\
& + \sum_{\substack{n=-\infty \\ k_{nm} = 0}}^{\infty} \sum_{m=1}^{\infty} \alpha_{nm}^+ \ \underline{e}_{nm}^m \ e^{jn\phi}
\end{aligned} \tag{2-36}$$

From (2-28), (2-29) and (2-36), we can write for $\underline{H}_b$:

$$\begin{aligned}
\underline{H}_b = {} & (\underline{H}_b \cdot \hat{z})\hat{z} + \frac{1}{\eta_b} (-\alpha_o^+ e^{jk_b z} + \alpha_o^- e^{-jk_b z}) \ \underline{h}^{TEM} \\
& + \sum_{\substack{n=-\infty \\ k_{nm} \neq 0}}^{\infty} \sum_{m=1}^{\infty} Y_{nm} (-\alpha_{nm}^+ e^{jk_{nm} z} + \alpha_{nm}^- e^{-jk_{nm} z}) \ \underline{h}_{nm}^m \ e^{jn\phi} \\
& + \sum_{\substack{n=-\infty \\ k'_{nm} \neq 0}}^{\infty} \sum_{m=1}^{\infty} Y'_{nm} (-\beta_{nm}^+ e^{jk'_{nm} z} + \beta_{nm}^- e^{-jk'_{nm} z}) \ \underline{h}_{nm}^e \ e^{jn\phi} \\
& + \sum_{\substack{n=-\infty \\ k_{nm} = 0}}^{\infty} \sum_{m=1}^{\infty} \frac{-j}{\eta_b} (k_b z \ \alpha_{nm}^+ + B_{nm}) \ \underline{h}_{nm}^m \ e^{jn\phi} \\
& + \sum_{\substack{n=-\infty \\ k'_{nm} = 0}}^{\infty} \sum_{m=1}^{\infty} \frac{1}{-j\eta_b k_b} \beta_{nm}^+ \ \underline{h}_{nm}^e \ e^{jn\phi}
\end{aligned} \tag{2-37}$$

where B_{nm} is a constant and

$$\underline{h}^{TEM} = \hat{z} \times \underline{e}^{TEM}, \qquad \underline{h}^{m}_{nm} = \hat{z} \times \underline{e}^{m}_{nm}, \qquad \underline{h}^{e}_{nm} = \hat{z} \times \underline{e}^{e}_{nm} \tag{2-38}$$

From (2-12), (2-13), (2-36) and the orthonormal relationships among $\underline{e}^{TEM}$, $\underline{e}^{m}_{nm}$ and $\underline{e}^{e}_{nm}$, we obtain

$$\alpha_o^+ + \alpha_o^- = (\underline{h}^{TEM}, \underline{M}_1^o)$$

$$\alpha_o^+ e^{jk_b d} + \alpha_o^- e^{-jk_b d} = -(\underline{h}^{TEM}, \underline{M}_2^o)$$

$$\left.\begin{aligned} &\alpha^+_{nm} + \alpha^-_{nm} = (\underline{h}^m_{nm}, \underline{M}^n_1) \\ &\alpha^+_{nm} e^{jk_{nm}d} + \alpha^-_{nm} e^{-jk_{nm}d} = -(\underline{h}^m_{nm}, \underline{M}^n_2) \end{aligned}\right\} \quad \text{for } k_{nm} \neq 0$$

$$\alpha^+_{nm} = \langle \underline{h}^m_{nm}, \underline{M}^n_1 \rangle = -(\underline{h}^m_{nm}, \underline{M}^n_2) \qquad \text{for } k_{nm} = 0$$

$$\left.\begin{aligned} &\beta^+_{nm} + \beta^-_{nm} = (\underline{h}^e_{nm}, \underline{M}^n_1) \\ &\beta^+_{nm} e^{jk'_{nm}d} + \beta^-_{nm} e^{-jk'_{nm}d} = -(\underline{h}^e_{nm}, \underline{M}^n_2) \end{aligned}\right\} \quad \text{for } k'_{nm} \neq 0$$

$$\left.\begin{aligned} &\beta^-_{nm} = (\underline{h}^e_{nm}, \underline{M}^n_1) \\ &\beta^+_{nm} d + \beta^-_{nm} = -(\underline{h}^e_{nm}, \underline{M}^n_2) \end{aligned}\right\} \quad \text{for } k'_{nm} = 0 \tag{2-39}$$

where

$$\underline{M}^n_i = M^n_{i\rho}\hat{\rho} + M^n_{i\phi}\hat{\phi} = \frac{1}{2\pi}\left[\hat{\rho}\int_0^{2\pi} (\underline{M}_i \cdot \hat{\rho}) e^{-jn\phi}\, d\phi + \hat{\phi}\int_0^{2\pi} (\underline{M}_i \cdot \hat{\phi}) e^{-jn\phi}\, d\phi\right]$$

or

$$\underline{M}_i = \sum_{n=-\infty}^{\infty} (M^n_{i\rho}\hat{\rho} + M^n_{i\phi}\hat{\phi}) e^{jn\phi} \qquad i = 1,2, \tag{2-40b}$$

$$i = 1,2 \tag{2-40a}$$

From (2-39), we obtain

$$\begin{cases} \alpha_o^{\pm} = \dfrac{\pm j(\underline{h}^{TEM},\ e^{\mp jk_b d}\ \underline{M}_1^o + \underline{M}_2^o)}{2 \sin k_b d} & \text{if } k_b d \neq \pi, 2\pi, \ldots \\ \alpha_o^{+} + \alpha_o^{-} = (\underline{h}^{TEM},\ \underline{M}_1^o),\ (\underline{h}^{TEM},\ \underline{M}_1^o + \cos k_b d\ \underline{M}_2^o) & \text{if } k_b d = \pi, 2\pi, \ldots \end{cases} \tag{2-41a}$$

$$\begin{cases} \alpha_{nm}^{\pm} = \dfrac{\pm j\ (\underline{h}_{nm}^m,\ \ e^{\mp jk_{nm} d}\ \underline{M}_1^n + \underline{M}_2^n)}{2 \sin k_{nm} d} & \text{if } k_{nm} d \neq 0, \pi, 2\pi, \ldots \\ \alpha_{nm}^{+} + \alpha_{nm}^{-} = (\underline{h}_{nm}^m,\ \underline{M}_1^n),\ \ (\underline{h}_{nm}^m,\ \underline{M}_1^n + \cos k_{nm} d\ \underline{M}_2^n) = 0 & \text{if } k_{nm} d = \pi, 2\pi, \ldots \\ \alpha_{nm}^{+} = (\underline{h}_{nm}^m,\ \underline{M}_1^n),\ \ (\underline{h}_{nm}^m,\ \underline{M}_1^n + \underline{M}_2^n) = 0 & \text{if } k_{nm} d = 0 \end{cases} \tag{2-41b}$$

$$\begin{cases} \beta_{nm}^{\pm} = \dfrac{j(\underline{h}_{nm}^e,\ e^{\mp jk'_{nm} d}\ \underline{M}_1^n + \underline{M}_2^n)}{2 \sin k'_{nm} d} & \text{if } k'_{nm} d \neq 0, \pi, 2\pi, \ldots \\ \beta_{nm}^{+} + \beta_{nm}^{-} = (\underline{h}_{nm}^e,\ \underline{M}_1^n),\ (\underline{h}_{nm}^e, \underline{M}_1^n + \cos k'_{nm} d\ \underline{M}_2^n) = 0 & \text{if } k'_{nm} d = \pi, 2\pi, \ldots \\ \beta_{nm}^{+} = \dfrac{-(\underline{h}_{nm}^e,\ \underline{M}_1^n + \underline{M}_2^n)}{d}\ ,\ \ \beta_{nm}^{-} = (\underline{h}_{nm}^e,\ \underline{M}_1^n) & \text{if } k'_{nm} d = 0 \end{cases} \tag{2-41c}$$

We substitute (2-41) into (2-36) and obtain

$$\underline{E}_b = (\underline{E}_b \cdot \hat{z})\hat{z} + \underline{e}^{TEM} \begin{cases} -\csc k_b d(\underline{h}^{TEM}, \sin k_b (z-d)\underline{M}_1^o + \sin k_b z \underline{M}_2^o) & \text{if } \sin k_b d \neq 0 \\ (\underline{h}^{TEM},\ \underline{M}_1^o)\cos k_b z + j(\alpha_o^{+} - \alpha_o^{-})\sin k_b z & \text{if } \sin k_b d = 0 \end{cases}$$

$$- \sum_{\substack{n=-\infty \\ \sin k_{nm} d \neq 0}}^{\infty} \sum_{m=1}^{\infty} \csc k_{nm} d(\underline{h}_{nm}^m,\ \sin k_{nm}(z-d)\underline{M}_1^n + \sin k_{nm} z \underline{M}_2^n)\ \underline{e}_{nm}^m\ e^{jn\phi}$$

$$- \sum_{\substack{n=-\infty \\ \sin k'_{nm} d \neq 0}}^{\infty} \sum_{m=1}^{\infty} \csc k'_{nm} d\ (\underline{h}_{nm}^e,\ \sin k'_{nm}(z-d)\underline{M}_1^n + \sin k'_{nm} z \underline{M}_2^n)\underline{e}_{nm}^e\ e^{jn\phi}$$

$$+ \sum_{\substack{n=-\infty \\ k_{nm}d=\pi,2\pi,\ldots}}^{\infty} \sum_{m=1}^{\infty} [(\underline{h}_{nm}^{m}, \underline{M}_{1}^{n})\cos k_{nm}z + j(\alpha_{nm}^{+}-\alpha_{nm}^{-})\sin k_{nm}z]\underline{e}_{nm}^{m} e^{jn\phi}$$

$$+ \sum_{\substack{n=-\infty \\ k'_{nm}d=\pi,2\pi,\ldots}}^{\infty} \sum_{m=1}^{\infty} [(\underline{h}_{nm}^{e}, \underline{M}_{1}^{n})\cos k'_{nm}z + j(\beta_{nm}^{+}-\beta_{nm}^{-})\sin k'_{nm}z]\underline{e}_{nm}^{e} e^{jn\phi}$$

$$+ \sum_{\substack{n=-\infty \\ k_{nm}=0}}^{\infty} \sum_{m=1}^{\infty} (\underline{h}_{nm}^{m}, \underline{M}_{1}^{n})\underline{e}_{nm}^{m} e^{jn\phi}$$

$$+ \sum_{\substack{n=-\infty \\ k'_{nm}=0}}^{\infty} \sum_{m=1}^{\infty} (\underline{h}_{nm}^{e}, (1-\frac{z}{d})\underline{M}_{1}^{n} - \frac{z}{d}\underline{M}_{2}^{n})\underline{e}_{nm}^{e} e^{jn\phi} \qquad (2\text{-}42)$$

We substitute (2-41) into (2-37) and obtain

$$\underline{H}_b = L_b^{w}(-\underline{M}_1, -\underline{M}_2)$$

$$= (\underline{H}_b \cdot \hat{z})\hat{z} - \frac{j}{\eta_b}\underline{h}^{TEM}\begin{cases} \csc k_b d(\underline{h}^{TEM}, \cos k_b(z-d)\underline{M}_1^{o} + \cos k_b z\underline{M}_2^{o}) & \text{if } \sin k_b d \neq 0 \\ (\underline{h}^{TEM}, \underline{M}_1^{o})\sin k_b z + C_o \cos k_b z & \text{if } \sin k_b d = 0 \end{cases}$$

$$- \sum_{\substack{n=-\infty \\ \sin k_{nm}d\neq 0}}^{\infty} \sum_{m=1}^{\infty} j\, Y_{nm}\csc k_{nm}d(\underline{h}_{nm}^{m}, \cos k_{nm}(z-d)\underline{M}_1^{n} + \cos k_{nm}z\underline{M}_2^{n})\underline{h}_{nm}^{m} e^{jn\phi}$$

$$- \sum_{\substack{n=-\infty \\ \sin k'_{nm}d\neq 0}}^{\infty} \sum_{m=1}^{\infty} j\, Y'_{nm}\csc k'_{nm}d(\underline{h}_{nm}^{e}, \cos k'_{nm}(z-d)\underline{M}_1^{n} + \cos k'_{nm}z\underline{M}_2^{n})\underline{h}_{nm}^{e} e^{jn\phi}$$

$$- \sum_{\substack{n=-\infty \\ k_{nm}d=\pi,2\pi,\ldots}}^{\infty} \sum_{m=1}^{\infty} j\, Y_{nm}[(\underline{h}_{nm}^{m}, \underline{M}_1^{n})\sin k_{nm}z + C_{nm}\cos k_{nm}z]\underline{h}_{nm}^{m} e^{jn\phi}$$

$$- \sum_{\substack{n=-\infty \\ k'_{nm}d=\pi,2\pi,\ldots}}^{\infty} \sum_{m=1}^{\infty} j\, Y'_{nm} [(\underline{h}^e_{nm}, \underline{M}_1^n) \sin k'_{nm} z + D_{nm} \cos k'_{nm} z] \underline{h}^e_{nm}\, e^{jn\phi}$$

$$- \sum_{\substack{n=-\infty \\ k_{nm}=0}}^{\infty} \sum_{m=1}^{\infty} [\frac{j}{\eta_b} (\underline{h}^m_{nm}, \underline{M}_1^n) k_b z + B_{nm}] \underline{h}^m_{nm}\, e^{jn\phi}$$

$$- \sum_{\substack{n=-\infty \\ k'_{nm}=0}}^{\infty} \sum_{m=1}^{\infty} \frac{j}{\eta_b} \frac{(\underline{h}^e_{nm}, \underline{M}_1^n + \underline{M}_2^n)}{k_b d} \underline{h}^e_{nm}\, e^{jn\phi} \qquad (2\text{-}43)$$

where

$$C_o = - j(\alpha_o^+ - \alpha_o^-),\ C_{nm} = - j(\alpha_{nm}^+ - \alpha_{nm}^-),\ D_{nm} = - j(\beta_{nm}^+ - \beta_{nm}^-) \qquad (2\text{-}44)$$

$L_b^w(-\underline{M}_1, -\underline{M}_2)$ gives the magnetic field inside the waveguide region b for the equivalent situation in Fig. 6. Note again that the TEM mode can only exist when $R_{in} \neq 0$. Also, we note that in (2-43), corresponding to each undetermined constant (not determined from $\underline{M}_1$ and $\underline{M}_2$ but can be determined through other information) C_o, B_{nm}, C_{nm} or D_{nm}, there is a condition on the magnetic currents as shown in (2-41). This correspondence is summarized in Table 1. The z-components of the fields in the above analysis are not investigated in detail because they are not used in the operator equations which we introduce in the next section.

Situation	Undetermined Coefficient	Condition on the Current
$k_b d = \pi, 2\pi, \ldots$	C_o	$(\underline{h}^{TEM}, \underline{M}_1^o) = -\cos k_b d\,(\underline{h}^{TEM}, \underline{M}_2^o)$
$k_{nm} = 0$	B_{nm}	$(\underline{h}_{nm}^m, \underline{M}_1^n) = -(\underline{h}_{nm}^m, \underline{M}_2^n)$
$k_{nm} d = \pi, 2\pi, \ldots$	C_{nm}	$(\underline{h}_{nm}^m, \underline{M}_1^n) = -\cos k_{nm} d\,(\underline{h}_{nm}^m, \underline{M}_2^n)$
$k'_{nm} d = \pi, 2\pi, \ldots$	D_{nm}	$(\underline{h}_{nm}^e, \underline{M}_1^n) = -\cos k'_{nm} d\,(\underline{h}_{nm}^e, \underline{M}_2^n)$

Table 1. Summary of correspondence between undetermined coefficients in L_b^w and conditions on the magnetic currents.

2.4. Basic Operator Equations

So far we have developed the equivalent situations for the three regions a, b and c. In each region the electromagnetic fields can be obtained from the surface equivalent currents through the operators introduced in the last section. For region a, magnetic current $2\underline{M}_1$ on S_1, together with the impressed sources $\underline{J}_i$ and $\underline{M}_i$ and their images $\underline{J}'_i$ and $\underline{M}'_i$, radiate into unbounded medium (ϵ_a, μ_a) to give $\underline{E}_a$, $\underline{H}_a$, as shown in Fig. 4(b). Therefore, we have

$$\underline{E}_a = [L_a^e(\eta_a \underline{J}_i + \eta_a \underline{J}'_i) - L_a^h(\underline{M}_i + \underline{M}'_i)] - 2L_a^h(\underline{M}_1) \tag{2-45}$$

$$\underline{H}_a = \frac{1}{\eta_a}[L_a^e(\underline{M}_i + \underline{M}'_i) + L_a^h(\eta_a \underline{J}_i + \eta_a \underline{J}'_i)] + \frac{2}{\eta_a} L_a^e(\underline{M}_1) \tag{2-46}$$

where the field point is anywhere in the region $z < 0$. For region c,

the situation is very similar except that no impressed sources are in this region. Therefore, we have

$$\underline{E}_c = - 2L_c^h(\underline{M}_2) \tag{2-47}$$

$$\underline{H}_c = \frac{2}{\eta_c} L_c^e(\underline{M}_2) \tag{2-48}$$

For region b, we have magnetic currents $-\underline{M}_1$ on S_1 and $-\underline{M}_2$ on S_2. These magnetic currents, together with the electric current on the entire S, radiate into unbounded medium (ε_b, μ_b) to give $\underline{E}_b$, $\underline{H}_b$ in region b. Therefore, we have

$$\underline{E}_b = - L_b^e(\eta_b \underline{J}) + L_b^h(\underline{M}_1) + L_b^h(\underline{M}_2) \tag{2-49}$$

$$\underline{H}_b = - \frac{1}{\eta_b} [L_b^e(\underline{M}_1) + L_b^e(\underline{M}_2) + L_b^h(\eta_b \underline{J})] \tag{2-50}$$

If we substitute (2-4) and (2-8) into (2-45) and (2-47), we find that tangential $\underline{E}_a$ is zero everywhere on the plane z = 0 except in S_1. In S_1, let the field point approach from z < 0 (i.e., $\hat{n}_o = - \hat{z}$ in (2-8)) and obtain $\hat{z} \times \underline{E}_a = \underline{M}_1$. Also $\underline{z} \times \underline{E}_c$ is zero everywhere on z = d except in S_2, let the field point approach from z > d (i.e., $\hat{n}_o = \hat{z}$ in (2-8)), and obtain $\hat{z} \times \underline{E}_c = - \underline{M}_2$. These boundary conditions are expected because of the way the equivalent situations were set up for regions a and c. For region b, however, the condition that fields be zero outside S still has to be enforced. This can be done by requiring either the tangential electric field or the tangential magnetic field be zero just outside S. We choose to use the condition on the electric field.

$$\hat{n} \times \hat{n} \times [L_b^h(\underline{M}_1) + L_b^h(\underline{M}_2) - L_b^e(\eta_b \underline{J})] = 0 \quad \text{on } S^+ \tag{2-51}$$

Note that since the field is evaluated on S^+, we have $\hat{n}_o = - \hat{n}$ for L_b^h.

If (2-51) is satisfied, we immediately have from (2-49) that $\hat{z} \times \underline{E}_b$ is zero on S_3 and

$$\hat{z} \times \underline{E}_b = \underline{M}_1 = \hat{z} \times \underline{E}_a \qquad \text{in } S_1 \tag{2-52}$$

$$\hat{z} \times \underline{E}_b = -\underline{M}_2 = \hat{z} \times \underline{E}_c \qquad \text{in } S_2 \tag{2-53}$$

Therefore, if (2-51) is satisfied, our tangential electric field will be zero on all conductor surfaces and continuous through the two aperture faces S_1 and S_2. The boundary condition yet to be satisfied is the continuity of tangential magnetic field through S_1 and S_2. To compute tangential $\underline{H}_b$ on S_1 and S_2, we note that when (2-51) is satisfied Ampere's law states

$$\hat{n} \times \hat{n} \times \underline{H}_b = -\hat{n} \times \underline{J} \qquad \text{in } S_1 \text{ and } S_2 \tag{2-54}$$

To compute the tangential $\underline{H}_a$ in S_1, we note that the contribution from the impressed sources and their images is twice that radiated by $\underline{J}_1$, $\underline{M}_1$ into unbounded (ε_a, μ_a). Therefore

$$\hat{n} \times \hat{n} \times \underline{H}_a = \hat{n} \times \hat{n} \times [2\underline{H}_1 + \frac{2}{\eta_a} L_a^e(\underline{M}_1)] \qquad \text{on } S_1 \tag{2-55}$$

The tangential $\underline{H}_c$ in S_2 is simply, from (2-48),

$$\hat{n} \times \hat{n} \times \underline{H}_c = \hat{n} \times \hat{n} \times \frac{2}{\eta_c} L_c^e(\underline{M}_2) \qquad \text{on } S_2 \tag{2-56}$$

Therefore, the continuity of tangential magnetic field can be written in the following form:

$$\hat{n} \times \hat{n} \times L_a^e(\underline{M}_1) + \frac{\eta_a}{2} \hat{n} \times \underline{J} = -\eta_a \hat{n} \times \hat{n} \times \underline{H}_i \qquad \text{on } S_1 \qquad (2\text{-}57)$$

$$\hat{n} \times \hat{n} \times L_c^e(\underline{M}_2) + \frac{\eta_c}{2} \hat{n} \times \underline{J} = 0 \qquad \text{on } S_2 \qquad (2\text{-}58)$$

Equations (2-57), (2-58), and (2-51) rewritten below,

$$\hat{n} \times \hat{n} \times [L_b^h(\underline{M}_1) + L_b^h(\underline{M}_2) - L_b^e(\eta_b \underline{J})] = 0 \qquad \text{on } S^+ \qquad (2\text{-}59)$$

form the basic operator equations for the general problem, where $\underline{M}_1$, $\underline{M}_2$ and $\underline{J}$ are the unknowns.

When region b represents a waveguide region, the fields in region b can be written in terms of $\underline{M}_1$ and $\underline{M}_2$ alone. The electric current $\underline{J}$ is no longer needed and the boundary conditions on the waveguide walls are built into the waveguide modes. Therefore, all we need to consider is the continuity of the tangential magnetic field across S_1 and S_2:

$$\hat{n} \times \hat{n} \times L_a^e(\underline{M}_1) + \frac{\eta_a}{2} \hat{n} \times \hat{n} \times L_b^w(\underline{M}_1, \underline{M}_2) = -\eta_a \hat{n} \times \hat{n} \times H_i \qquad \text{on } S_1 \qquad (2\text{-}60)$$

$$\hat{n} \times \hat{n} \times L_c^e(\underline{M}_2) + \frac{\eta_c}{2} \hat{n} \times \hat{n} \times L_b^w(\underline{M}_1, \underline{M}_2) = 0 \qquad \text{on } S_2 \qquad (2\text{-}61)$$

(2-60) and (2-61) are the basic operator equations for the special case when region b is a waveguide region.

2.5. Fourier Decomposition

So far we have not taken advantage of the rotational symmetry of the geometry assumed in the problem. In this section this property is used to reduce the system of equations to a smaller set of equations. To do this, we first define the Fourier coefficients of the unknowns as follows:

$$\underline{J}^n(t) = J_t^n(t)\hat{\underline{t}} + J_\phi^n(t)\hat{\underline{\phi}}$$

$$= \frac{\hat{\underline{t}}}{2\pi}\int_0^{2\pi}[\underline{J}(t,\phi)\cdot\hat{\underline{t}}]e^{-jn\phi}\,d\phi + \frac{\hat{\underline{\phi}}}{2\pi}\int_0^{2\pi}[\underline{J}(t,\phi)\cdot\hat{\underline{\phi}}]e^{-jn\phi}\,d\phi \qquad (2\text{-}62a)$$

$$\underline{M}_1^n(t) = M_{1t}^n(t)\hat{\underline{t}} + M_{1\phi}^n\hat{\underline{\phi}}$$

$$= \frac{\hat{\underline{t}}}{2\pi}\int_0^{2\pi}[\underline{M}_1(t,\phi)\cdot\hat{\underline{t}}]e^{-jn\phi}\,d\phi + \frac{\hat{\underline{\phi}}}{2\pi}\int_0^{2\pi}[\underline{M}_1(t,\phi)\cdot\hat{\underline{\phi}}]e^{-jn\phi}\,d\phi \qquad (2\text{-}62b)$$

$$\underline{M}_2^n(t) = M_{2t}^n(t)\hat{\underline{t}} + M_{2\phi}^n(t)\hat{\underline{\phi}}$$

$$= \frac{\hat{\underline{t}}}{2\pi}\int_0^{2\pi}[\underline{M}_1(t,\phi)\cdot\hat{\underline{t}}]e^{-jn\phi}\,d\phi + \frac{\hat{\underline{\phi}}}{2\pi}\int_0^{2\pi}[\underline{M}_2(t,\phi)\cdot\hat{\underline{\phi}}]e^{-jn\phi}\,d\phi \qquad (2\text{-}62c)$$

where n = 0, ±1, ±2,... . Since the field point in the operator equations is always on the surface S and only the tangential component is used, it is convenient to define field quantities in the same fashion as for the sources in (2-62):

$$L_\alpha^{en}(J) = \frac{\hat{\underline{t}}}{2\pi}\int_0^{2\pi}[L_\alpha^e(\underline{J})\cdot\hat{\underline{t}}]e^{-jn\phi}\,d\phi + \frac{\hat{\underline{\phi}}}{2\pi}\int_0^{2\pi}[L_\alpha^e(\underline{J})\cdot\hat{\underline{\phi}}]e^{-jn\phi}\,d\phi \qquad (2\text{-}63)$$

$$L_\alpha^{hn\pm}(\underline{J}) = \frac{\hat{\underline{t}}}{2\pi}\int_0^{2\pi}[L_\alpha^h(\underline{J})\cdot\hat{\underline{t}}]e^{-jn\phi}\,d\phi + \frac{\hat{\underline{\phi}}}{2\pi}\int_0^{2\pi}[L_\alpha^h(\underline{J})\cdot\hat{\underline{\phi}}]e^{-jn\phi}\,d\phi \qquad (2\text{-}64)$$

where for L_α^{hn+}, the field point is on the side of the surface that $\hat{\underline{n}}$ points away from. L_α^{hn-} in the meanwhile, is used for field point on the other side. Substituting (2-4) and (2-8) into (2-63) and (2-64), we find

$$L_\alpha^{en}(\underline{J}) = L_\alpha^{en}(\underline{J}^n)$$

$$= [L_{\alpha tt}^{en}(J_t^n) + L_{\alpha t\phi}^{en}(J_\phi^n)]\hat{\underline{t}} + [L_{\alpha\phi t}^{en}(J_t^n) + L_{\alpha\phi\phi}^{en}(J_\phi^n)]\hat{\underline{\phi}} \qquad (2\text{-}65)$$

$$L_\alpha^{hn\pm}(\underline{J}) = L_\alpha^{hn\pm}(\underline{J}^n)$$

$$= [L_{\alpha tt}^{hn}(J_t^n) + L_{\alpha t\phi}^{hn\pm}(J_\phi^n)]\underline{\hat{t}} + [L_{\alpha\phi t}^{hn\pm}(J_t^n) + L_{\alpha\phi\phi}^{hn}(J_\phi^n)]\underline{\hat{\phi}} \qquad (2\text{-}66)$$

What (2-65) and (2-66) mean is that the Fourier coefficient of either the t or ϕ-component of the field is a function of only the Fourier coefficients of the t and ϕ-components of the source in the same mode. The new operators introduced in (2-65) and (2-66) are defined as:

$$L_{\alpha tt}^{en}(f) = \frac{-j}{2\pi}\{k_\alpha^2\int[\frac{1}{2}\sin v \sin v'(g_{n+1}+g_{n-1}) + \cos v \cos v' g_n]f(t')\rho' dt'$$

$$+ \frac{d}{dt}\int g_n \frac{d}{dt'}(\rho' f(t'))dt'\} \qquad (2\text{-}67a)$$

$$L_{\alpha t\phi}^{en}(f) = \frac{1}{2\pi}\{k_\alpha^2\int\frac{1}{2}\sin v(g_{n+1} - g_{n-1})\, f(t')\rho' dt'$$

$$+ n\int g_n f(t')dt'\} \qquad (2\text{-}67b)$$

$$L_{\alpha\phi t}^{en}(f) = \frac{1}{2\pi}\{- k_\alpha^2\int\frac{1}{2}\sin v'(g_{n+1} - g_{n-1})f(t')\rho' dt'$$

$$+ \frac{n}{\rho}\int g_n \frac{d}{dt'}(\rho' f(t'))dt'\} \qquad (2\text{-}67c)$$

$$L_{\alpha\phi\phi}^{en}(f) = \frac{-j}{2\pi}\{k_\alpha^2\int\frac{1}{2}(g_{n+1} + g_{n-1})f(t')\rho' dt'$$

$$- \frac{n^2}{\rho}\int g_n f(t')dt'\} \qquad (2\text{-}67d)$$

$$L_{\alpha tt}^{hn}(f) = \frac{jk_\alpha^3}{2\pi}\int[\rho'\sin v\cos v' - \rho\sin v'\cos v - (z'-z)\sin v\sin v']G_3 f(t')\rho' dt \qquad (2\text{-}67e)$$

$$L_{\alpha t\phi}^{hn\pm}(f) = \pm\frac{f(t)}{2} + \frac{k_\alpha^3}{2\pi}\int[\rho'\cos v G_1 + ((\rho'-\rho)\cos v - (z'-z)\sin v)G_2]f(t')\rho' dt' \qquad (2\text{-}67f)$$

$$L_{\alpha\phi t}^{hn\pm}(f) = \mp\frac{f(t)}{2} + \frac{k_\alpha^3}{2\pi}\int[\rho\cos v' G_1 - ((\rho'-\rho)\cos v' - (z'-z)\sin v')G_2]f(t')\rho' dt' \qquad (2\text{-}67g)$$

$$L^{hn}_{\alpha\phi\phi}(f) = -\frac{jk_\alpha^3}{2\pi}\int (z'-z)G_3 f(t')\rho' dt' \tag{2-67h}$$

where

$$\cos v = \underline{\hat{t}} \cdot \underline{\hat{z}}\ , \qquad \sin v = \underline{\hat{t}} \cdot \underline{\hat{\rho}} \tag{2-68a}$$

$$\cos v' = \underline{\hat{t}}' \cdot \underline{\hat{z}}\ , \qquad \sin v' = \underline{\hat{t}}' \cdot \underline{\hat{\rho}} \tag{2-68b}$$

$$g_n(t,t') = \int_0^\pi \cos n\phi\, \frac{e^{-jk_\alpha R}}{k_\alpha R}\, d\phi \tag{2-69}$$

$$G_1(t,t') = \int_0^\pi \frac{(1 + jk_\alpha R)e^{-jk_\alpha R}}{k_\alpha^3 R^3} \sin^2\frac{\phi}{2} \cos n\phi\, d\phi \tag{2-70}$$

$$G_2(t,t') = \int_0^\pi \frac{(1 + jk_\alpha R)e^{-jk_\alpha R}}{k_\alpha^3 R^3} \cos\phi \cos n\phi\, d\phi \tag{2-71}$$

$$G_3(t,t') = \int_0^\pi \frac{(1 + jk_\alpha R)e^{-jk_\alpha R}}{k_\alpha^3 R^3} \sin\phi \cos n\phi\, d\phi \tag{2-72}$$

$$R = \sqrt{(\rho - \rho')^2 + (z - z')^2 + 4\rho\rho' \sin^2\frac{\phi}{2}} \tag{2-73}$$

Note that in (2-67), f(t) represents the source function and all integrals are along the generating curve where f(t) is not zero. For the operator L_b^w, if we define

$$L_b^{wn}(\underline{M}_1, \underline{M}_2) = \frac{\hat{\rho}}{2\pi}\int_0^{2\pi} [L_b^w(\underline{M}_1, \underline{M}_2) \cdot \hat{\rho}]e^{-jn\phi}\, d\phi + \frac{\hat{\phi}}{2}\int_0^{2\pi} [L_b^w(\underline{M}_1, \underline{M}_2) \cdot \hat{\phi}]e^{-jn\phi}\, d\phi \tag{2-74}$$

it follows from (2-43) that

$$L_b^{wn}(\underline{M}_1, \underline{M}_2) = L_b^{wn}(\underline{M}_1^n, \underline{M}_2^n)$$

$$= \begin{cases} \frac{j}{\eta_b} \operatorname{csc} k_b d(\underline{h}^{TEM}, \cos k_b(z-d)\underline{M}_1^o + \cos k_b z \underline{M}_2^o)\underline{h}^{TEM} & \text{if } n=0,\ R_{in}\neq 0 \text{ and } \sin k_b d\neq 0 \\ \frac{j}{\eta_b}\left[(\underline{h}^{TEM}, \underline{M}_1^o)\sin k_b z + C_o \cos k_b z\right]\underline{h}^{TEM} & \text{if } n=0,\ R_{in}\neq 0 \text{ and } \sin k_b d=0 \\ 0 & \text{if } n\neq 0 \text{ or } R_{in}=0 \end{cases}$$

$$+ j \sum_{\substack{m=1 \\ \sin k_{nm} d\neq 0}}^{\infty} Y_{nm} \csc k_{nm} d(\underline{h}_{nm}^m, \cos k_{nm}(z-d)\underline{M}_1^n + \cos k_{nm} z \underline{M}_2^n)\underline{h}_{nm}^m$$

$$+ j \sum_{\substack{m=1 \\ \sin k'_{nm} d\neq 0}}^{\infty} Y'_{nm} \csc k'_{nm} d(\underline{h}_{nm}^e, \cos k'_{nm}(z-d)\underline{M}_1^n + \cos k'_{nm} z \underline{M}_2^n)\underline{h}_{nm}^e$$

$$+ j \sum_{\substack{m=1 \\ k_{nm} d=\pi, 2\pi, \ldots}}^{\infty} Y_{nm}\left[(\underline{h}_{nm}^m, \underline{M}_1^n) \sin k_{nm} z + C_{nm} \cos k_{nm} z\right]\underline{h}_{nm}^m$$

$$+ j \sum_{\substack{m=1 \\ k'_{nm} d=\pi, 2\pi, \ldots}}^{\infty} Y'_{nm}\left[(\underline{h}_{nm}^e, \underline{M}_1^n) \sin k'_{nm} z + D_{nm} \cos k'_{nm} z\right]\underline{h}_{nm}^e$$

$$+ \frac{j}{\eta_b} \begin{cases} \left[(\underline{h}_{nq}^m, \underline{M}_1^n)\, k_b z + B_{nq}\right]\underline{h}_{nq}^m & \text{if there exists } k_{nq} = 0 \\ \dfrac{(\underline{h}_{nq}^e, \underline{M}_1^n + \underline{M}_2^n)}{k_b d}\, \underline{h}_{nq}^e & \text{if there exists } k'_{nq} = 0 \end{cases} \qquad (2\text{-}75)$$

Note that all x_{nm} and x'_{nm} for a fixed n are interlaced, and therefore at most one of all k_{nm} and k'_{nm} can be zero. Also note that the conditions on the currents as shown in Table 1 should be considered as part of the definition of the operator.

From (2-64) to (2-67), we can rewrite (2-57) to (2-59) as:

$$-L_a^{en}(\underline{M}_1^n) + \frac{\eta_a}{2}\,\hat{\underline{n}} \times \underline{J}^n = \eta_a \underline{H}_i^n \qquad \text{on } \Gamma_1 \tag{2-76}$$

$$-L_c^{en}(\underline{M}_2^n) + \frac{\eta_c}{2}\,\hat{\underline{n}} \times \underline{J}^n = 0 \qquad \text{on } \Gamma_2 \tag{2-77}$$

$$-L_b^{hn+}(\underline{M}_1^n) + L_b^{hn+}(\underline{M}_2^n) - L_b^{en}(\eta_b\,\underline{J}^n) = 0 \quad \text{on } \Gamma \tag{2-78}$$

From (2-74) and (2-75), we can rewrite (2-60) and (2-61) as:

$$-L_a^{en}(\underline{M}_1^n) - \frac{\eta_a}{2}\,L_a^{wn}(\underline{M}_1^n, \underline{M}_2^n) = \eta_a \underline{H}_i^n \qquad \text{on } \Gamma_1 \tag{2-79}$$

$$-L_c^{en}(\underline{M}_2^n) - \frac{\eta_c}{2}\,L_b^{wn}(\underline{M}_1^n, \underline{M}_2^n) = 0 \qquad \text{on } \Gamma_2 \tag{2-80}$$

For both sets of equations above, we have n = 0, ±1, ±2,... and H_i^n is defined as

$$\underline{H}_i^n = H_{i\rho}^n \hat{\underline{\rho}} + H_{i\phi}^n \hat{\underline{\phi}}$$

$$= \frac{\hat{\underline{\rho}}}{2\pi} \int_0^{2\pi} (\underline{H}_i \cdot \hat{\underline{\rho}}) e^{-jn\phi}\, d\phi + \frac{\hat{\underline{\phi}}}{2\pi} \int_0^{2\pi} (\underline{H}_i \cdot \hat{\underline{\phi}}) e^{-jn\phi}\, d\phi \tag{2-81}$$

Our problem has now been reduced to solving (2-76) to (2-78) for the general case and solving (2-79) and (2-80) for a special case. Although

an infinite number of modes exist, higher order modes are not important unless frequency is high. Also, for axial plane wave incidence, $\underline{H}_1$ is constant in S_1 and therefore, from (2-81), only the $n \pm 1$ modes are excited.

Chapter 3

NUMERICAL SOLUTION

3.1. Generating Curve, Basis Functions and Symmetric Product

The geometry of our problem can be fully specified by the generating curve Γ. This curve, in general, can be fully described by a pair of parametric functions

$$\rho = h_1(t), \quad z = h_2(t) \qquad (\phi \text{ fixed}) \tag{3-1}$$

In our numerical solution, a finite number of points, (ρ_1, z_1) $(\rho_2, z_2),\ldots,$ are specified on the curve. Γ is approximated by connecting successive points with straight line segments. t_i denotes the t-coordinate of the ith point (ρ_i, z_i). Therefore, we have

$$\rho = h_1(t) = \rho_i + \left(\frac{t - t_i}{\Delta t_i}\right)(\rho_{i+1} - \rho_i) \tag{3-2}$$

$$z = h_2(t) = z_i + \left(\frac{t - t_i}{\Delta t_i}\right)(z_{i+1} - z_i) \tag{3-3}$$

where

$$\Delta t_i = t_{i+1} - t_i \tag{3-4}$$

For Γ_2, we have $t_1 \leq t \leq t_{N_1}$. For Γ_1, we have $t_{N_2} \leq t \leq t_{N_3}$. For Γ_3, if S_3 is doubly connected (if there is a center conductor in region b), we have $t_{N_1} \leq t \leq t_{N_2}$ and $t_{N_3} \leq t \leq t_{N_4+1}$. If S_3 is singly connected, we only have $t_{N_1} \leq t \leq t_{N_2}$ for Γ_3. This arrangement is shown in Fig. 8(a) and Fig. 8(b) for the two cases.

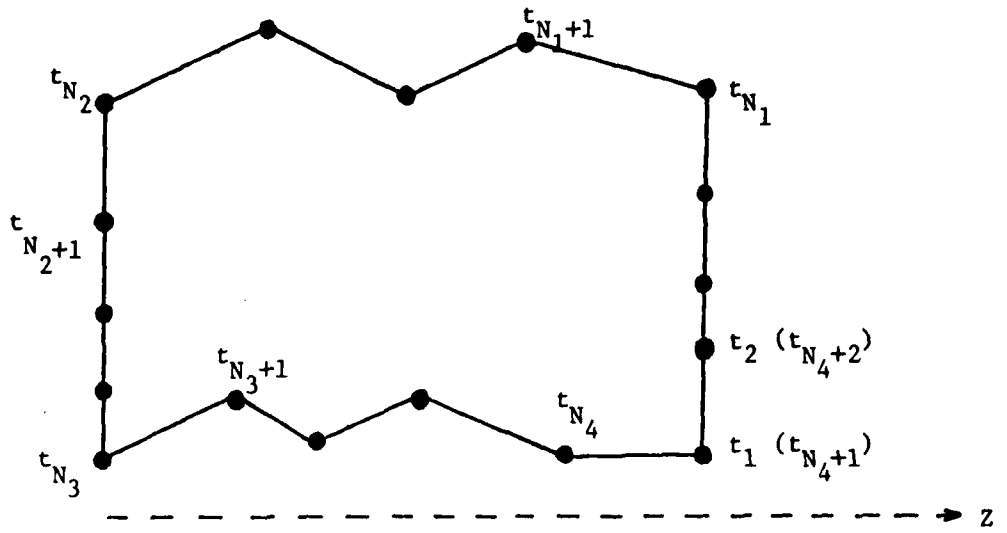

Fig. 8(a). Approximate generating curve, S_3 doubly connected.

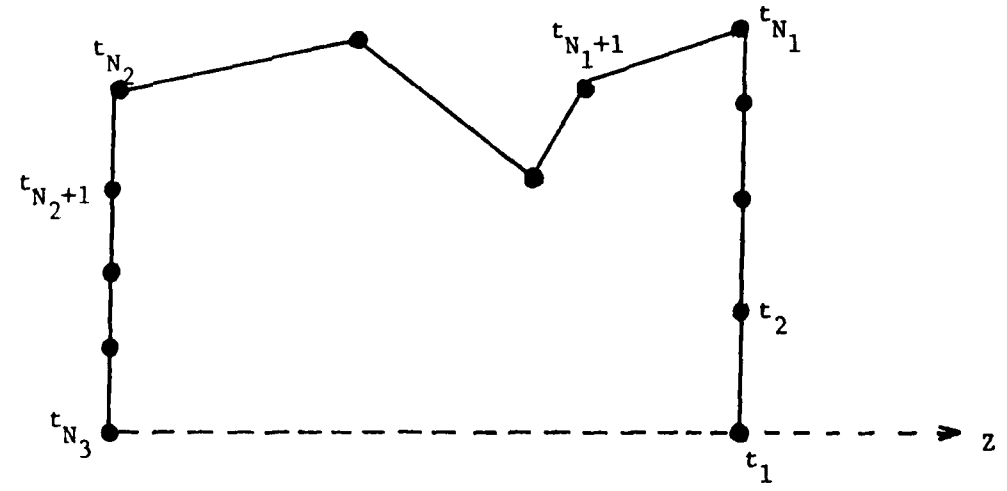

Fig. 8(b). Approximate generating curve, S_3 simply connected.

We now define a set of basis functions, $\{\underline{u}_{ti},\ \underline{u}_{\phi j} \mid i = 1,2,\ldots N_t;\ j = 1,2,\ldots N_\phi\}$, on S:

$$\underline{u}_{ti} = \frac{T_i(t)}{\rho}\,\hat{\underline{t}} \qquad i = 1,2,\ldots, N_t \tag{3-5}$$

$$\underline{u}_{\phi i} = \frac{P_i(t)}{\rho_i^+}\,\hat{\underline{\phi}} \qquad i = 1,2,\ldots,N_\phi \tag{3-6}$$

where

$$T_i(t) = \begin{cases} \dfrac{t - t_i}{t_{i+1} - t_i} & \text{for } t_i \le t \le t_{i+1} \\ \dfrac{t_{i+2} - t}{t_{i+2} - t_{i+1}} & \text{for } t_{i+1} \le t \le t_{i+2} \\ 0 & \text{for } t \text{ elsewhere} \end{cases} \tag{3-7}$$

$$P_i(t) = \begin{cases} 1 & \text{for } t_i \le t \le t_{i+1} \\ 0 & \text{for } t \text{ elsewhere} \end{cases} \tag{3-8}$$

and

$$\rho_i^+ = \frac{1}{2}\,(\rho_i + \rho_{i+1}) \tag{3-9}$$

$$N_t = \begin{cases} N_3 - 2 & \text{for } S_3 \text{ simply connected} \\ N_4 & \text{for } S_3 \text{ doubly connected} \end{cases} \tag{3-10}$$

$$N_\phi = \begin{cases} N_3 - 1 & \text{for } S_3 \text{ simply connected} \\ N_4 & \text{for } S_3 \text{ doubly connected} \end{cases} \tag{3-11}$$

Note that when S_3 is doubly connected, as shown in Fig. 8(a), we use:

$$(\rho_{N_4+1},\ z_{N_4+1}) = (\rho_1,\ z_1) \qquad (\rho_{N_4+2},\ z_{N_4+2}) = (\rho_2,\ z_2) \tag{3-12}$$

The symmetric product, $\langle \underline{a}, \underline{b} \rangle$ of two vector functions is defined as:

$$\langle \underline{a}, \underline{b} \rangle = \int_{\Gamma} \underline{a} \cdot \underline{b} \rho \, dt \tag{3-13}$$

3.2. Matrix Equation for the Nonmodal Formulation

The moment method [17] is used to reduce the set of linear operator equations (2-76) to (2-78) to a matrix equation. To do this, we first expand our unknowns $\underline{M}_1^n$, $\underline{M}_2^n$ and $\underline{J}^n$ as linear combinations of the basis functions defined in the last section:

$$\underline{M}_1^n = \sum_{q=1}^{m_{1t}} V_{1tq}^n \, \underline{u}_{t,q+N_2-1} + \sum_{q=1}^{m_{1\phi}} V_{1\phi q}^n \, \underline{u}_{\phi,q+N_2-1} \tag{3-14}$$

$$\underline{M}_2^n = \sum_{q=1}^{m_{2t}} V_{2tq}^n \, \underline{u}_{tq} + \sum_{q=1}^{m_{2\phi}} V_{2\phi q}^n \, \underline{u}_{\phi q} \tag{3-15}$$

$$\eta_b \underline{J} = \sum_{q=1}^{N_t} I_{tq}^n \, \underline{u}_{tq} + \sum_{q=1}^{N_\phi} I_{\phi q}^n \, \underline{u}_{\phi q} \tag{3-16}$$

where

$$m_{1t} = N_3 - N_2 - 1 \quad , \quad m_{1\phi} = N_3 - N_2 \quad , \quad m_{2t} = N_1 - 2, \quad m_{2\phi} = N_1 - 1 \tag{3-17}$$

Note that the boundary conditions that the components of $\underline{M}_1^n$ and $\underline{M}_2^n$ normal to the edge of the apertures be zero are satisfied by (3-14) and (3-15). Equations (3-14) to (3-16) are substituted into (2-78). Next, we test

(2-76) with every element in the set $\{\underline{u}_{ti}, \underline{u}_{\phi j} \mid i = N_2,\ldots,N_3-2;$ $j = N_2, \ldots, N_3-1\}$. *In other words, we require that the symmetric* product of both sides of (2-76) with every element in the above set be equal. Similarly, (2-77) is tested with the set $\{\underline{u}_{ti}, \underline{u}_{\phi j} \mid i=1,2,\ldots,N_1-2;$ $j = 1,2,\ldots, N_1-1\}$ and (2-78) is tested with the set $\{\underline{u}_{ti}, \underline{u}_{\phi j} \mid i=1,2,\ldots,N_t;$ $j = 1,2,\ldots, N_\phi\}$. This moment method procedure results in the matrix equation

$$\begin{bmatrix} Z^{an}_{tt} & Z^{an}_{t\phi} & 0 & 0 & U^{1}_{tt} & U^{1}_{t\phi} \\ Z^{an}_{\phi t} & Z^{an}_{\phi\phi} & 0 & 0 & U^{1}_{\phi t} & U^{1}_{\phi\phi} \\ 0 & 0 & Z^{cn}_{tt} & Z^{cn}_{t\phi} & U^{2}_{tt} & U^{2}_{t\phi} \\ 0 & 0 & Z^{cn}_{\phi t} & Z^{cn}_{\phi\phi} & U^{2}_{\phi t} & U^{2}_{\phi\phi} \\ Y^{1bn}_{tt} & Y^{1bn}_{t\phi} & Y^{2bn}_{tt} & Y^{2bn}_{t\phi} & Z^{bn}_{tt} & Z^{bn}_{t\phi} \\ Y^{1bn}_{\phi t} & Y^{1bn}_{\phi\phi} & Y^{2bn}_{\phi t} & Y^{2bn}_{\phi\phi} & Z^{bn}_{\phi t} & Z^{bn}_{\phi\phi} \end{bmatrix} \begin{bmatrix} \bar{V}^{n}_{1t} \\ \bar{V}^{n}_{1\phi} \\ \bar{V}^{n}_{2t} \\ \bar{V}^{n}_{2\phi} \\ \bar{I}^{n}_{t} \\ \bar{I}^{n}_{\phi} \end{bmatrix} = \begin{bmatrix} \bar{p}^{n}_{t} \\ \bar{p}^{n}_{\phi} \\ 0 \\ 0 \\ 0 \\ 0 \end{bmatrix} \tag{3-18}$$

where the Y's, Z's and U's are submatrices. Their elements in the ith row and jth column are defined as:

$$[Z^{an}_{pq}]_{ij} = - \langle \underline{u}_{p,i+N_2-1}, L^{en}_{a}(\underline{u}_{q,j+N_2-1}) \rangle$$

$$p,q = t,\phi$$

$$i = 1,2,\ldots, m_{1p}$$

$$j = 1,2,\ldots, m_{1q} \tag{3-19}$$

$$[Z^{cn}_{pq}]_{ij} = - \langle \underline{u}_{pi}, L^{en}_{c}(\underline{u}_{qj}) \rangle$$

$$p, q = t,\phi$$

$$i = 1, 2,\ldots, m_{2p}$$

$$j = 1,2,\ldots, m_{2q} \tag{3-20}$$

$$[Z^{bn}_{pq}]_{ij} = - \langle \underline{u}_{pi}, L_b^{en}(\underline{u}_{qj}) \rangle$$

$$p,q = t,\phi$$

$$i = 1,2,\ldots, N_p$$

$$j = 1,2,\ldots, N_q \qquad (3\text{-}21)$$

$$[Y^{1bn}_{pq}]_{ij} = \langle \underline{u}_{pi}, L_b^{hn+}(\underline{u}_{q,j+N_2-1}) \rangle$$

$$p,q = t,\phi$$

$$i = 1,2,\ldots, N_p$$

$$j = 1,2,\ldots, m_{1q} \qquad (3\text{-}22)$$

$$[Y^{2bn}_{pq}]_{ij} = \langle \underline{u}_{pi}, L_b^{hn+}(\underline{u}_{qj}) \rangle$$

$$p,q = t,\phi$$

$$i = 1,2,\ldots, N_p$$

$$j = 1,2,\ldots, m_{2q} \qquad (3\text{-}23)$$

$$[U^{l}_{pq}]_{ij} = \frac{\eta_a}{2\eta_b} \langle \underline{u}_{p,i+N_2-1}, \hat{\underline{n}} \times \underline{u}_{qj} \rangle$$

$$= \begin{cases} \dfrac{\eta_a \Delta_j}{4\eta_b \rho^+_j} (\delta_{i+N_2,j} + \delta_{i+N_2-1,j}) & \text{if } p=t,\ q=\phi \\ \dfrac{-\eta_a \Delta_{i+N_2-1}}{4\eta_b \rho^+_{i+N_2-1}} (\delta_{i+N_2-1,j} + \delta_{i+N_2-2,j}) & \text{if } p=\phi,\ q=t \\ 0 & \text{if } p = q \end{cases} \qquad (3\text{-}24)$$

$$p,q = t,\phi$$

$$i = 1,2,\ldots,m_{1p}$$

$$j = 1,2,\ldots,N_q$$

$$[U^2_{pq}]_{ij} = \frac{\eta_c}{2\eta_b} \langle \underline{u}_{pi}, \hat{\underline{n}} \times \underline{u}_{qj} \rangle$$

$$= \begin{cases} \dfrac{\eta_c \, \Delta_j}{4\eta_b \, \rho_j^+} (\delta_{ij} + \delta_{i+1,j}) & \text{if } p=t,\ q=\phi \\ \dfrac{-\eta_c \, \Delta_i}{4\eta_b \rho_i^+} (\delta_{ij} + \delta_{i-1,j} + \delta_{il} \, \delta_{j,N_4}) & \text{if } p=\phi\ ,\ q=t \\ 0 & \text{if } p = q \end{cases}$$

$$p,q = t,\phi$$

$$i = 1,2,\ldots, m_{2p}$$

$$j = 1,2,\ldots, N_q \qquad (3\text{-}25)$$

Note that explicit formulas are obtained for elements of the U's because the evaluation is very easy. The Kronecker delta is used in (3-24) and (3-25). The evaluation of (3-19) to (3-23) requires complicated double integration. Numerical methods are used in the computation. The evaluation of the g's and G's in (2-69) to (2-72) is important because of the special care required in handling the singularities of the integrands. The singular part, or a function that has the same singularity, is integrated analytically for each integrand that has a singularity. The difference, which is regular, is then integrated numerically. The details are explained by Mautz and Harrington in [18], [19], and [20].

$\bar{V}^n_{1t}$, $\bar{V}^n_{1\phi}$, $\bar{V}^n_{2t}$, $\bar{V}^n_{2\phi}$, $\bar{I}^n_t$ and $\bar{I}^n_\phi$ are column matrices defined as

$$\bar{V}_{is}^{n} = \begin{bmatrix} V_{is1}^{n} \\ V_{is2}^{n} \\ \cdot \\ \cdot \\ \cdot \\ V_{ism_{is}}^{n} \end{bmatrix} \qquad \begin{matrix} i = 1,2 \\ s = t, \phi \end{matrix} \tag{3-26}$$

$$\bar{I}_{s}^{n} = \begin{bmatrix} I_{s1}^{n} \\ I_{s2}^{n} \\ \cdot \\ \cdot \\ \cdot \\ I_{sN_s}^{n} \end{bmatrix} \qquad s = t,\phi \tag{3-27}$$

Their elements are the unknown coefficients of the expansions in (3-14) to (3-16). $\bar{p}_{t}^{n}$ and $\bar{P}_{\phi}^{n}$ are column matrices of lengths m_{1t} and $m_{1\phi}$ respectively. Their elements are defined as

$$p_{sj}^{n} = \eta_a \langle \underline{u}_{s,j+N_2-1}, \underline{H}_{i}^{n} \rangle \qquad \begin{matrix} s = t,\phi \\ j = 1,2,\ldots,m_{1s} \end{matrix} \tag{3-28}$$

A more detailed examination of the "excitation matrix" defined in (3-28) is discussed in a later section.

3.3 Matrix Equation for the Modal Formulation

To discuss the modal formulation, we first note that the complete systems of equations for this formulation consists of the operator equations (2-79) and (2-80) plus the equations that set the conditions on the

magnetic currents, when required, as summarized in Table 1. When the operator L_b^{wn} is used, a finite number of modes are used instead of an infinite number of them. The unknown magnetic curretns $\underline{M}_1^n$ and $\underline{M}_2^n$ are expanded as in the last section:

$$\underline{M}_1^n = \sum_{i=1}^{m_{1t}} V_{1ti}^n \, \underline{u}_{t,i+N_2-1} + \sum_{i=1}^{m_{1\phi}} V_{1\phi i}^n \, \underline{u}_{\phi,i+N_2-1} \tag{3-29}$$

$$\underline{M}_2^n = \sum_{i=1}^{m_{2t}} V_{2ti}^n \, \underline{u}_{t,i} + \sum_{i=1}^{m_{2\phi}} V_{2\phi i}^n \, \underline{u}_{\phi,i} \tag{3-30}$$

We substitute (3-29) and (3-30) into (2-79) and (2-80). Equations (2-79) and (2-80) are then tested by $\{\underline{u}_{ti}, \underline{u}_{\phi j} | i = N_2, \ldots, N_3-2; j = N_2, \ldots, N_3-1\}$ and $\{\underline{u}_{ti}, \underline{u}_{\phi j} | i = 1,2,\ldots, N_1-2; j = 1,2,\ldots, N_1-1\}$, respectively, using the symmetric product defined in (3-13). The resulting equations can be written in the following form:

$$\begin{bmatrix} Z_{tt}^{an} + W_{tt}^{bn11} & Z_{t\phi}^{an} + W_{t\phi}^{bn11} & W_{tt}^{bn12} & W_{t\phi}^{bn12} & X_{1t}^n \\ Z_{\phi t}^{an} + W_{\phi t}^{bn11} & Z_{\phi\phi}^{an} + W_{\phi\phi}^{bn11} & W_{\phi t}^{bn12} & W_{\phi\phi}^{bn12} & X_{1\phi}^n \\ W_{tt}^{bn21} & W_{t\phi}^{bn21} & Z_{tt}^{cn} + W_{t\phi}^{bn22} & Z_{t\phi}^{cn} + W_{t\phi}^{bn22} & X_{2t}^n \\ W_{\phi t}^{bn21} & W_{\phi\phi}^{bn21} & Z_{\phi t}^{cn} + W_{\phi t}^{bn22} & Z_{\phi\phi}^{cn} + W_{\phi\phi}^{bn22} & X_{2\phi}^n \end{bmatrix} \begin{bmatrix} \bar{V}_{1t}^n \\ \bar{V}_{1\phi}^n \\ \bar{V}_{2t}^n \\ \bar{V}_{2\phi}^n \\ \bar{C}^n \end{bmatrix} = \begin{bmatrix} \bar{p}_t^n \\ \bar{p}^n \\ 0 \\ 0 \end{bmatrix} \tag{3-31}$$

where the Z's and $\bar{V}$'s and $\bar{p}$'s are defined the same as in (3-26) and (3-28). The elements in the W's are defined in the following:

$$W_{pq}^{bn11} = \frac{\eta_a}{2j\eta_b}\left\{ \sum_{\substack{m=1 \\ \sin k_{nm} d \neq 0}}^{N^m} \frac{k_b}{k_{nm}} \cot(k_{nm} d)\, \bar{x}_{nm}^{m1p}\, \bar{x}_{nm}^{m1q^+} \right.$$

$$+ \sum_{\substack{m=1 \\ \sin k'_{nm} d \neq 0}}^{N^e} \frac{k'_{mn}}{k_b} \cot(k'_{nm} d)\, \bar{x}_{nm}^{e1p}\, \bar{x}_{nm}^{e1q^+}$$

$$+ \cot(k_b d)\, \bar{x}_1^{TEM}\, \bar{x}_1^{TEM^+} \quad (\text{if } n=0,\ R_{in} \neq 0,\ \sin k_b d \neq 0 \text{ and } p=q=\phi)$$

$$\left. + \frac{1}{k_b d}\, \bar{x}_{nk}^{e1p}\, \bar{x}_{nk}^{e1q^+} \quad (\text{if there exists a } k'_{nk} = 0) \right\}$$

$$p,\ q = t, \phi \qquad (3\text{-}32)$$

$$W_{pq}^{bn22} = \frac{\eta_c}{2j\eta_b}\left\{ \sum_{\substack{m=1 \\ \sin k_{nm} d \neq 0}}^{N^m} \frac{k_b}{k_{nm}} \cot(k_{nm} d)\, \bar{x}_{nm}^{m2p}\, \bar{x}_{nm}^{m2q^+} \right.$$

$$+ \sum_{\substack{m=1 \\ \sin k'_{nm} d \neq 0}}^{N^e} \frac{k'_{nm}}{k_b} \cot(k'_{nm} d)\, \bar{x}_{nm}^{e2p}\, \bar{x}_{nm}^{e2q^+}$$

$$+ \cot(k_b d)\, \bar{x}_2^{TEM}\, \bar{x}_2^{TEM^+} \quad (\text{if } n=0,\ R_{in} \neq 0,\ \sin k_b d \neq 0 \text{ and } p=q=\phi)$$

$$\left. + \frac{1}{k_b d}\, \bar{x}_{nk}^{e2p}\, \bar{x}_{nk}^{e2q^+} \quad (\text{if there exists a } k'_{nk} = 0) \right\}$$

$$p,\ q = t, \phi \qquad (3\text{-}33)$$

$$W_{pq}^{bn12} = \frac{\eta_a}{2j\eta_b}\Bigg\{ \sum_{\substack{m=1 \\ \sin k_{nm}d\neq 0}}^{N^m} \frac{k_b}{k_{nm}} \csc k_{nm}d \; \bar{x}_{nm}^{m1p} \; \bar{x}_{nm}^{m2q^+}$$

$$+ \sum_{\substack{m=1 \\ \sin k'_{nm}\neq 0}}^{N^e} \frac{k'_{mn}}{k_b} \csc k'_{nm}d \; \bar{x}_{nm}^{e1p} \; \bar{x}_{nm}^{e2q^+}$$

$$+ \csc k_b d \; \bar{x}_1^{TEM} \; \bar{x}_2^{TEM^+} \quad (\text{if } n=0, R_{in}\neq 0, \sin k_b d\neq 0, \text{ and } p=q=\phi)$$

$$+ \frac{1}{k_b d} \; \bar{x}_{nk}^{e1p} \; \bar{x}_{nk}^{e2q^+} \quad (\text{if there exists a } k'_{nk} = 0)\Bigg\}$$

$$p,q = t,\phi \qquad (3\text{-}34)$$

$$W_{pq}^{bn21} = \frac{\eta_c}{2j\eta_b}\Bigg\{ \sum_{\substack{m=1 \\ \sin k_{nm}d\neq 0}}^{N^m} \frac{k_b}{k_{nm}} \csc k_{nm}d \; \bar{x}_{nm}^{m2p} \; \bar{x}_{nm}^{m1q^+}$$

$$\sum_{\substack{m=1 \\ \sin k'_{nm}d\neq 0}}^{N^e} \frac{k'_{nm}}{k_b} \csc k'_{nm}d \; \bar{x}_{nm}^{e2p} \; \bar{x}_{nm}^{e1q^+}$$

$$+ \csc k_b d \; \bar{x}_2^{TEM} \; \bar{x}_1^{TEM^+} \quad (\text{if } n=0, R_{in}\neq 0, \sin k_b d\neq 0 \text{ and } p=q=\phi)$$

$$+ \Bigg\{ \begin{array}{l} \frac{1}{k_b d} \; \bar{x}_{nk}^{e2p} \; \bar{x}_{nk}^{e1q^+} \quad (\text{if there exists a } k'_{nk} = 0) \\ \\ k_b d \; \bar{x}_{nk}^{m2p} \; \bar{x}_{nk}^{m1q^+} \quad (\text{if there exists a } k_{nk} = 0) \end{array} \Bigg\}$$

$$p,q = t,\phi \qquad (3\text{-}35)$$

where $\bar{x}^{mlp}_{nm}$, $\bar{x}^{elp}_{nm}$,..., etc., are column matrices. Their elements are defined as

$$[\bar{x}^{mlt}_{nm}]_i = \langle \underline{u}_{t,i+N_2-1}, \underline{h}^m_{nm} \rangle = jn \int_{R_{in}}^{R_{out}} \frac{T_{i+N_2-1}}{\rho} \psi^m_{nm} d\rho \qquad (3\text{-}36)$$

$$i=1,2,\ldots,m_{1t}$$

$$[\bar{x}^{ml\phi}_{nm}]_i = \langle \underline{u}_{\phi,i+N_2-1}, \underline{h}^m_{nm} \rangle = \int_{R_{in}}^{R_{out}} \frac{P_{i+N_2-1}}{\rho^+_{i+N_2-1}} \psi^{m'}_{nm} d\rho \qquad (3\text{-}37)$$

$$i=1,2,\ldots,m_{1\phi}$$

$$[\bar{x}^{elt}_{nm}]_i = \langle \underline{u}_{t,i+N_2-1}, \underline{h}^e_{nm} \rangle = \int_{R_{in}}^{R_{out}} T_{i+N_2-1} \psi^{e'}_{nm} d\rho \qquad (3\text{-}38)$$

$$i = 1,2,\ldots,m_{1t}$$

$$[\bar{x}^{el\phi}_{nm}]_i = \langle \underline{u}_{\phi,i+N_2-1}, \underline{h}^e_{nm} \rangle = -jn \int_{R_{in}}^{R_{out}} \frac{P_{i+N_2-1}}{\rho^+_{i+N_2-1}} \psi^e_{nm} d\rho \qquad (3\text{-}39)$$

$$i = 1,2,\ldots,m_{1\phi}$$

$$[\bar{x}^{TEM}_1]_i = \langle \underline{u}_{\phi,i+N_2-1}, \underline{h}^{TEM} \rangle = \frac{\Lambda_{i+N_2-1}}{\rho^+_{i+N_2-1}\sqrt{\ln (R_{out}/R_{in})}} \qquad (3\text{-}40)$$

$$i = 1,2,\ldots,m_{1\phi}$$

$$[\bar{x}^{m2t}_{nm}]_i = \langle \underline{u}_{ti}, \underline{h}^m_{nm} \rangle = -jn \int_{R_{in}}^{R_{out}} \frac{T_i}{\rho} \psi^m_{nm} d\rho \qquad (3\text{-}41)$$

$$i = 1,2,\ldots,m_{2t}$$

$$[\bar{x}^{m2\phi}_{nm}]_i = \langle \underline{u}_{\phi i}, \underline{h}^m_{nm} \rangle = \int_{R_{in}}^{R_{out}} \frac{P_i}{\rho_i^+} \psi^{m'}_{nm} \rho \, d\rho \qquad (3\text{-}42)$$

$$i = 1,2,\ldots,m_{2\phi}$$

$$[\bar{x}^{e2t}_{nm}]_i = \langle \underline{u}_{ti}, \underline{h}^e_{nm} \rangle = - \int_{R_{in}}^{R_{out}} T_i \, \psi^{e'}_{nm} \, d\rho \qquad (3\text{-}43)$$

$$i = 1,2,\ldots,m_{2t}$$

$$[\bar{x}^{e2\phi}_{nm}]_i = \langle \underline{u}_{\phi i}, \underline{h}^e_{nm} \rangle = - jn \int_{R_{in}}^{R_{out}} \frac{P_i}{\rho_i^+} \psi^e_{nm} \, d\rho \qquad (3\text{-}44)$$

$$i = 1,2,\ldots,m_{2\phi}$$

$$[\bar{x}^{TEM}_2]_i = \langle \underline{u}_{\phi i}, \underline{h}^{TEM} \rangle = \frac{\Lambda_i}{\rho_i^+ \sqrt{\ln (R_{out}/R_{in})}} \qquad (3\text{-}45)$$

$$i = 1,2,\ldots,m_{2\phi}$$

ψ^m_{nm}, ψ^e_{nm}, T_i and P_i are defined in (2-21), (2-22), (3-7) and (3-8). The superscript "+" on a matrix denotes its complex conjugate transpose. N^m and N^e are the numbers of TM and TE modes used in the approximation of L_b^{wn}. We normally choose them such that $\psi^m_{nm}(\rho)$ and $\psi^e_{nm}(\rho)$ have a number of oscillations in any given subsection.

The $\bar{X}$'s and the column matrix $\bar{C}^n$ exist only when at least one "cavity resonance" occurs. By "cavity resonance," we mean any of the situations listed in Table 1. The elements of the column matrix $\bar{C}^n$ are the unknown coefficients C_o, B_{nm}, C_{nm}, and D_{nm} when their corresponding resonance occurs. If such an unknown coefficient exists as the ith ele-

ment of $\bar{C}^n$, then there exists a corresponding ith column in each of the X^n_{1t}, $X^n_{1\phi}$, X^n_{2t} and $X^n_{2\phi}$. This corresponding column is of the following form:

$$\frac{Y}{2j}\begin{bmatrix} \eta_a \, \bar{x}^{1t} \\ \eta_a \, \bar{x}^{1\phi} \\ \eta_c \cos kd \, \bar{x}^{2t} \\ \eta_c \cos kd \, \bar{x}^{2\phi} \end{bmatrix} \tag{3-46}$$

where the $\bar{x}$'s and Y and k used in (3-46) depend on the particular "cavity resonance" under consideration. The correspondence between the unknown coefficients and the $\bar{x}$'s and Y and k in (3-46) are summarized in Table 2.

Coefficient	Y	k	$\bar{x}^{is}$ $i=1,2$ $s=t,\phi$
C_o	$1/\eta_b$	k_b	x_i^{-TEM} for $s=\phi$ 0 for $s=t$
B_{nm}	$1/\eta_b$	k_{nm}	$\bar{x}^m_{nm}$
C_{nm}	Y_{nm}	k_{nm}	$\bar{x}^m_{nm}$
D_{nm}	Y'_{nm}	k'_{nm}	$\bar{x}^e_{nm}$

Table 2. Correspondence between $\bar{x}$'s and Y and k in (3-46) and the coefficients associated with cavity resonances.

Next we consider the conditions on the magnetic currents when cavity resonances occur. Substituting (3-29) and (3-30) into the

conditions listed in Table 1, we find

$$\begin{bmatrix} \frac{\eta_c}{\eta_a} X_{1t}^{n+} & \frac{\eta_c}{\eta_a} X_{1\phi}^{n+} & X_{2t}^{n+} & X_{2\phi}^{n+} \end{bmatrix} \begin{bmatrix} \bar{V}_{1t}^n \\ \bar{V}_{1\phi}^n \\ \bar{V}_{2t}^n \\ \bar{V}_{2\phi}^n \end{bmatrix} = 0 \tag{3-47}$$

Combining (3-38) and (3-54), we obtain, for the modal formulation,

$$\begin{bmatrix} Z_{tt}^{an} + W_{tt}^{bn11} & Z_{t\phi}^{an} + W_{t\phi}^{bn11} & W_{tt}^{bn12} & W_{t\phi}^{bn12} & X_{1t}^n \\ Z_{\phi t}^{an} + W_{\phi t}^{bn11} & Z_{\phi\phi}^{an} + W_{\phi\phi}^{bn11} & W_{\phi t}^{bn12} & W_{\phi\phi}^{bn12} & X_{1\phi}^n \\ W_{tt}^{bn21} & W_{t\phi}^{bn21} & Z_{tt}^{cn} + W_{tt}^{bn22} & Z_{t\phi}^{cn} + W_{t\phi}^{bn22} & X_{2t}^n \\ W_{\phi t}^{bn21} & W_{\phi\phi}^{bn21} & Z_{\phi t}^{cn} + W_{\phi t}^{bn22} & Z_{\phi\phi}^{an} + W_{\phi\phi}^{bn22} & X_{2\phi}^n \\ \nu_{ca} X_{1t}^{n+} & \nu_{ca} X_{1\phi}^{n+} & X_{2t}^{n+} & X_{2\phi}^{n+} & 0 \end{bmatrix} \begin{bmatrix} \bar{V}_{1t}^n \\ \bar{V}_{1\phi}^n \\ \bar{V}_{2t}^n \\ \bar{V}_{2\phi}^n \\ \bar{C}^n \end{bmatrix} = \begin{bmatrix} \bar{p}_t^n \\ \bar{p}_\phi^n \\ 0 \\ 0 \\ 0 \end{bmatrix} \tag{3-48}$$

where

$$\nu_{ca} = \eta_c / \eta_a \tag{3-49}$$

3.4. Far Field Measurement and Plane Wave Excitation

The modal and nonmodal formulation discussed in previous sections share the same excitation matrix defined in (3-28). The values of the matrix elements depend upon the specific type of incident field under consideration. In this section we consider plane wave incidence. This plane wave can be considered as the field radiated by an electric dipole

located so far away from the aperture region such that the distance between the dipole and the aperture region is much greater than the linear dimension of the aperture. Therefore, from (3-28), the computation of the excitation matrix involves calculating the reaction [16, Sec. 7-7] between the magnetic field due to an electric dipole and the basis functions of the magnetic current in the aperture S_1. Furthermore, from reciprocity [16, Sec. 3-8] the problem can be thought of as calculating the reaction between the electric field due to the basis functions of the magnetic current and the distant electric dipole. This situation is very similar to the one we have when the far field on the transmitted side is considered. In that situation, each of the two components (tangential to the radiation sphere) of the radiation electric field can be thought of as the reaction between the electric field due to a linear combination of the basis functions of the magnetic current and a distant electric dipole of unit magnitude, pointing in the appropriate direction. Therefore, the far field measurement and the plane wave excitation share basically the same analysis.

First, let us consider the plane wave excitation. The plane wave considered here is of either the θ-polarization or the ϕ-polarization. The electric and magnetic fields of these two types are of the following form:

$$\left.\begin{aligned} \underline{E}_i^{\theta} &= E_o^{\theta}\, \underline{\hat{\theta}}_i\, e^{-j\underline{k}_i \cdot \underline{r}} \\ \underline{H}_i^{\theta} &= \frac{1}{\eta_a}\, \underline{k}_i \times \underline{E}_i \end{aligned}\right\} \quad \theta\text{-polarization} \qquad (3\text{-}50)$$

$$\left.\begin{aligned} \underline{E}_i^{\phi} &= E_o^{\phi}\,\hat{\underline{\phi}}_i\, e^{-j\underline{k}_i\cdot\underline{r}} \\ \underline{H}_i^{\phi} &= \frac{1}{\eta_a}\,\hat{\underline{k}}_i \times \underline{E}_i^{\phi} \end{aligned}\right\} \qquad \phi\text{-polarization} \qquad (3\text{-}51)$$

where

$$\hat{\underline{k}}_i = \hat{\underline{\phi}}_i \times \hat{\underline{\theta}}_i \quad , \qquad \underline{k}_i = k_a \hat{\underline{k}}_i \quad , \qquad (3\text{-}52)$$

$\hat{\underline{\theta}}_i$ and $\hat{\underline{\phi}}_i$ are the unit vectors in the spherical coordinate system at the point, (r_i, θ_i, ϕ_i), where the distant incident source is located. This situation is shown in Fig. 9. A general plane wave is a linear combination of (3-50) and (3-51). Substituting (2-81), (3-50) and (3-51) into (3-28), we obtain

$$p_{sj}^{nq} = \frac{E_o^q}{2\pi} \int_{t_{N_2}}^{t_{N_3}} dt_\rho \,(\hat{\underline{s}}\cdot\underline{u}_{s,j+N_2-1}) \int_0^{2\pi} d\phi\,(\hat{\underline{s}}\cdot\hat{\underline{k}}_i \times \hat{\underline{q}}_i) e^{-j\underline{k}_i\cdot\underline{r}-jn\phi}$$

$$\begin{aligned} s &= t,\phi \\ q &= \theta,\phi \\ j &= 1,2,\ldots,m_{1s} \end{aligned} \qquad (3\text{-}53)$$

The extra superscript q denotes the type of polarization under consideration. Substituting (3-5), (3-6) and (3-52) into (3-53), we obtain

$$\begin{aligned} \bar{p}_t^{n\theta} &= \frac{E_o^{\theta}\, e^{-jn\phi_i}}{2\pi k_a}\,\bar{R}_n^{t\phi} \\ \bar{p}_{\phi}^{n\theta} &= \frac{-E_o^{\theta}\, e^{-jn\phi_i}}{2\pi k_a}\,\bar{R}_n^{\phi\phi} \\ \bar{p}_t^{n\phi} &= \frac{E_o^{\phi}\, e^{-jn\phi_i}}{2\pi k_a}\,\bar{R}_n^{t\theta} \\ \bar{p}_{\phi}^{n\phi} &= \frac{-E_o^{\phi}\, e^{-jn\phi_i}}{2\pi k_a}\,\bar{R}_n^{\phi\theta} \end{aligned} \qquad (3\text{-}54)$$

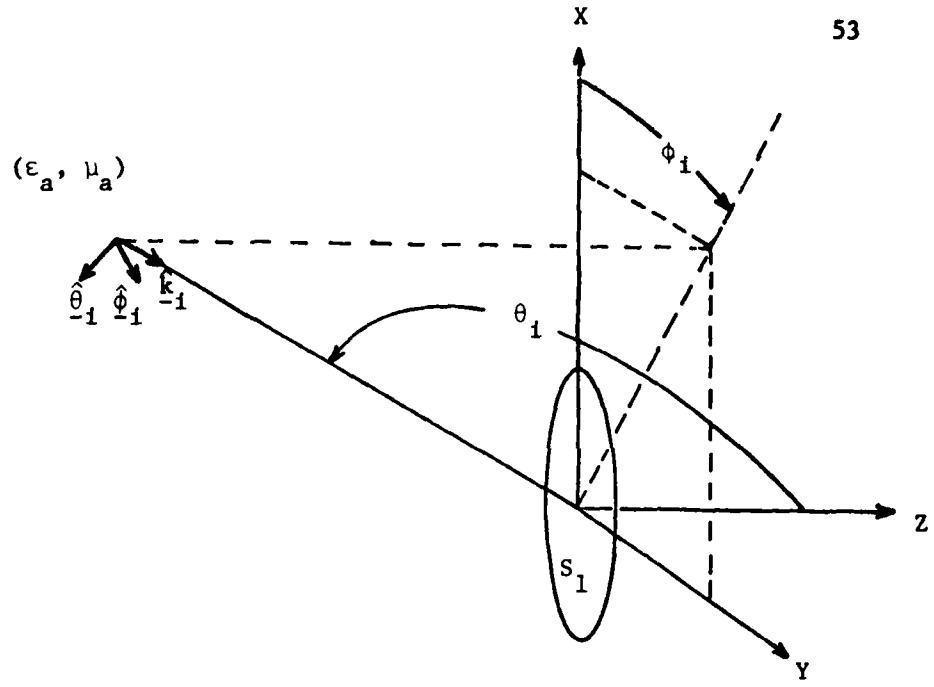

Fig. 9. Coordinates for the incident wave.

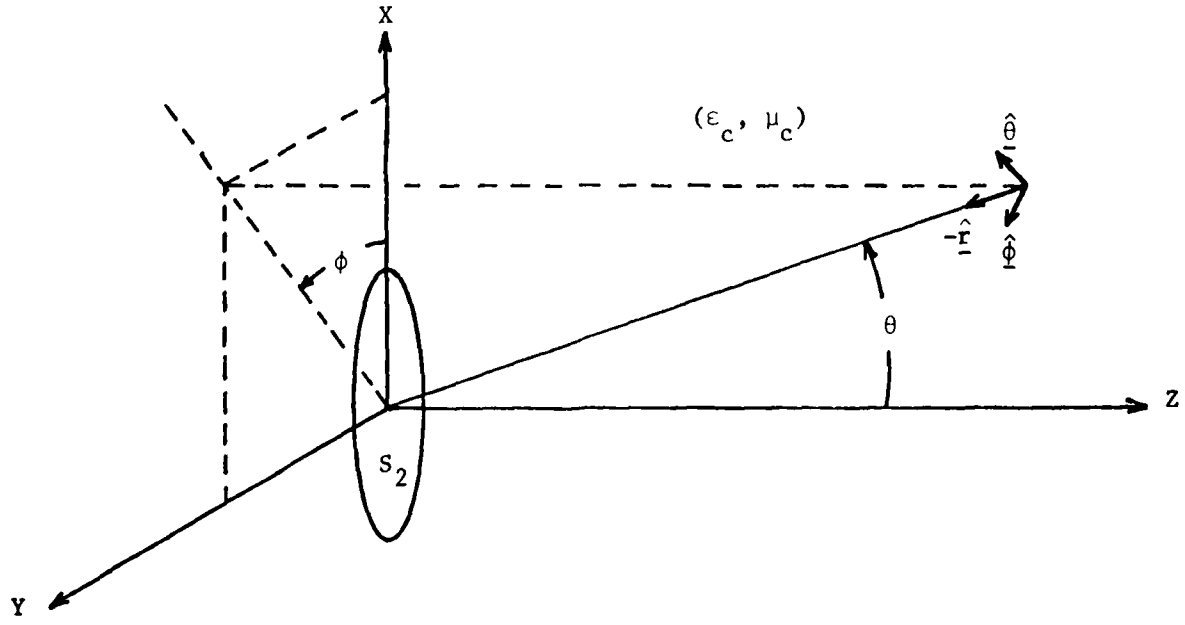

Fig. 10. Coordinates for the transmitted far field.

where the elements of the column matrices, $\bar{R}$'s, are defined as

$$R_{nj}^{t\theta} = j^{n+1} \pi k_a \cos\theta_i \int_{t_{N_2}}^{t_{N_3}} T_{j+N_2-1}(t)[J_{n+1}(k_a\rho \sin\theta_i) - J_{n-1}(k_a\rho \sin\theta_i)] \sin\nu \, dt$$

$$R_{nj}^{\phi\theta} = - j^n \pi \, k_a \cos\theta_i \int_{t_{N_2}}^{t_{N_3}} \frac{P_{j+N_2-1}(t)}{\rho^+_{j+N_2-1}} [J_{n+1}(k_a\rho \sin\theta_i) + J_{n-1}(k_a\rho \sin\theta_i)] \rho \, dt$$

$$R_{nj}^{t\phi} = j^n \pi k_a \int_{t_{N_2}}^{t_{N_3}} T_{j+N_2-1}(t) [J_{n+1}(k_a\rho \sin\theta_i) + J_{n-1}(k_a\rho \sin\theta_i)] \sin\nu \, dt$$

$$R_{nj}^{\phi\phi} = j^{n+1} \pi \, k_a \int_{t_{N_2}}^{t_{N_3}} \frac{P_{j+n_2-1}(t)}{\rho^+_{j+N_2-1}} [J_{n+1}(k_a\rho \sin\theta_i) - J_{n-1}(k_a\rho \sin\theta_i)] \rho \, dt \qquad (3\text{-}55)$$

The J_n's denote the Bessel functions of the first kind. The definition of the $\bar{R}$'s is to link quantities in this work to those in [21].

Next, we consider the far field pattern on the transmitted side. From the equivalent situation discussed in section 2.2., we know that the far field is due to $2\underline{M}_2$ in S_2, radiated into the unbounded medium (ε_c, μ_c). By reciprocity, we have

$$\underline{E}_c \cdot I\hat{\underline{\ell}} = \int_{S_2} L_c^h(I\hat{\underline{\ell}}) \cdot 2\underline{M}_2(\underline{r}')da' \tag{3-56}$$

where $I\hat{\underline{\ell}}$ is an electric dipole situated at the point (r,θ,ϕ) distant from the aperture in region C. $\hat{\underline{\ell}}$ is either $\hat{\underline{\theta}}$ or $\hat{\underline{\phi}}$ since it is along the directions of these two unit vectors that the far field is to be computed. This situation is shown in Fig. 10. Notice that we have moved the origin to the center of S_2 for convenience. Since either $\hat{\underline{\theta}}$ or $\hat{\underline{\phi}}$ is tangential to the radiation sphere of $I\hat{\underline{\ell}}$ in the vicinity of S_2, we can write

$$L_c^h(I\hat{\underline{\ell}}) = \frac{jk_c(\hat{\underline{r}} \times I\hat{\underline{\ell}})\, e^{-jk_c r}}{4\pi r} e^{j\hat{\underline{r}} \cdot \underline{r}'} \qquad \ell = \theta,\phi \tag{3-57}$$

From (2-62b) and (2-62c), we obtain

$$\underline{M}_p = \sum_{n=-\infty}^{\infty} [M_{pt}^n \underline{\hat{t}} + M_{p\phi}^n \hat{\underline{\phi}}] e^{jn\phi} \qquad p = 1,2 \tag{3-58}$$

Substituting (3-57), (3-58) and (3-15) into (3-56), we obtain

$$\underline{E}_{cr} \cdot \hat{\underline{\ell}} = E_{cr}^{\ell}$$

$$= \frac{jk_c e^{-jk_c r}}{2\pi r} \sum_{n=-\infty}^{\infty} \Bigg\{ \sum_{j=1}^{N_1-2} V_{2tj}^n \int_{t_1}^{t_{N_1}} dt' T_j(t') \int_0^{2\pi} d\phi' \underline{\hat{t}}' \cdot (\hat{\underline{r}} \times \hat{\underline{\ell}}) e^{j\hat{\underline{r}} \cdot \underline{r}' + jn\phi}$$

$$+ \sum_{j=1}^{N_1-1} V_{2\phi j}^n \int_{t_1}^{t_{N_1}} dt' \rho_j^+ \frac{P_j(t')}{\rho_j^+} \int_0^{2\pi} d\phi' (\hat{\underline{\phi}}' \cdot \hat{\underline{r}} \times \hat{\underline{\ell}}) e^{-j\hat{\underline{r}} \cdot \underline{r}' + jn\phi} \Bigg] \tag{3-59}$$

Here the extra subscript r denotes radiation field and the superscript ℓ denotes the component (θ or ϕ) of the field. The integrals in (3-59) are very similar to those in (3-53). It is not difficult to find that

$$\begin{bmatrix} E^{\theta}_{cr} \\ \\ E^{\phi}_{cr} \end{bmatrix} = \frac{-jk_c\, e^{-jk_c r}}{2\pi r} \sum_{n=-\infty}^{\infty} e^{jn\phi} \begin{bmatrix} -\tilde{\bar{R}}^{t\phi}_{n} & -\tilde{\bar{R}}^{\phi\phi}_{n} \\ \\ \tilde{\bar{R}}^{t\theta}_{n} & \tilde{\bar{R}}^{\phi\theta}_{n} \end{bmatrix} \begin{bmatrix} \bar{V}^{n}_{2t} \\ \\ \bar{V}^{n}_{2\phi} \end{bmatrix}$$

where the $\tilde{\bar{R}}$'s are the transpose of the $\bar{R}$'s defined as in (3-55) with $(k_a, \theta_i, t_{N_2}, t_{N_3})$ changed to $(k_c, \theta, t_1, t_{N_1})$ and the subscript $j+N_2-1$ on T, P and ρ^+ changed to j. The lengths of the matrices also change from m_{1t}, $m_{1\phi}$ to m_{2t} and $m_{2\phi}$ accordingly. Note sin ν is -1 in S_1 and is 1 in S_2.

It is appropriate to discuss the symmetry with respect to n at this time. From (3-56) it is apparent that

$$\begin{bmatrix} \bar{R}^{t\theta}_{-n} & \bar{R}^{t\phi}_{-n} \\ \\ \bar{R}^{\phi\theta}_{-n} & \bar{R}^{\phi\phi}_{-n} \end{bmatrix} = \begin{bmatrix} \bar{R}^{t\theta}_{n} & -\bar{R}^{t\phi}_{n} \\ \\ -\bar{R}^{\phi\theta}_{n} & \bar{R}^{\phi\phi}_{n} \end{bmatrix} \tag{3-61}$$

From (3-19) to (3-23) and (2-67) to (2-73), we find

$$\begin{bmatrix} Z^{\alpha,-n}_{tt} & Z^{\alpha,-n}_{t\phi} \\ \\ Z^{\alpha,-n}_{\phi t} & Z^{\alpha,-n}_{\phi\phi} \end{bmatrix} = \begin{bmatrix} Z^{\alpha n}_{tt} & -Z^{\alpha n}_{t\phi} \\ \\ -Z^{\alpha n}_{\phi t} & Z^{\alpha n}_{\phi\phi} \end{bmatrix} \tag{3-62}$$

$$\alpha = a,b,c$$

and

$$\begin{bmatrix} Y_{tt}^{jb,-n} & Y_{t\phi}^{jb,-n} \\ Y_{\phi t}^{jb,-n} & Y_{\phi\phi}^{jb,-n} \end{bmatrix} = \begin{bmatrix} -Y_{tt}^{jbn} & Y_{t\phi}^{jbn} \\ Y_{\phi t}^{jbn} & -Y_{\phi\phi}^{jbn} \end{bmatrix} \qquad j = 1,2 \qquad (3\text{-}63)$$

The elements of the U's do not depend on n, as shown in (3-24) and (3-25). Therefore, from (3-54) and the above discussion, we find

$$\begin{aligned} \bar{V}_{jt}^{-n\theta} &= -\bar{V}_{jt}^{n\theta}, \quad \bar{V}_{jt}^{-n\phi} = \bar{V}_{jt}^{n\phi} \qquad j = 1,2 \\ \bar{V}_{jt}^{-n\theta} &= \bar{V}_{j\phi}^{n\theta}, \quad \bar{V}_{j\phi}^{-n\phi} = -\bar{V}_{jt}^{n\phi} \qquad j = 1,2 \qquad (3\text{-}64) \\ \bar{I}_{t}^{-n\theta} &= \bar{I}_{t}^{n\theta}, \quad \bar{I}_{t}^{-n\phi} = -\bar{I}_{t}^{n\phi} \\ \bar{I}_{\phi}^{-n\theta} &= -\bar{I}_{\phi}^{n\theta}, \quad \bar{I}_{\phi}^{-n\phi} = \bar{I}_{\phi}^{n\phi} \end{aligned}$$

Here the extra superscripts θ and ϕ denote the solution of (3-18) for the particular polarization of the incidence. From (3-14), (3-15), (3-58) and (3-64), we obtain

$$M_{1t}^{\theta}\Big|_{t=t_{i+N_2}} = 2j \sum_{n=1}^{\infty} \frac{V_{1ti}^{n\theta}}{\rho_{i+N_2}} \sin n\phi \qquad i=1,2,\ldots,m_{1t}$$

$$M_{1\phi}^{\theta}\Big|_{t=t_{i+N_2-1}^{+}} = \frac{V_{1\phi i}^{o\theta}}{\rho_{i+N_2-1}^{+}} + 2 \sum_{n=1}^{\infty} \frac{V_{1\phi i}^{n\theta}}{\rho_{i+N_2-1}^{+}} \cos n\phi \qquad i=1,2,\ldots,m_{1\phi}$$

$$M_{2t}^{\theta}\Big|_{t=t_{i+1}} = 2j \sum_{n=1}^{\infty} \frac{V_{2ti}^{n\theta}}{\rho_{i+1}} \sin n\phi \qquad i=1,2,\ldots,m_{2t}$$

$$M^{\theta}_{2\phi}\Big|_{t=t^{+}_{i}} = \frac{V^{o\theta}_{2\phi i}}{\rho^{+}_{i}} + 2\sum_{n=1}^{\infty}\frac{V^{n\theta}_{2\phi i}}{\rho^{+}_{i}}\cos n\phi \qquad i = 1,2,\ldots,m_{2\phi}$$

$$M^{\phi}_{1t}\Big|_{t=t_{i+N_2}} = \frac{V^{o\phi}_{1ti}}{\rho_{i+N_2}} + 2\sum_{n=1}^{\infty}\frac{V^{o\phi}_{1ti}}{\rho_{i+N_2}}\cos n\phi \qquad i = 1,2,\ldots,m_{1t}$$

$$M^{\phi}_{1\phi}\Big|_{t=t^{+}_{i+N_2-1}} = 2j\sum_{n=1}^{\infty}\frac{V^{n\phi}_{1\phi i}}{\rho^{+}_{i+N_2-1}}\sin n\phi \qquad i = 1,2,\ldots,m_{1\phi}$$

$$M^{\phi}_{2t}\Big|_{t=t_{i+1}} = \frac{V^{o\phi}_{2ti}}{\rho_{i+1}} + 2\sum_{n=1}^{\infty}\frac{V^{n\phi}_{2ti}}{\rho_{i+1}}\cos n\phi \qquad i = 1,2,\ldots,m_{2t}$$

$$M^{\phi}_{2\phi}\Big|_{t=t^{+}_{i}} = 2j\sum_{n=1}^{\infty}\frac{V^{n\phi}_{2\phi i}}{\rho^{+}_{i}}\sin n\phi \qquad i=1,2,\ldots,M_{2\phi} \quad (3\text{-}65)$$

The extra superscript on M's again denotes the polarization of the incident wave. The electric current $\underline{J}$ exhibits similar behavior. J^{θ}_{t} and J^{θ}_{ϕ} have the same angular behavior in each mode as that of M^{ϕ}_{1t} and $M^{\phi}_{1\phi}$. J^{ϕ}_{t} and J^{ϕ}_{ϕ} have the same angular behavior in each mode as that of M^{θ}_{1t} and $M^{\theta}_{1\phi}$:

$$\eta_b J^{\theta}_{t}\Big|_{t=t_{i+1}} = \frac{I^{o\theta}_{ti}}{\rho_{i+1}} + 2\sum_{n=1}^{\infty}\frac{I^{n\theta}_{ti}}{\rho_{i+1}}\cos n\phi \qquad i = 1,2,\ldots, N_t$$

$$\eta_b J^{\theta}_{\phi}\Big|_{t=t^{+}_{i}} = 2j\sum_{n=1}^{\infty}\frac{I^{n\theta}_{\phi i}}{\rho^{+}_{i}}\sin n\phi \qquad i = 1,2,\ldots,N_{\phi}$$

$$\eta_b J_t^{\phi}\Big|_{t=t_{i+1}} = 2j \sum_{n=1}^{\infty} \frac{I_{ti}^{n\phi}}{\rho_{i+1}} \sin n\phi \qquad i = 1,2,\ldots,N_t$$

$$\eta_b J_{\phi}^{\phi}\Big|_{t=t_i^+} = \frac{\bar{I}_{\phi}^{o\phi}}{\rho_i^+} + 2 \sum_{n=1}^{\infty} \frac{I_{\phi i}^{n\phi}}{\rho_i^+} \cos n\phi \qquad i = 1,2,\ldots,N_{\phi} \tag{3-66}$$

From (3-60) and (3-64), we obtain

$$\begin{bmatrix} E_{cr}^{\theta\theta} & E_{cr}^{\theta\phi} \\ E_{cr}^{\phi\theta} & E_{cr}^{\phi\phi} \end{bmatrix} = \frac{-jk_c e^{-jk_c r}}{2\pi r} \begin{bmatrix} -\tilde{\bar{R}}_o^{\phi\phi} \bar{V}_{2\phi}^{o\theta} & 0 \\ 0 & \tilde{\bar{R}}_o^{t\theta} \bar{V}_{2t}^{o\phi} \end{bmatrix}$$

$$+ 2 \sum_{n=1}^{\infty} \begin{bmatrix} \cos n\phi & 0 \\ 0 & j \sin n\phi \end{bmatrix} \begin{bmatrix} -\tilde{\bar{R}}_n^{t\phi} & -\tilde{\bar{R}}_n^{\phi\phi} \\ \tilde{\bar{R}}_n^{t\theta} & \tilde{\bar{R}}_n^{\phi\theta} \end{bmatrix} \begin{bmatrix} \bar{V}_{2t}^{n\theta} & 0 \\ \bar{V}_{2\phi}^{n\theta} & 0 \end{bmatrix}$$

$$+ 2 \sum_{n=1}^{\infty} \begin{bmatrix} j \sin n\phi & 0 \\ 0 & \cos n\phi \end{bmatrix} \begin{bmatrix} -\tilde{\bar{R}}^{t\phi} & -\tilde{\bar{R}}^{\phi\phi} \\ \tilde{\bar{R}}^{t\theta} & \tilde{\bar{R}}^{\phi\theta} \end{bmatrix} \begin{bmatrix} 0 & \bar{V}_{2t}^{n\phi} \\ 0 & \bar{V}_{2\phi}^{n\phi} \end{bmatrix} \tag{3-67}$$

The first superscript of E_{cr} denotes the component of the far field and the second superscript denotes the polarization of the incidence.

Chapter 4

EQUIVALENT CIRCUIT AND LOW FREQUENCY APPROXIMATION OF THE NARROW ANNULAR SLOT

In this chapter, the narrow annular slot shown in Fig. 11 is considered. Now region b inside the thick screen is a coaxial region. For simplicity, regions a and c are assumed to be air filled with $k_a = k_c = k_o$ and $\eta_a = \eta_c = \eta_o$. The word "narrow" means the following:

$$k_o w << 1 \quad , \quad k_b w << 1 \tag{4-1}$$

$$w << R_a \qquad (\gamma \cong 1) \tag{4-2}$$

where w and R_a are the width and the mean radius of the slot.

$$w = R_{out} - R_{in} \tag{4-3}$$

$$R_a = \frac{1}{2}(R_{out} + R_{in}) \tag{4-4}$$

The thickness of the screen, d, is assumed to be finite. The power through any cross section of the coaxial region is the sum of the powers associated with each coaxial mode. This is due to the orthogonality relationship among the modes. Under condition (4-2), x_{nm} and x'_{nm} defined in (2-26) can be approximated by [22, 23]:

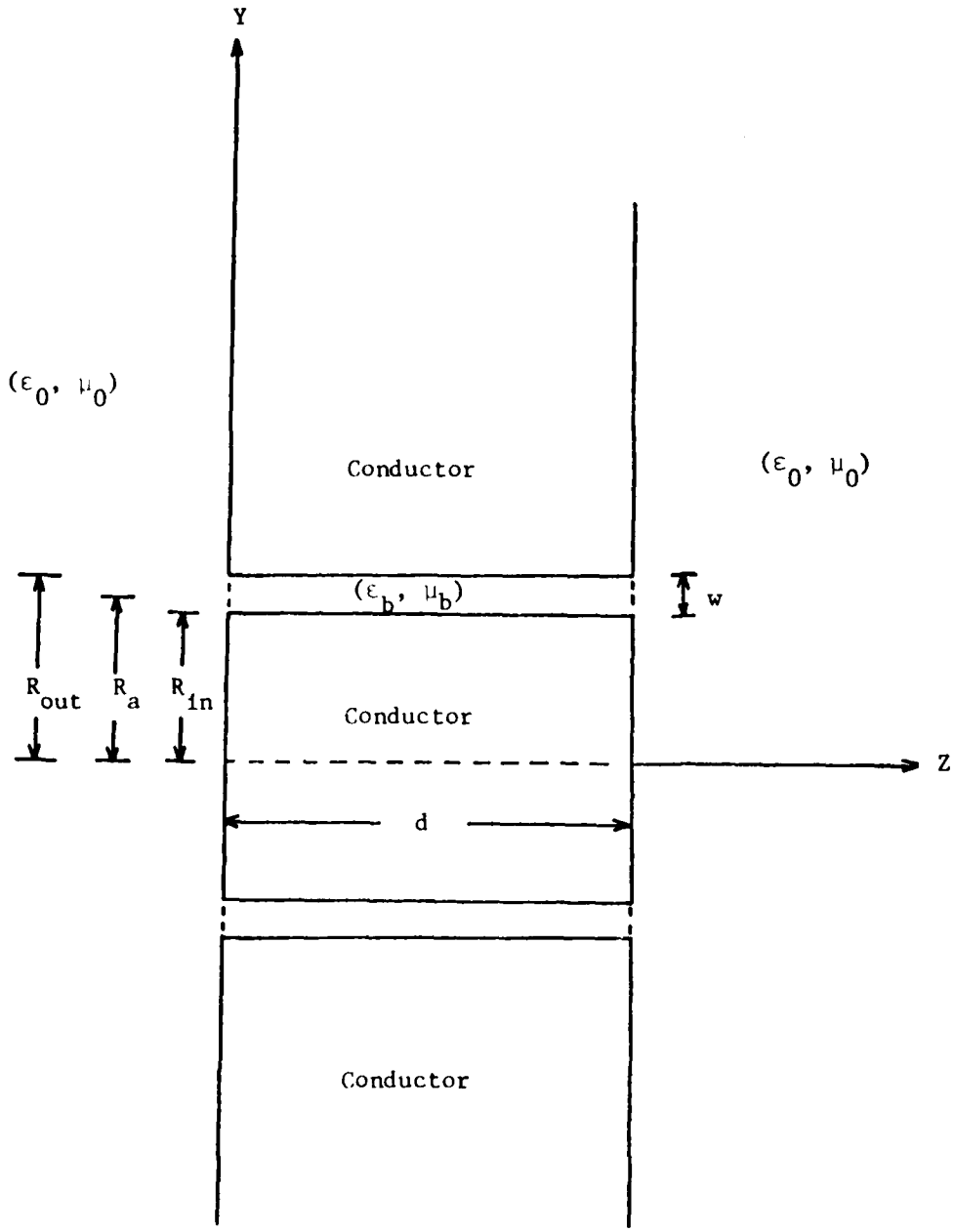

Fig. 11. A narrow annular slot in a thick screen, cross section in the y-z plane.

$$
\begin{aligned}
x_{nm} &= \frac{m\pi}{(1-\gamma)} && n = 0,1,2,\ldots \\
& && m = 1,2,\ldots \\
x'_{om} &= \frac{m\pi}{(1-\gamma)} && m = 1,2,\ldots, \\
x'_{n,m+1} &= \frac{m\pi}{(1-\gamma)} && n = 1,2,\ldots \\
& && m = 1,2,\ldots \\
x'_{n1} &= n && n = 1,2,\ldots
\end{aligned} \tag{4-5}
$$

It is then straightforward to see that if (4-1) and (4-2) are true, and if

$$k_b R_{out} < x'_{11} \cong 1 , \tag{4-6}$$

then the TEM mode is the only mode that propagates. Therefore, the power associated with the TEM mode is of special interest since, when (4-6) is true, it can be responsible for most of the power transmitted.

In the following sections, we develop an equivalent circuit for the problem based on the analysis of the TEM mode. Resonant behavior of the power transmission is observed and the electric polarizability is discussed for a small and narrow annular slot in the thick screen.

4.1. Equivalent Circuit

The time averaged power transmitted through the aperture, denoted P_{trans}, can be obtained by integrating the complex Poynting ector over the aperture surface S_2. Therefore, we have

$$P_{trans} = \mathrm{Re} \int_{S_2} \underline{E}_b \cdot \underline{H}_b^* \cdot \hat{\underline{z}}\, da = - \mathrm{Re} \int_{S_2} \underline{M}_2 \cdot \underline{H}_b^* da \tag{4-7}$$

Substituting (2-43) into 4-7) and retaining only the contribution from the TEM mode, we obtain

$$P^{o}_{trans} = - \mathrm{Re}(V_2 \; I_2^{*}) \tag{4-8}$$

where the superscript "o" denotes the contribution from the TEM mode, and the quantities on the right hand side of (4-8) are defined in the following:

$$I_2 = -\frac{j}{\eta_b}\csc\,(k_b d)V_1 - \frac{j}{\eta_b}\cot\,(k_b d)V_2 \tag{4-9}$$

$$V_j = \sqrt{2\pi}\;(\underline{h}^{TEM},\, \underline{M}^{o}_{j}) = \sqrt{\frac{2\pi}{-\ln\gamma}}\int_{R_{in}}^{R_{out}} M^{o}_{j\phi}\,d\rho \qquad j = 1,2 \tag{4-10}$$

Equations (4-9) and (4-10) define three of the four parameters of a two-port network that we introduce later. The fourth is defined as

$$I_1 = -\frac{j}{\eta_b}\cot\,(k_b d)V_1 - \frac{j}{\eta_b}\csc\,(k_b d)V_2 \tag{4-11}$$

We now proceed to develop the equivalent circuit of the problem, starting with the operator equations (2-79) and (2-80). Substituting (2-65), (2-67a) to (2-67d) and (2-75) into (2-79) and 2-80) for n = 0, and separating the the ϕ and t components, we obtain, for the ϕ-component,

$$\frac{jk_o\hat{\phi}}{\pi\eta_o}\int_{R_{in}}^{R_{out}} d\rho'\rho' M^{o}_{1\phi}(\rho')\int_{0}^{\pi}\frac{\cos\phi e^{-jk_o R}}{R}\,d\phi - \frac{j}{\sqrt{2\pi}\,\eta_b}\,[\cot(k_b d)V_1 + \csc(k_b d)V_2]\underline{h}^{TEM}$$

$$-j\sum_{m=1}^{\infty} Y_{om}[\cot(k_{om}d)(\underline{h}^{m}_{om},\underline{M}^{o}_{1}) + \csc(k_{om}d)(\underline{h}^{m}_{om},\underline{M}^{o}_{2})]\underline{h}^{m}_{om}$$

$$= ?H^{o}_{i\phi}\hat{\phi} \tag{4-12}$$

$$\frac{jk_o\hat{\phi}}{\pi\eta_o}\int_{R_{in}}^{R_{out}} d\rho'\rho' M_{2\phi}^{o}(\rho')\int_0^{\pi}\frac{\cos\phi e^{-jk_oR}}{R}d\phi - \frac{j}{\sqrt{2\pi}\,\eta_b}[\csc(k_bd)V_1+\cot(k_bd)V_2]\underline{h}^{TEM}$$

$$-j\sum_{m=1}^{\infty} Y_{om}[\csc(k_{om}^m d)(\underline{h}_{om}^m, \underline{M}_1^o) + \cot(k_{om}^m d)(\underline{h}_{om}^m, \underline{M}_1^o)]\underline{h}_{om}^m$$

$$= 0 \qquad (4\text{-}13)$$

where

$$R = \sqrt{\rho^2 + \rho'^2 - 2\rho\rho'\cos\phi} \qquad (4\text{-}14)$$

Note that for n = 0, the TM modes have only the ϕ-component and the TE modes have only the ρ-component. Next, we equate the inner products of $\underline{h}^{TEM}$ with each side of (4-12) and (4-13). The result is

$$\frac{\sqrt{2}\,jk_o^2}{\sqrt{-\pi\ln\gamma}\,\eta_o}\int_{R_{in}}^{R_{out}} d\rho\int_{R_{in}}^{R_{out}} g_1\, M_{1\phi}^{o}(\rho')\rho' d\rho'$$

$$-\frac{j}{\eta_b}[\cot(k_bd)V_1 + \csc(k_bd)V_2] = \frac{2\sqrt{2\pi}}{\sqrt{-\ln\gamma}}\int_{R_{in}}^{R_{out}} H_{i\phi}^{o}(\rho)d\rho \qquad (4\text{-}15)$$

$$\frac{\sqrt{2}\,jk_o^2}{\sqrt{-\pi\ln\gamma}\,\eta_o}\int_{R_{in}}^{R_{out}} d\rho\int_{R_{in}}^{R_{out}} g_1\, M_{2\phi}^{o}(\rho')\rho' d\rho'$$

$$-\frac{j}{\eta_b}[\csc(k_bd)V_1 + \cot(k_bd)V_2] = 0 \qquad (4\text{-}16)$$

where

$$g_1 = \int_0^{\pi}\frac{\cos\phi\, e^{-jk_oR}}{k_oR}d\phi \qquad (4\text{-}17)$$

and is the same as defined in (2-69). Under the condition (4-2), g_1 can be written as

$$g_1 \cong -\frac{1}{k_o R_a}\left\{\left[\ln\frac{e^2|\rho-\rho'|}{8R_a}-\frac{\pi}{2}\int_0^{2k_oR_a}E_2(x)dx\right]+\frac{j\pi}{2}\int_0^{2k_oR_a}J_2(x)dx\right\} \tag{4-18}$$

where J_2 and E_2 are the Bessel and Weber functions of the second order. The proof of (4-18) is given in Appendix A. Substituting (4-18) into (4-15) and (4-16) and using the approximation $\rho' \cong R_a$, we obtain

$$\frac{k_o w}{\eta_o}\left\{\left[\frac{1}{2}\int_0^{2k_oR_a}J_2(x)dx+\frac{j}{2}\int_0^{2k_oR_a}E_2(x)dx\right]V_1-\frac{j\sqrt{2\pi}}{\pi w\sqrt{-\ln\gamma}}\int_{R_{in}}^{R_{out}}d\rho\int_{R_{in}}^{R_{out}}\ln\left(\frac{e^2|\rho-\rho'|}{8R_a}\right)M_{1\phi}^o(\rho')d\rho'\right\}$$

$$-\frac{j}{\eta_b}\left[\cot(k_bd)V_1+\csc(k_bd)V_2\right]=\frac{2\sqrt{2\pi}}{\sqrt{-\ln\gamma}}\int_{R_{in}}^{R_{out}}H_{i\phi}^o(\rho)d\rho \tag{4-19}$$

$$\frac{k_o w}{\eta_o}\left\{\left[\frac{1}{2}\int_0^{2k_oR_a}J_2(x)dx+\frac{j}{2}\int_0^{2k_oR_a}E_2(x)dx\right]V_2-\frac{j\sqrt{2\pi}}{\pi w\sqrt{-\ln\gamma}}\int_{R_{in}}^{R_{out}}d\rho\int_{R_{in}}^{R_{out}}\ln\left(\frac{e^2|\rho-\rho'|}{8R_a}\right)M_{2\phi}^o(\rho')d\rho'\right\}$$

$$-\frac{j}{\eta_b}\left[\csc(k_bd)V_1+\cot(k_bd)V_2\right]=0 \tag{4-20}$$

We now examine the double integral in (4-19). Changing the order of integration, we obtain

$$\int_{R_{in}}^{R_{out}} d\rho \int_{R_{in}}^{R_{out}} M_{1\phi}^{o}(\rho')\ln\left(\frac{e^2|\rho-\rho'|}{8R_a}\right)d\rho' = \int_{R_{in}}^{R_{out}} M_{1\phi}^{o}(\rho')f(\rho')d\rho' \quad (4\text{-}21)$$

where

$$f(\rho') = \int_{R_{in}}^{R_{out}} \ln\left(\frac{e^2|\rho-\rho'|}{8R_a}\right)d\rho$$

$$= w \ln\frac{e^2}{8R_a} - w + (R_{out} - \rho')\ln(R_{out} - \rho') + (\rho' - R_{in})\ln(\rho' - R_{in}) \quad (4\text{-}22)$$

$f(\rho')$ is an even function about $\rho' = R_a$ and has its minimum value $f_{min} = (w \ln\frac{e^2 w}{8R_a} - w)$ occurring at $\rho' = R_{in}$ and $\rho' = R_{out}$. Its maximum value $f_{max} = (w \ln\frac{e^2 w}{16R_a} - w)$ occurs at $\rho' = R_a$. When $w << R_a$, $f(\rho')$ is almost constant. Therefore, the value of the double integral in (4-21) is essentially proportional to the integral of $M_{1\phi}^{o}$, i.e., V_1, and is insensitive with respect to the actual functional form of $M_{1\phi}^{o}(\rho')$. Various values can be obtained for this integral by assuming different functional forms for $M_{1\phi}^{o}(\rho')$. They converge to the same value as the ratio $\frac{w}{R_a}$ becomes very small. The same argument is valid for the double integral involving $M_{2\phi}^{o}$ in (4-20). Equations (4-19) and (4-20) are now written in the following form:

$$Y^{hs}V_1 + Y_{11}^{b}V_1 + Y_{12}^{b}V_2 = I_s \quad (4\text{-}23)$$

$$Y^{hs}V_2 + Y_{21}^{b}V_1 + Y_{22}^{b}V_2 = 0 \quad (4\text{-}24)$$

where

$$\begin{bmatrix} Y_{11}^b & Y_{12}^n \\ Y_{21}^b & Y_{22}^b \end{bmatrix} = \begin{bmatrix} -\frac{j}{\eta_b}\cot k_b d & -\frac{j}{\eta_b}\csc k_b d \\ -\frac{j}{\eta_b}\csc k_b d & -\frac{j}{\eta_b}\cot k_b d \end{bmatrix} \tag{4-25}$$

$$Y^{hs} = G + jB \tag{4-26}$$

$$G = \frac{k_o w}{2\eta_o} \int_0^{2k_o R_a} J_2(x)dx \tag{4-27}$$

$$B = \frac{k_o w}{\eta_o}\left\{\frac{1}{2}\int_0^{2k_o R_a} E_2(x)dx - \frac{\int_{R_{in}}^{R_{out}} M_{trial}(\rho')f(\rho')d\rho'}{\pi w \int_{R_{in}}^{R_{out}} M_{trial}(\rho')d\rho'}\right\} \tag{4-28}$$

$$I_s = \frac{2\sqrt{2\pi}}{\sqrt{-\ln\gamma}} \int_{R_{in}}^{R_{out}} H_{i\phi}^o(\rho)d\rho \tag{4-29}$$

In (4-28), M_{trial} represents any particular functional form that we choose for $M_{1\phi}^o$ and $M_{2\phi}^o$. If we choose to use a constant, we obtain

$$B = \frac{k_o w}{\eta_o}\left\{\frac{1}{2}\int_0^{2k_o R_a} E_2(x)dx - \frac{1}{\pi}\ln\left(\frac{e^{1/2}w}{8R_a}\right)\right\} \tag{4-30}$$

If we choose to use for M_{trial} the quasistatic solution for a narrow annular slot in a infinitely thin screen [24], then

$$M_{trial}(\rho) \propto \frac{1}{\sqrt{(\frac{w}{2})^2 - (\rho - R_a)^2}} \tag{4-31}$$

and the result is

$$B = \frac{k_o w}{\eta_o}\left\{ \frac{1}{2} \int_0^{2k_o R_a} E_2(x)dx - \frac{1}{\pi} \ln (\frac{e^2 w}{32R_a})\right\} \tag{4-32}$$

Equations (4-23) and (4-24) can be viewed as the equations for the equivalent circuit shown in Fig. 12. This equivalent circuit can be used to analyze the TEM mode as long as (4-2) holds. The current source can be computed for plane wave incidence:

$$\underline{H}_i = \frac{-E_o^{\theta}}{\eta_o} \hat{\underline{\phi}}_i \, e^{-j\underline{k}_i \cdot \underline{r}} \tag{4-33}$$

Note that (4-33) represents the θ-polarized plane wave defined in (3-50), since a ϕ-polarized plane wave does not excite the TEM mode. Substituting (4-33) and (2-81) into (4-29) and using the condition (4-1), we obtain

$$I^s = \frac{-\, j\, 2\sqrt{2\pi}\, w\, E_o^{\theta}\, J_1(k_o R_a \sin\theta_i)}{\eta_o \sqrt{-\ln\gamma}} \tag{4-34}$$

In the above analysis we have assumed $\sin k_b d \neq 0$. This is evident because, when deriving (4-8), (4-12), and (4-13), we used (2-43) and (2-75) in the case where $\sin k_b d \neq 0$. It is not difficult to show that when $\sin k_b d = 0$, we have the following equations:

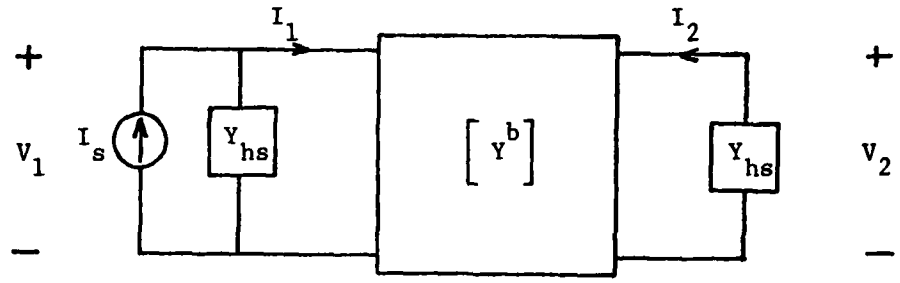

Fig. 12. Equivalent circuit for (4-23) and (4-24).

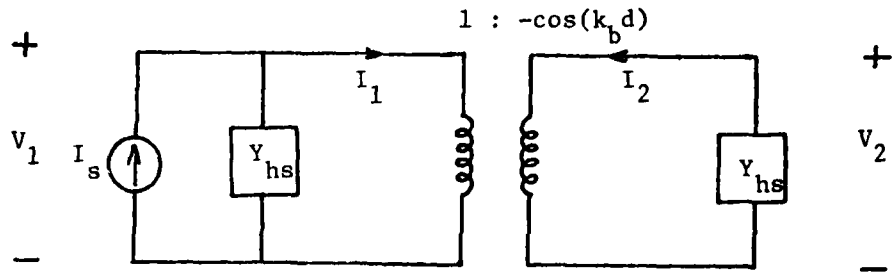

Fig. 13. Equivalent circuit for a cavity resonance case, (4-35),(4-36) and (4-37).

$$Y^{hs}V_1 + I_1^r = I_s \tag{4-35}$$

$$Y^{hs}V_2 + I_2^r = 0 \tag{4-36}$$

$$V_1 + V_2 \cos k_b d = 0 \tag{4-37}$$

where V_1 and V_2 are defined the same as in (4-10) while I_1^r and I_2^r are defined as

$$I_1^r = -\frac{j\sqrt{2\pi}}{\eta_b} C_o \tag{4-38a}$$

$$I_2^r = -\frac{j\sqrt{2\pi}\cos k_b d}{\eta_b} C_o \tag{4-38b}$$

C_o is the extra unknown constant associated with the case $\sin k_b d = 0$, introduced in Chapter 2. The equivalent circuit for this case can be constructed from (4-35) to (4-37) and is shown in Fig. 13. The power transmitted can be shown to be

$$P_{trans}^{o,r} = -\mathrm{Re}(V_2\, I_2^{r*}) \tag{4-39}$$

for this case.

4.2. Power Transmission and Resonant Behavior

The equivalent circuit shown in Fig. 12 is very similar to that of a narrow TE slot in a thick screen [25]. When the thickness of the screen is close to a multiple of a half wavelength, the waveguide

region can "tune" the aperture to transfer peak power. We show this by considering our equivalent circuit in Fig. 12. From the equivalent circuit, we obtain the power transmitted as

$$P^{o}_{trans} = - V_2 I_2^{*} = \left|\frac{I^{s}}{y_{12}}\right|^2 G \tag{4-40}$$

Here y_{12} is the transfer admittance defined as

$$y_{12} = \frac{I_s}{V_2} \tag{4-41}$$

and can be solved from the circuit as

$$y_{12} = - 2Y^{hs}\cos k_b d - \frac{j}{\eta_b}\left[1 + (\eta_b Y^{hs})^2\right]\sin k_b d \tag{4-42}$$

Equations (4-40) and (4-42) are valid even when $\sin k_b d$ is zero. This can be easily shown by solving the equivalent circuit in Fig. 13. Substituting (4-26), (4-27), (4-32), (4-34), and (4-42) into (4-40), we obtain

$$P^{o}_{trans} = \frac{|E^{o}_{\theta}|^2}{\eta_o} \frac{8\pi w R_a J_1^2(k_o R_a \sin\theta_i) G'}{[2G'\cos k_b d - 2G'B'\sin k_b d)]^2 + [2B'\cos k_b d + (1+G'^2-B'^2)\sin k_b d]^2} \tag{4-43}$$

where

$$G' = \eta_o G = \frac{k_o w}{2}\int_0^{2k_o R_a} J_2(x)dx \tag{4-44}$$

$$B' = \eta_o B = \frac{k_o w}{2}\left\{\int_0^{2k_o R_a} F_2(x)dx + \frac{2}{\pi}\left[\ln\frac{16(1+\gamma)}{(1-\gamma)} - 2\right]\right\} \tag{4-45}$$

For a finite $k_o R_a$, under the condition (4-1), we see from (4-44) and (4-45) that

$$G' \ll 1 , \quad B' \ll 1 \tag{4-46}$$

With (4-46) in mind, we see from (4-43) that, when sin $k_b d$ is not small, P^o_{trans} is approximately proportional to $\csc^2 k_b d$ and has its minimum in the neighborhood of $d = (\frac{n}{2} + \frac{1}{4})\lambda_b$. Furthermore, P^o_{trans} is large in the neighborhood of $d = \frac{n}{2}\lambda_b$. Looking at the denominator of P^o_{trans} in (4-23), we see that when $k_b d \cong n\pi$, the first term of the two is very insensitive to a small change in $k_b d$ and has the approximate value of $4G'^2$. The second term however, is very sensitive to a change in $k_b d$, and can be made zero by precisely choosing our $k_b d$. Therefore, the maximum of P^o_{trans} occurs when

$$\tan k_b d = - \frac{2B'}{(1 + G'^2 - B'^2)} \tag{4-47}$$

Equation (4-47) is our condition for "slot resonance" described above. Since B' is small, a first approximation of the solution of (4-47) is

$$d^{res} = (\frac{n}{2} - \frac{B'}{\pi})\lambda_b \tag{4-48}$$

The peak value of P^o_{trans} can be found by substituting (4-47) into (4-43). The result, after proper approximation, is

$$P^{o,res}_{trans} = \frac{|E^o_\theta|^2 \, 2\pi \, w \, R_a J_1^2(k_o R_a \sin \theta_i)}{\eta_o G'} \tag{4-49}$$

The superscript "res" that appears in (4-48) and (4-49) denotes the slot resonance, and is to be distinguished from the superscript "r"

in (4-35), (4-36), (4-38), and (4-39) where it denotes the situation when sin $k_b d$ is exactly zero.

Another quantity of interest is the width of the power transmission peak just discussed. We define this peak width as the distance between the two neighboring points of d^{res} where half of the peak power is transmitted. Therefore, we solve the equation

$$P^{o}_{trans} = \frac{1}{2} P^{o,res}_{trans} \tag{4-50}$$

Substituting (4-43) and (4-49) into (4-50) and using the approximations

$$\begin{aligned} k_b d &= k_b d^{res} + \delta \\ \cos k_b d &= (-1)^n \\ \sin k_b d &= (-1)^n(\delta - 2B') \end{aligned} \tag{4-51}$$

we obtain

$$\delta = \pm 2G' \tag{4-52}$$

Therefore, the half peak power transmission occurs at

$$d = d^{res} \pm \frac{G'}{\pi} \lambda_b \tag{4-53}$$

and the peak width is $\frac{2G'}{\pi}\lambda_b$. Notice that, in (4-51) and (4-52), δ represents a small number and is to be distinguished from the Kronecker delta used elsewhere in this work.

The transmission coefficient T is defined as

$$T = \frac{P_{trans}}{P_{in}} \tag{4-54}$$

where P_{trans} is defined in (4-7). P_{in} is the power that would be intercepted by the aperture S_1 if the incident plane wave were normal. Therefore,

$$P_{in} = \frac{2\pi\, w\, R_a\, |E^o|^2}{\eta_o} \tag{4-55}$$

where E^o is the magnitude of the incident electric field of the general plane wave of the form

$$\underline{E}_i = (E_o^{\theta}\hat{\underline{\theta}}_i + E_o^{\phi}\hat{\underline{\phi}}_i)\, e^{-j\underline{k}_i\cdot\underline{r}} \tag{4-56}$$

For the problem discussed in this chapter, if (4-6) is valid, we have

$$P_{trans} \cong P^o_{trans} \tag{4-57}$$

Substituting (4-43), (4-55), and (4-57) into (4-54), we obtain

$$T = \frac{|E_\theta^o|^2\, 4G' J_1^2(k_o R_a \sin\theta_i)}{|E^o|^2\, [2G'\cos k_b d - 2G'B'\sin k_b d]^2 + [2B'\cos k_b d + (1+G'^2-B'^2)\sin k_b d]^2} \tag{4-58}$$

Similarly, if (4-49) is used instead of (4-43), we obtain, for the slot resonance,

$$T^{res} = \frac{|E_\theta^o|^2\, J_1^2(k_o R_a \sin\theta_i)}{|E^o|^2 G'} \tag{4-59}$$

4.3. Small Apertures and the Electric Polarizability

If in addition to the conditions (4-1) and (4-2), we assume that the overall size of the aperture is small, i.e.,

$$k_o R_a << 1 \tag{4-60}$$

then some of the formulas in the previous sections can be simplified. These formulas are written below without detailed justification because they involve mostly simple small argument approximations of related functions.

$$G' = \eta_o G = \frac{1}{6} (k_o w) (k_o R_a)^3 \tag{4-61}$$

$$B' = \eta_o B = \frac{k_o w}{\pi} \ln \left(\frac{32R_a}{e^2 w}\right) \tag{4-62}$$

$$I_s = j \sqrt{\frac{2\pi}{-\ln\gamma}} \frac{k_o R_a w E_{iz}(0)}{\eta_o} \tag{4-63}$$

$$P_{trans} = TP_{in} = \frac{\pi w R_a (k_o w)(k_o R_a)^5 |E_{iz}(0)|^2}{3\eta_o \{[2G'\cos k_b d - 2G'B'\sin k_b d]^2 + [2B'\cos k_b d + (1+G'^2-B'^2)\sin k_b d]^2\}} \tag{4-64}$$

$$P_{trans}^{res} = T^{res} P_{in} = \frac{|E_{iz}(0)|^2}{\eta_o} \cdot \frac{3\lambda_o^2}{4\pi} \tag{4-65}$$

In (4-63) to (4-65), $E_{iz}(0)$ represents the z-component of the incident electric field evaluated at the aperture S_1. Also, when R_a is small, the fields in region c can be considered as due to an electric dipole $\underline{p}_e$ in S_2 in the presence of the shorted conducting screen. The dipole can be computed from the magnetic current,

$$\underline{p}_e = -\frac{\varepsilon_o}{2} \int_{S_2} \underline{r} \times \underline{M}_2 da$$

$$\simeq -\varepsilon_o R_a^2 \sqrt{\frac{-\pi \ln\gamma}{2}} V_2 \hat{\underline{z}} \tag{4-66}$$

Substituting (4-41) and (4-63) into (4-66), we obtain

$$\underline{p}_e = \varepsilon_o \alpha_e \, E_{iz}(0) \, \hat{\underline{z}} \tag{4-67}$$

where

$$\alpha_e = \frac{-j\pi \, k \, R_a^3}{\eta_o \, y_{12}} \tag{4-68}$$

is the electric polarizability of our narrow annular aperture in the thick screen. For slot resonance, we have $\mathrm{Im}(y_{12}) = 0$. Therefore, replacing $(\eta_o y_{12})$ by $(-2G' \cos k_b d)$ in (4-68) and using (4-61), we obtain

$$\alpha_e^{res} = \frac{3j \, \lambda_o^3 \cos k_b d}{8\pi^2} \tag{4-69}$$

where $\cos k_b d$ is approximately 1 or -1 depending on the situation. We notice that (4-69) is a much greater quantity than the electric polarizability for an annular aperture in an infinitely thin screen [24]. Note that the dipole moment $\underline{p}_e$ is equivalent to an electric current element $\underline{I\ell}$ in the following sense:

$$\underline{I\ell} = j\omega \, \underline{p}_e \tag{4-70}$$

Chapter 5

NUMERICAL RESULTS

The computational results of some typical examples are presented in this chapter. Five simple configurations are used. The cross sections of the apertures in the y-z plane for these configurations are shown in Figs. 14(a) to 14(e). Two narrow annular apertures shown in Figs. 36(a) and 36(b) are used to demonstrate the resonant behavior described in Chapter 4. Results from the matrix solution and the analytical prediction are compared and discussed. For the current plots, the magnetic current is normalized with respect to the amplitude of the incident E-field, and the electric current is normalized with respect to the amplitude of the incident H-field. The horizontal axis represents the variable t along the generating curve. Tick marks are placed to show how subsections along the curve are arranged in the matrix solution. The ϕ-component of either the magnetic or the electric current is represented by a combination of pulses, consistent with the true expansion functions in the solution. The t-component is represented by a linear function, constructed by connecting points representing the solution at each t_i's with straight line segments. This is an approximation to the true expansion because the expansion functions for the t-component are triangles divided by ρ. For cases to which the modal solution also apply, the results from both formulations are shown for comparison.

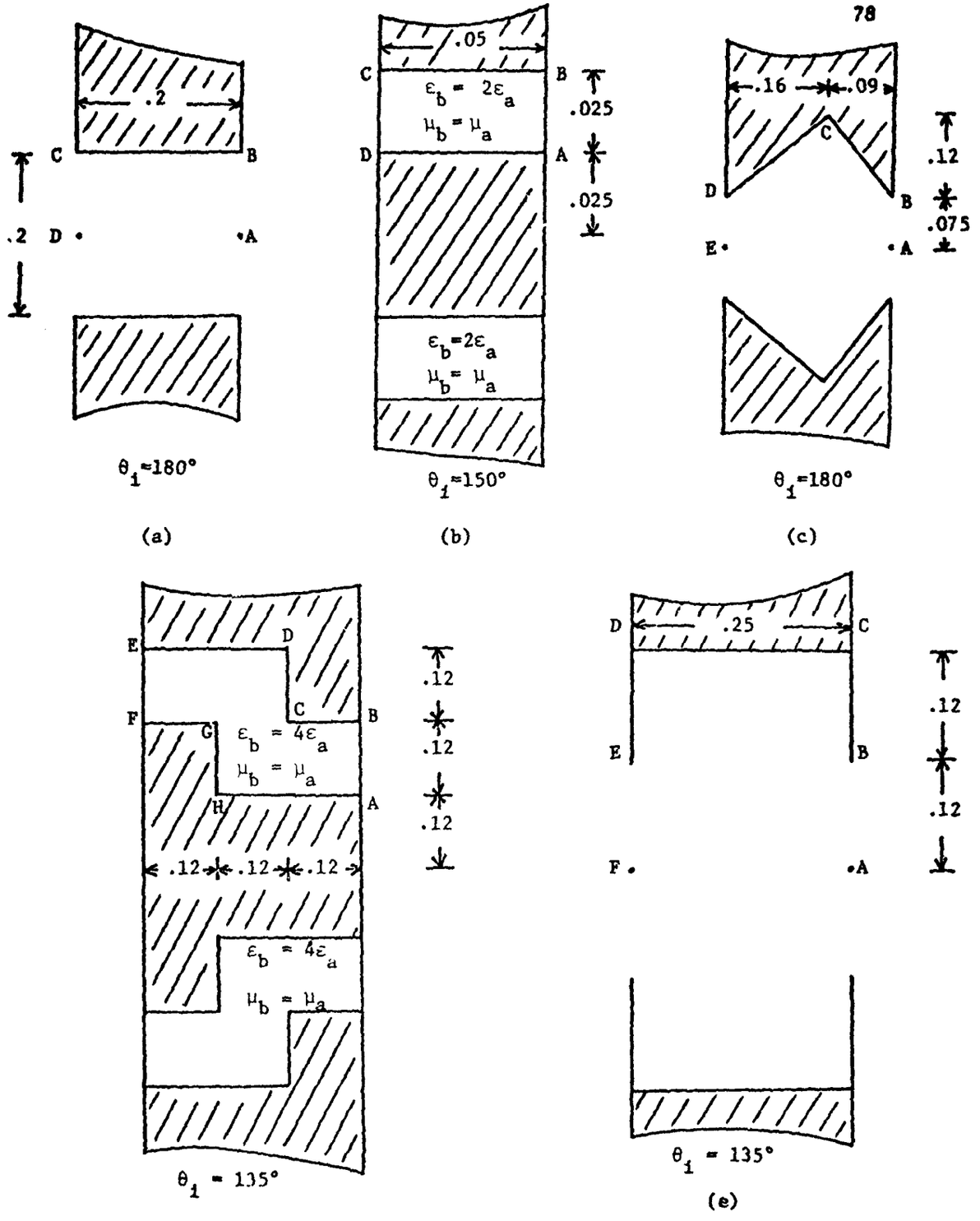

Fig. 14. Apertures of various cross sections, angles of incidence considered in each case are specified. The dimensions are in units of the wavelength in region a. Regions a and c are filled with the same medium. Region b is filled with the same medium except where explicitly labeled.

The ϕ and t-components of the modal solution are marked with triangles and squares, respectively, at a number of discrete points. Figures 14(a) and 14(b) show typical cases where both formulations are used. For the circular aperture in Fig. 14(a), normal incidence is considered. Only the $n = \pm 1$ modes are needed for this case, and the $n = 1$ mode currents are shown for an incident E-field polarized in the -x direction. The azimuth angle of incidence ϕ_i is assumed to be zero without loss of generality because of the symmetry. The magnetic current on the transmitted side shown in Fig. 16 is much smaller in magnitude than that on the illuminated side shown in Fig. 15, and the attenuation can be clearly seen from the electric currents, which represent components of the tangential H-field, in Fig. 17. The wall thickness in this case greatly reduces power transmission. The aperture with a filled coaxial region, shown in Fig. 14(b), exhibits different transmission characteristics. An oblique wave incident from $\theta_i = 150°$ is applied. The aperture is small electrically, and therefore only the $n = 0, \pm 1$ modes are needed. Figure 18 shows the circulating magnetic currents on each side of the aperture and the t-directed electric current on the walls, for $n = 0$, due to a θ-polarized incidence. This polarization couples to the TEM mode of the coaxial region. The effect of this propagating mode is seen in the current distribution. We don't see the great attenuation observed in the previous case, where all modes are evanescent. The currents for the $n = 1$ mode are also shown in Figs. 19 and 20. The attenuation of this mode is again present, and therefore the TEM mode transmits most of the energy.

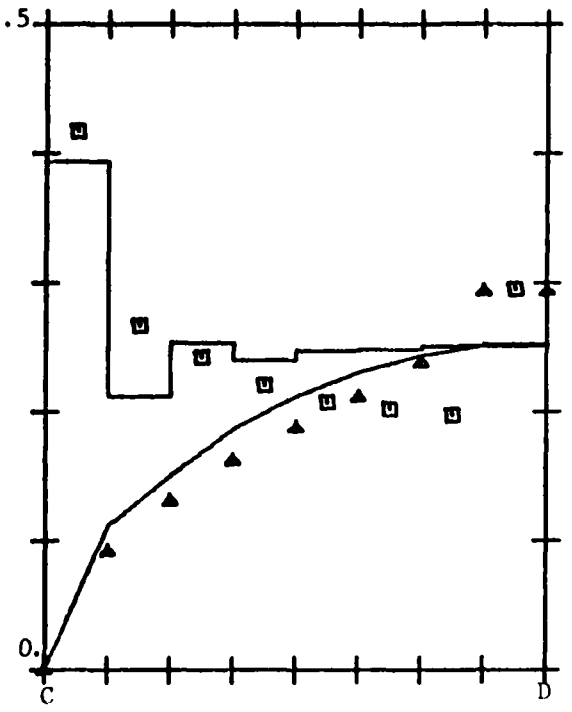

Fig. 15. M_{1t}^{1} and $M_{1\phi}^{1}$ of the example in Fig. 14(a).

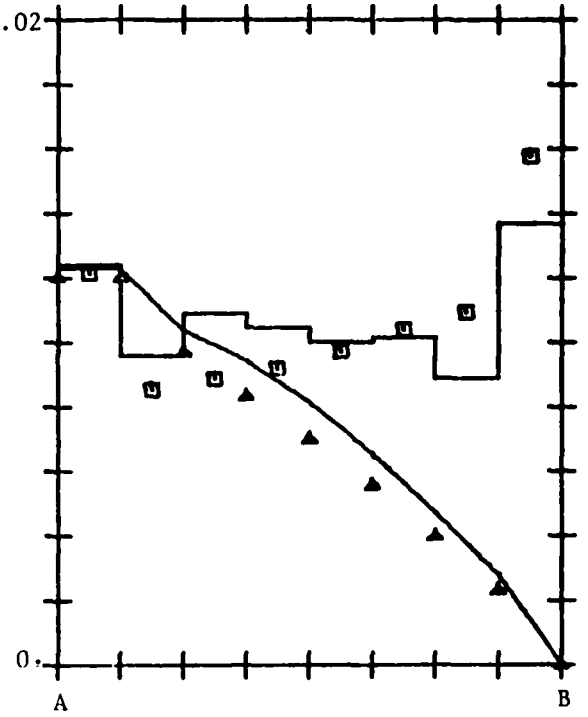

Fig. 16. M_{2t}^{1} and $-jM_{2\phi}^{1}$ of the example in Fig. 14(a).

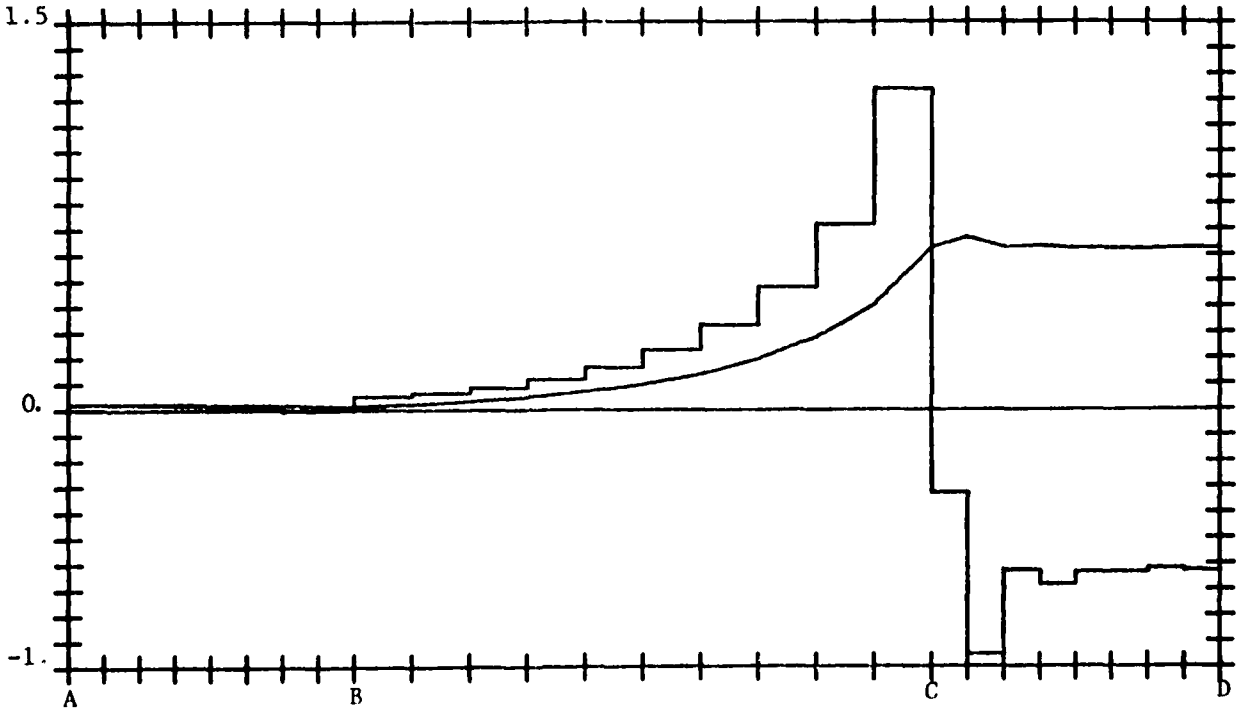

Fig. 17. J_{t}^{1} and $-jJ_{\phi}^{1}$ of the example in Fig. 14(a).

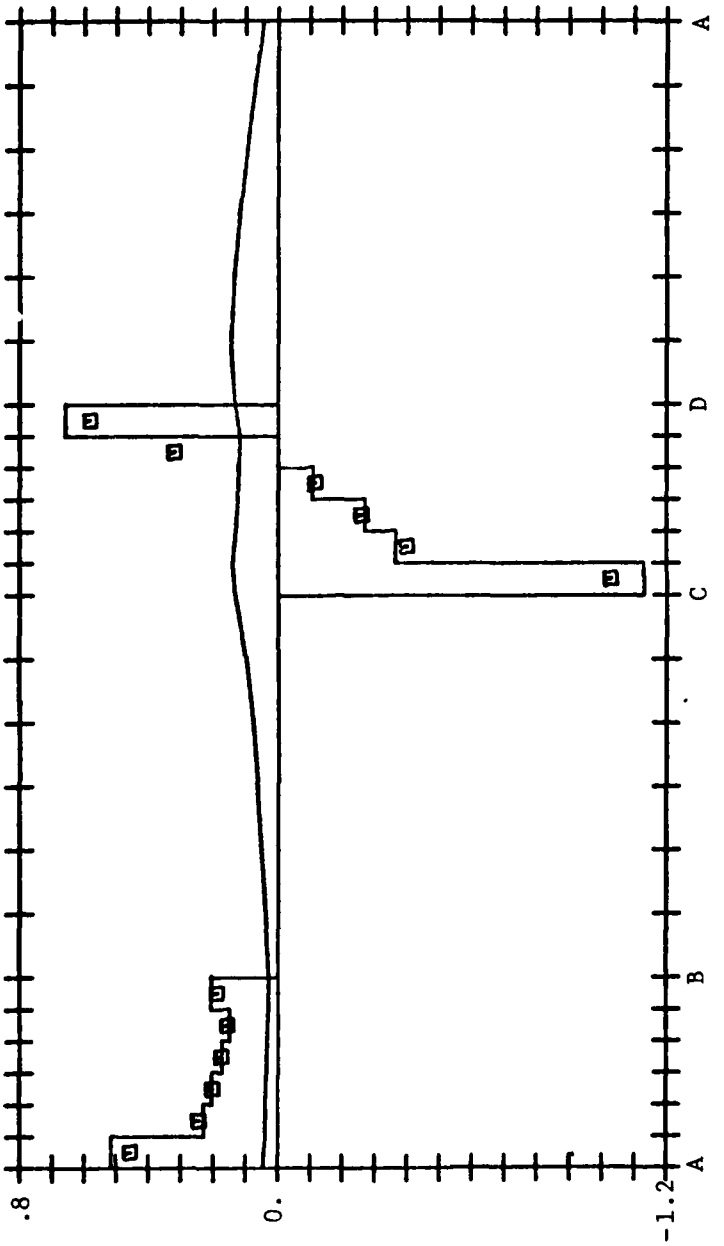

Fig. 18. $M_{1\phi}^{o}$, $M_{2\phi}^{o}$ and $-jJ_{t}^{o}$ of the example in Fig. 14(b), θ-polarization.

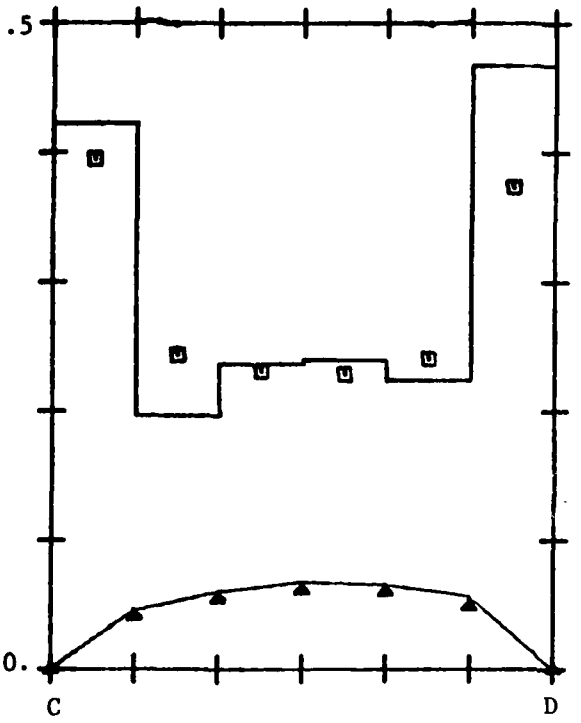

Fig. 19. M^1_{1t} and $jM^1_{1\phi}$ of the example in Fig. (b), θ-polarization.

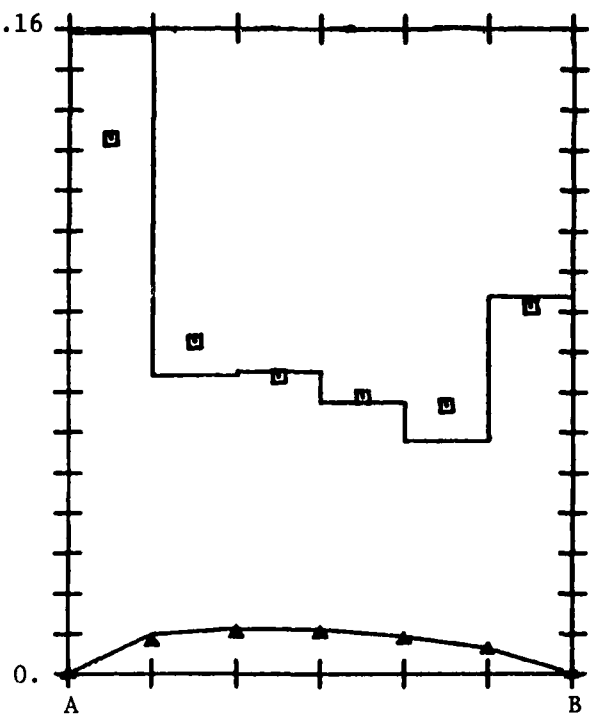

Fig. 20. M^1_{2t} and $-jM^1_{2\phi}$ of the example in Fig. 14(b), θ-polarization.

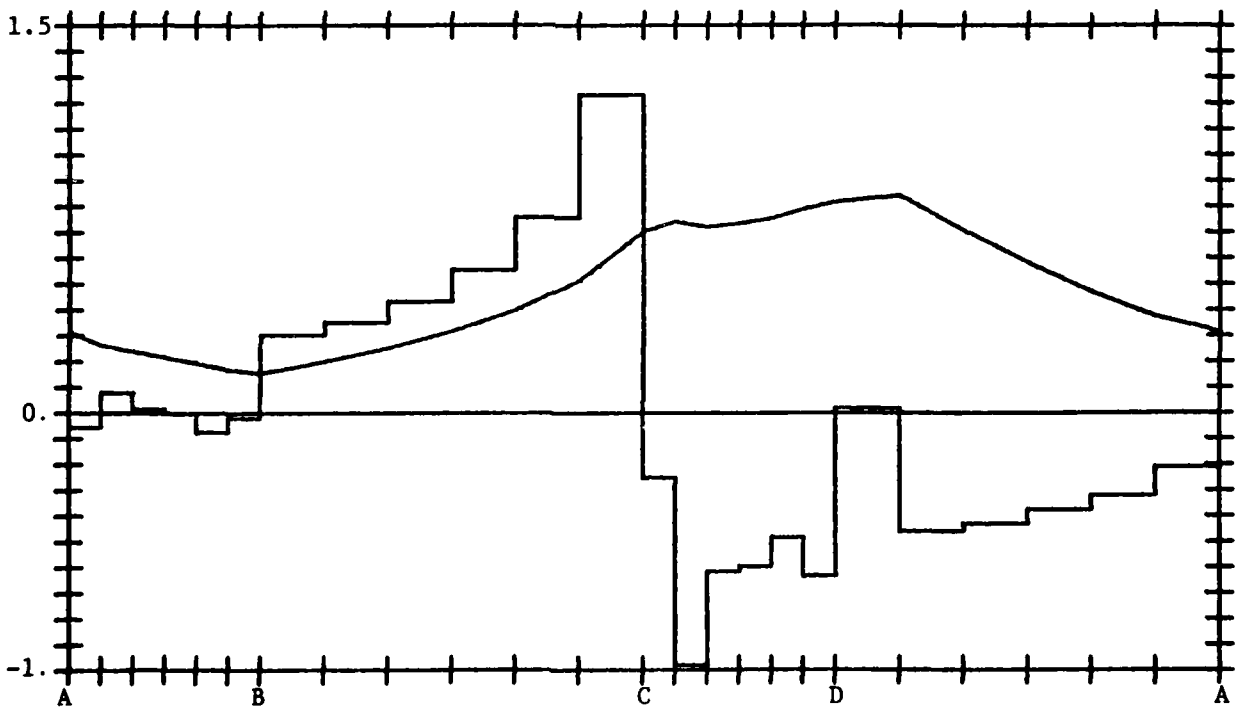

Fig. 21. J^1_t and $-jJ^1_\phi$ of the example in Fig. 14(b), θ-polarization.

Currents for the ϕ-polarized incidence are shown in Figs. 22 to 24. The currents for n = 1 mode are shown and they are very similar to that for θ-polarization. However, these currents are responsible for most of the energy transmission in this case, since power transmitted by the n = 0 mode is negligible now that it's not coupled to the TEM mode. The currents for the n = 0 mode in this case are not shown for this reason. Results for the magnetic currents from both formulations are compared for the above two configurations. The overall agreement is very good. The proper edge behavior of the magnetic current is also observed. One of the simplest geometries for which the modal approach is not applicable is shown in Fig. 14(c). The n = 1 mode currents are shown in Figs. 25 to 27 for normal incidence. The magnetic currents again exhibit a distribution similar to that which exists in a small circular aperture in a infinitesimally thin screen. The fields decrease rapidly from one side to the other. It is interesting to observe that most of the attenuation occurred before the sharp corner on the inner wall of the aperture. The configuration shown in 14(d) models a gasket in the thick screen. Oblique incidence of 135° with θ-polarization is considered. Figure 28 shows the circulating magnetic currents and the t-component of the electric current in the n = 0 mode. It is apparent that, although our waveguide region is no longer a straight coaxial region, the existence of the center conductor still enables the fields to propagate through the screen. Also, because of the size of the aperture, there is propagation even for the n = 1 mode. This can be seen from Figs. 29 to 31.

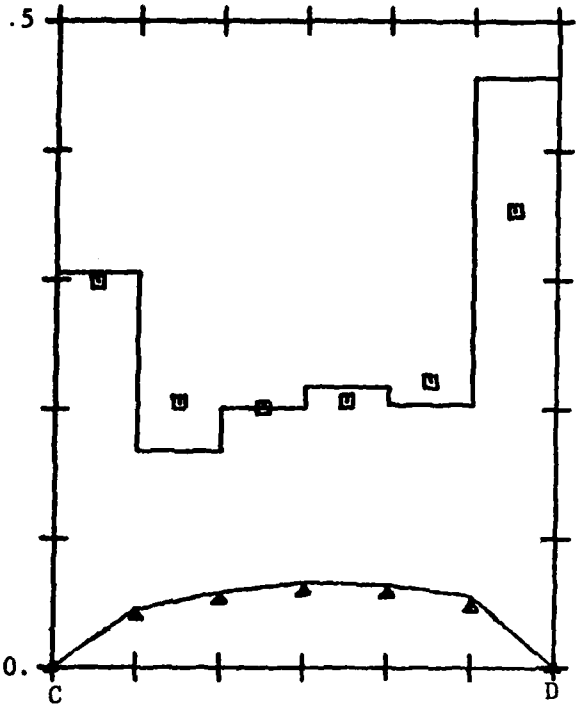

Fig. 22. $-jM^1_{1t}$ and $M^1_{1\phi}$ of the example in Fig. 14(b), ϕ-polarization.

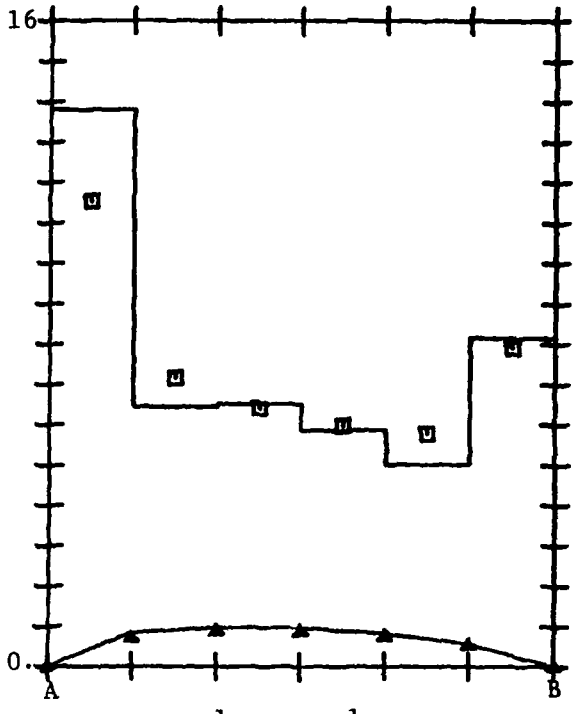

Fig. 23. $-jM^1_{2t}$ and $-M^1_{2\phi}$ of the example in Fig. 14(b), ϕ-polarization.

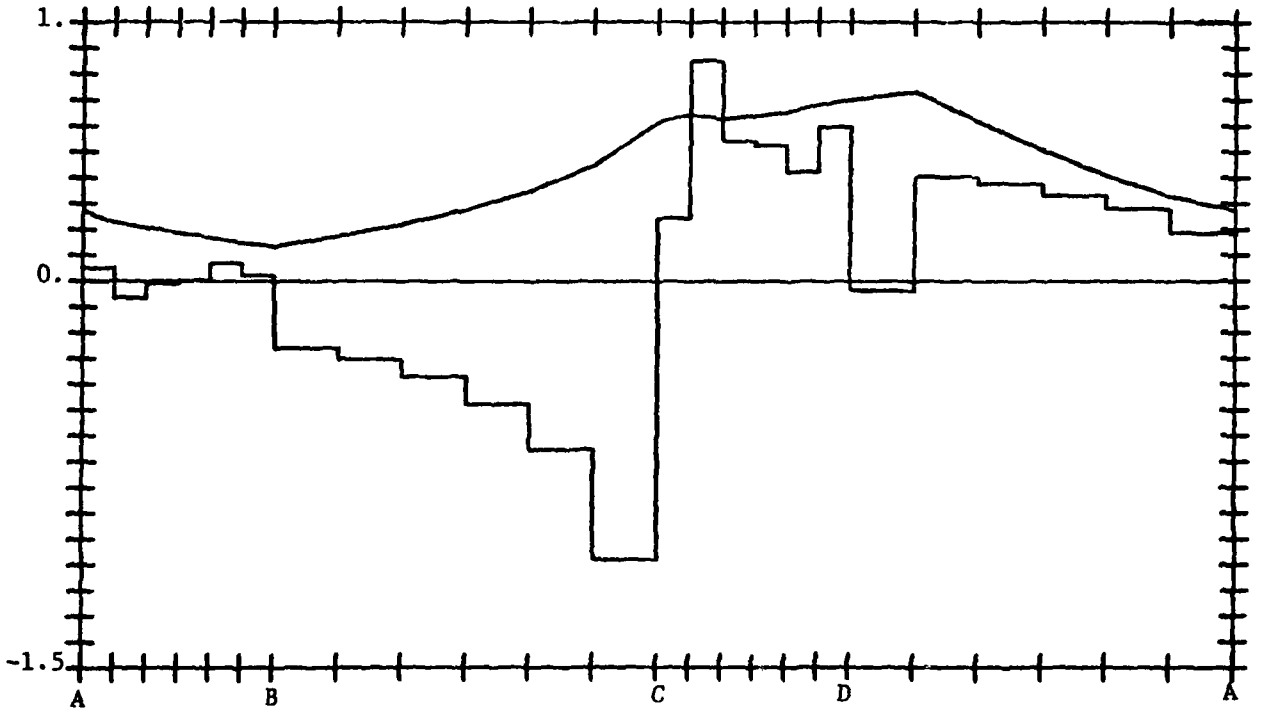

Fig. 24. $-jJ^1_t$ and J^1_ϕ of the example in Fig. 14(b), ϕ-polarization.

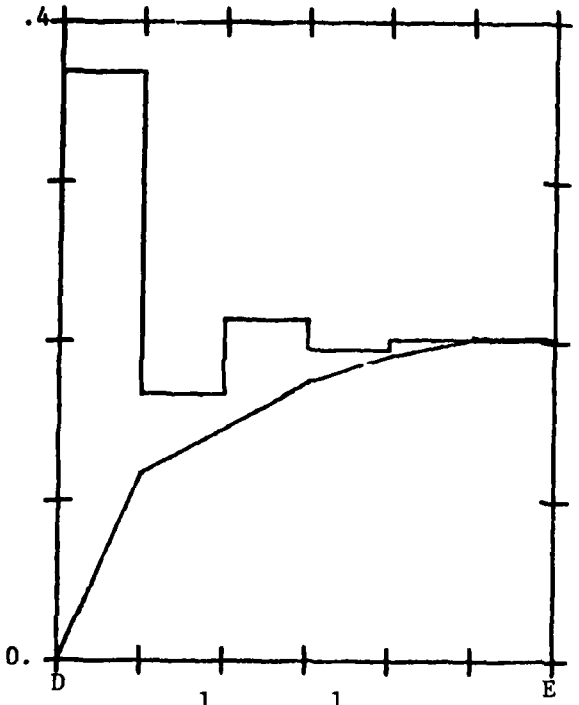

Fig. 25. M_{1t}^{1} and $jM_{1\phi}^{1}$ of the example in Fig. 14(c).

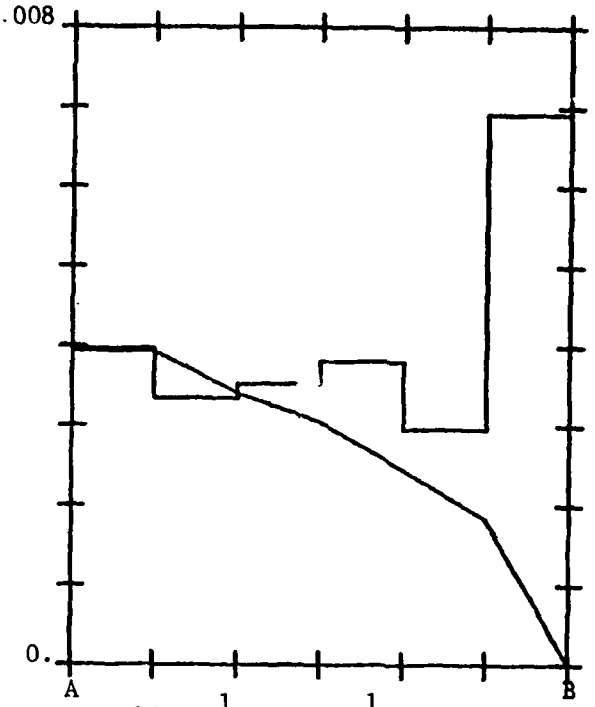

Fig. 26. M_{2t}^{1} and $-jM_{2\phi}^{1}$ of the example in Fig. 14(c).

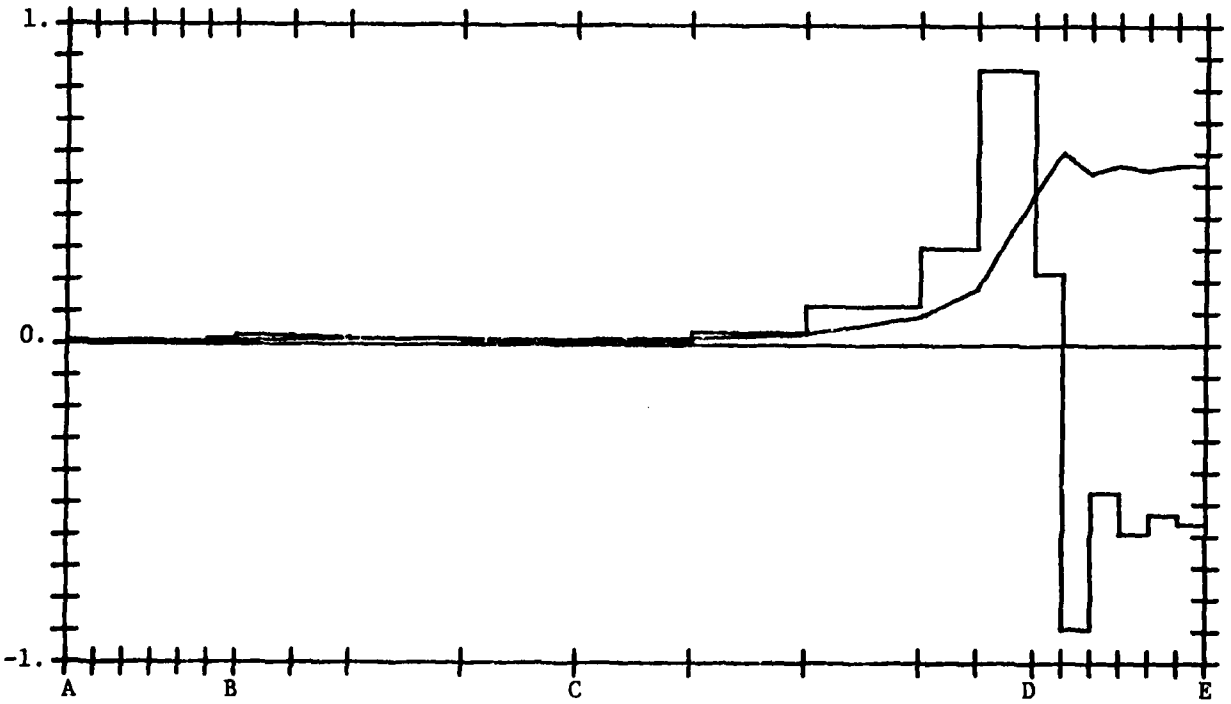

Fig. 27. J_{t}^{1} and $-jJ_{\phi}^{1}$ of the example in Fig. 14(c).

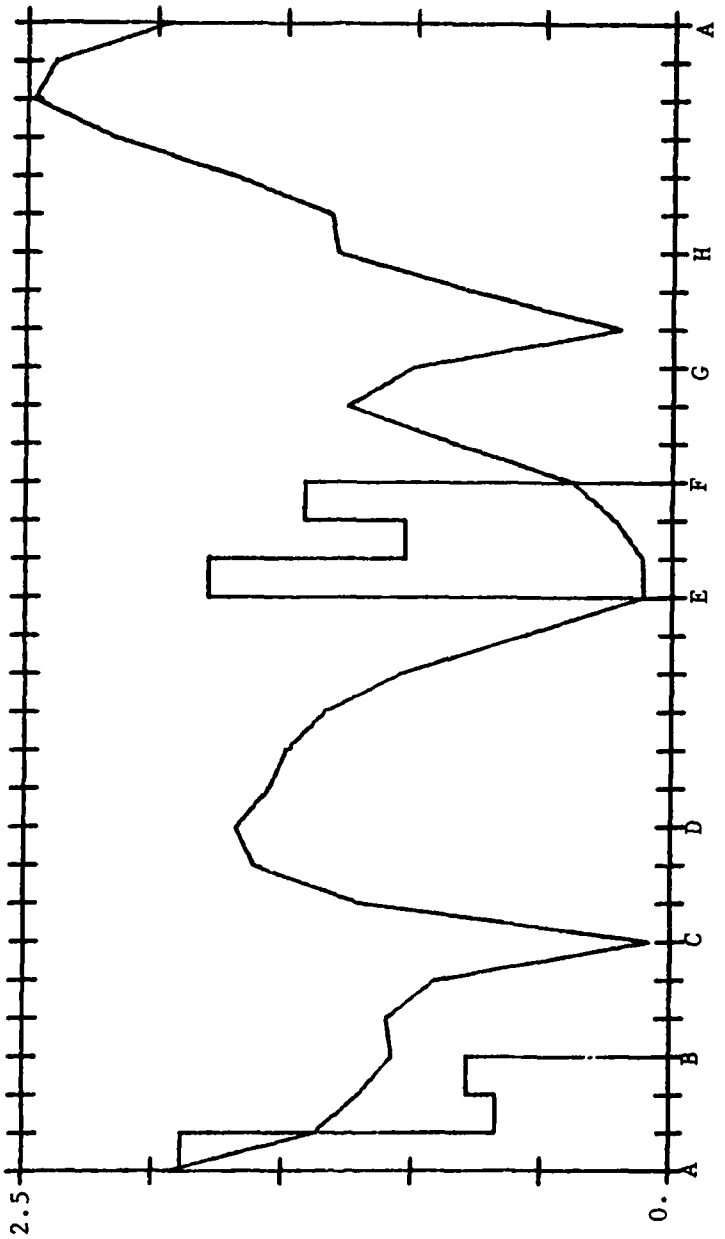

Fig. 28 $|M^{o}_{1\phi}|$, $|M^{o}_{2\phi}|$ and $|J^{o}_{t}|$ of the example in Fig. 14(d), θ-polarization.

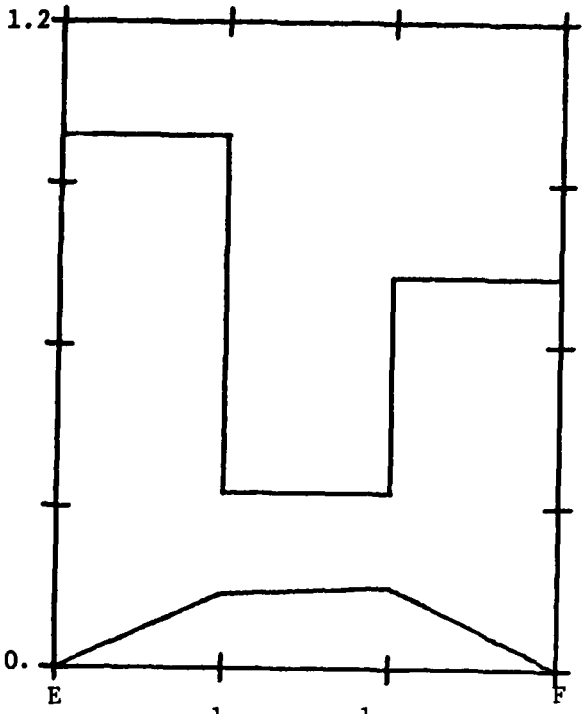

Fig. 29. $|M^1_{1t}|$ and $|M^1_{1\phi}|$ of the example in Fig. 14(d), θ-polarization.

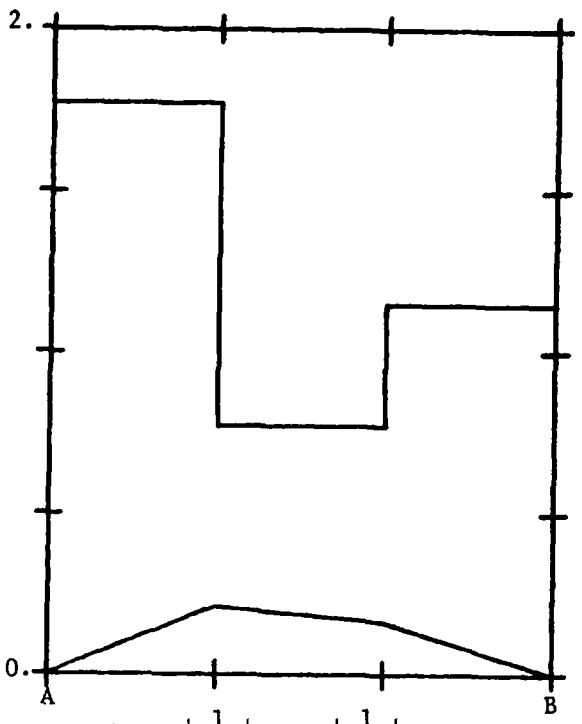

Fig. 30. $|M^1_{2t}|$ and $|M^1_{2\phi}|$ of the example in Fig. 14(d), θ-polarization.

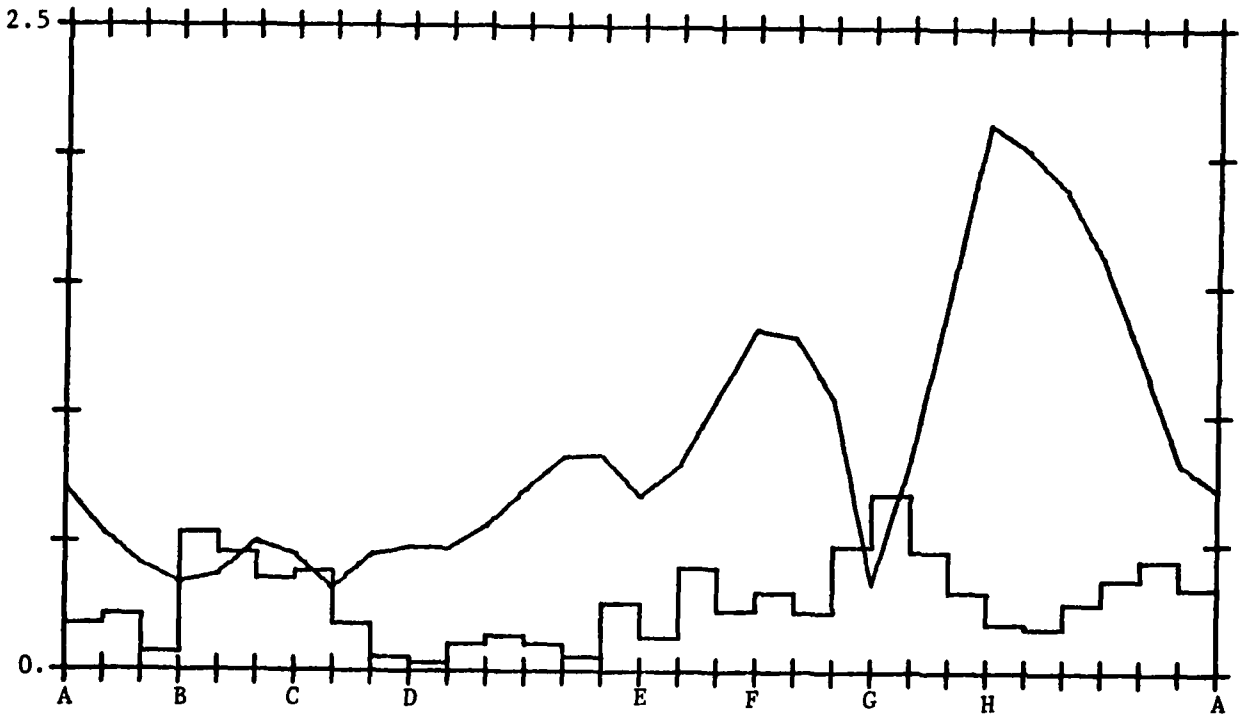

Fig. 31. $|J^1_t|$ and $|J^1_\phi|$ of the example in Fig. 14(d), θ-polarization.

Again, the ϕ-component of the magnetic currents becomes large at both edges of the aperture as expected. Our last example for currents is shown in Fig. 14(e). The incident wave is θ-polarized with a 135° angle of incidence. Currents for both the n = 0 and n = 1 modes are shown in Figs. 32 to 35. The system is below cutoff and the screen effectively attenuates the field.

The transmission coefficient T is computed for the two narrow annular slots shown in Figs. 36(a) and 36(b). Figure 37 shows the transmission coefficient for the aperture in Fig. 36(a) as a function of the screen thickness d. The computed results does show a repeated resonant phenomenon with period $\frac{\lambda}{2}$. Since the peaks are in general very narrow, only the result in the neighborhood of the first resonance is shown. The solid line represents the result from (4-58) and the circles represent the result from our modal matrix solution. The agreement is excellent except that the centers of the peaks are separated by a few ten thousandths of a wavelength. This can be explained as follows. From (4-53), the width of our resonant peak is approximately $\frac{2G'}{\pi} \lambda_b$. The center of the peak, from (4-48) is $\frac{B'}{\pi} \lambda_b$ away from half wavelength. For our particular problem, G' and B' can be found, from (4-44) and (4-45), to be roughly 0.00014 and 0.038. Therefore, a combined error of one percent from the two calculations of B' can cause the peaks to separate completely from each other. V_1 and V_2, the voltages defined in (4-10), are computed from the matrix solution also. They are shown in Fig. 38. The solid lines are the real and imaginary parts of V_1. The squares and triangles are the real

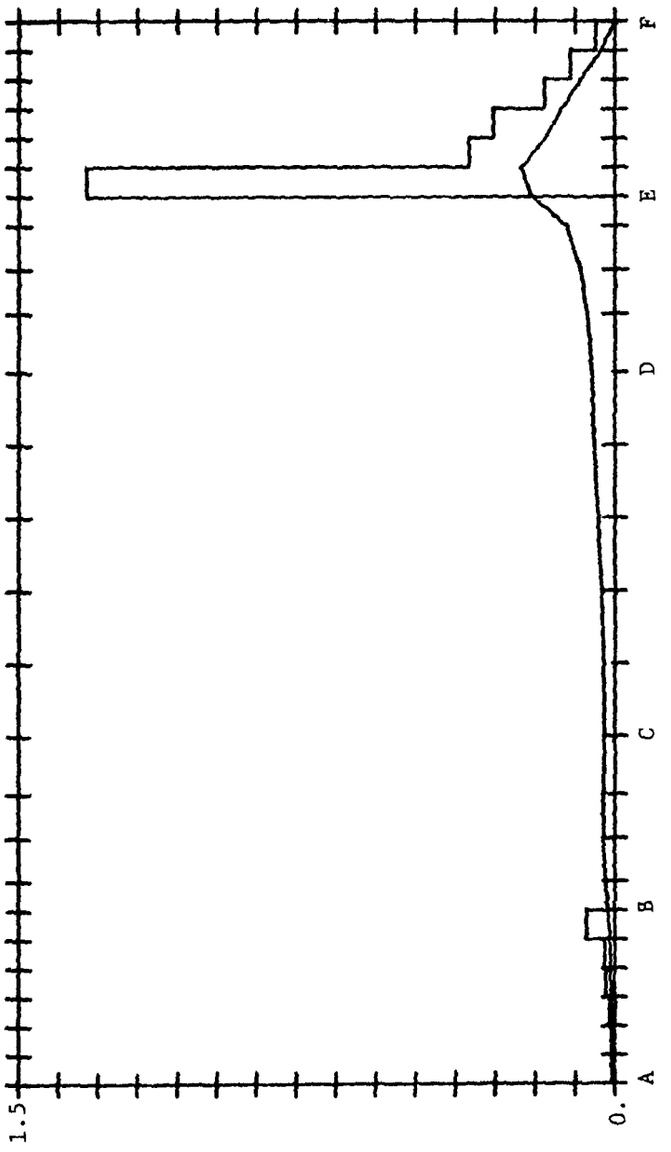

Fig. 32. $|M^o_{1\phi}|$, $|M^o_{2\phi}|$ and $|J^o_t|$ of the example in Fig. 14(e), θ-polarization.

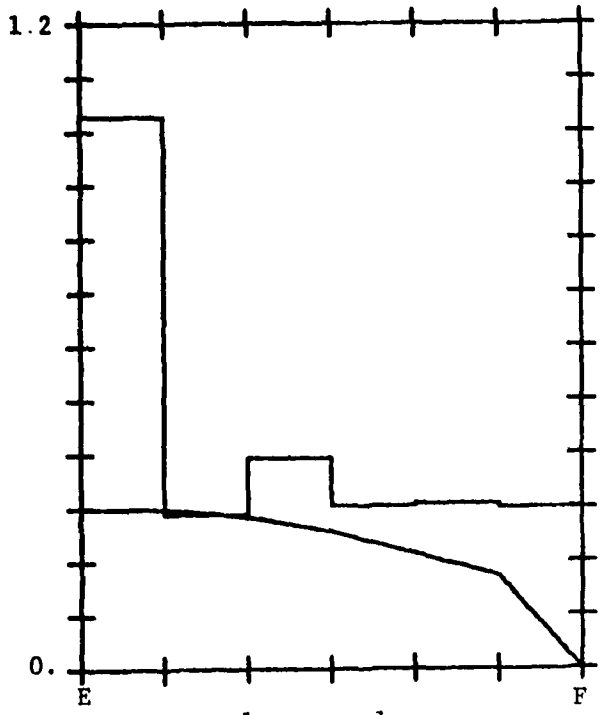

Fig. 33. M_{1t}^1 and $jM_{1\phi}^1$ of the example in Fig. 14(e), θ-polarization.

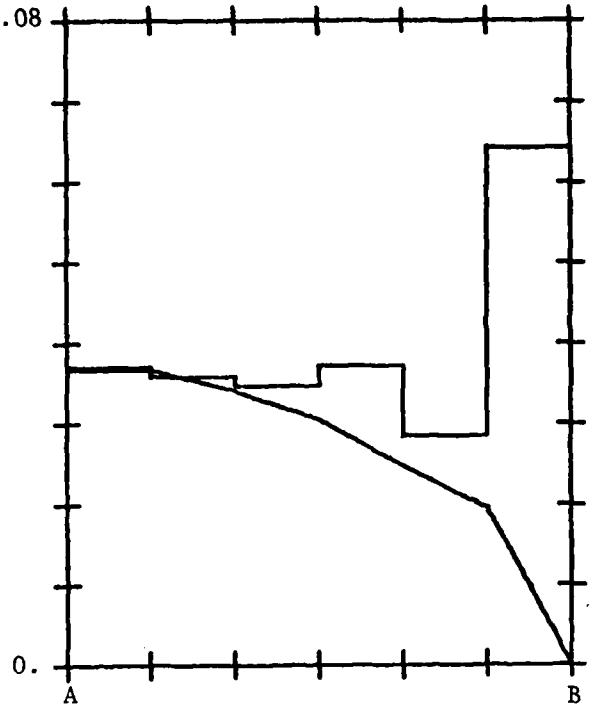

Fig. 34. M_{2t}^1 and $-jM_{2\phi}^1$ of the example in Fig. 14(e), θ-polarization.

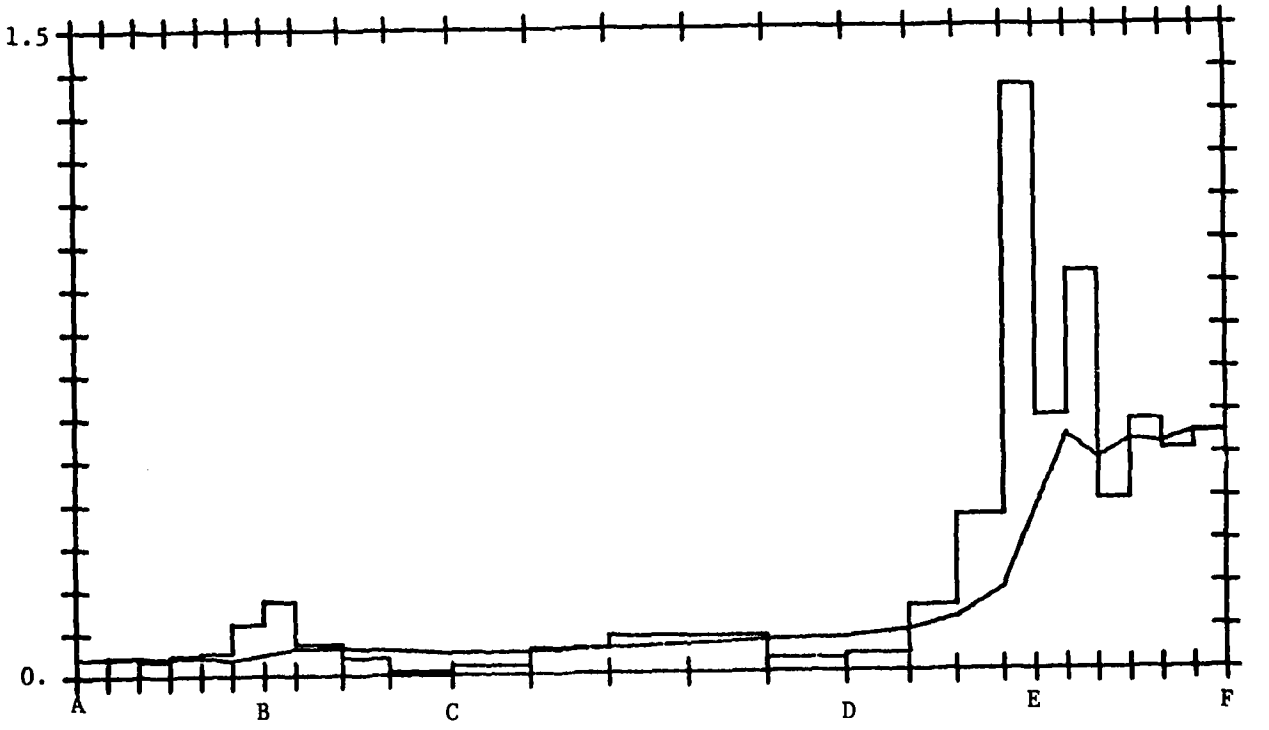

Fig. 35. $|J_t^1|$ and $|J_\phi^1|$ of the example in Fig. 14(e), θ-polarization.

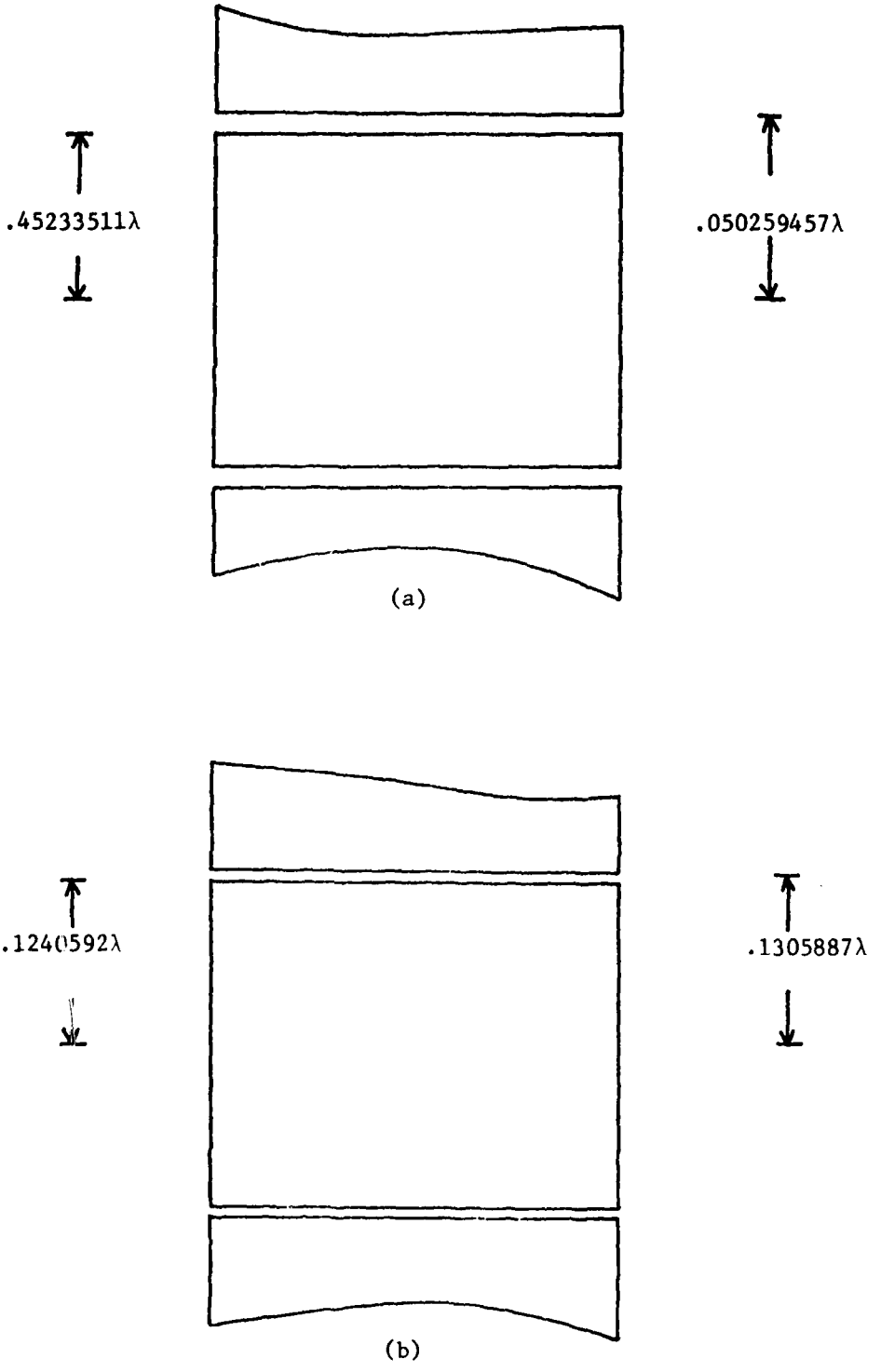

Fig. 36. Two narrow annular slots.

AD-A099 906 SYRACUSE UNIV NY DEPT OF ELECTRICAL AND COMPUTER EN--ETC F/G 20/14
ELECTROMAGNETIC TRANSMISSION THROUGH A ROTATIONALLY SYMMETRIC H--ETC(U)
JUN 81 C CHA, R F HARRINGTON N00014-76-C-0225
UNCLASSIFIED TR-81-2 NL

END
DATE FILMED
6-81
DTIC

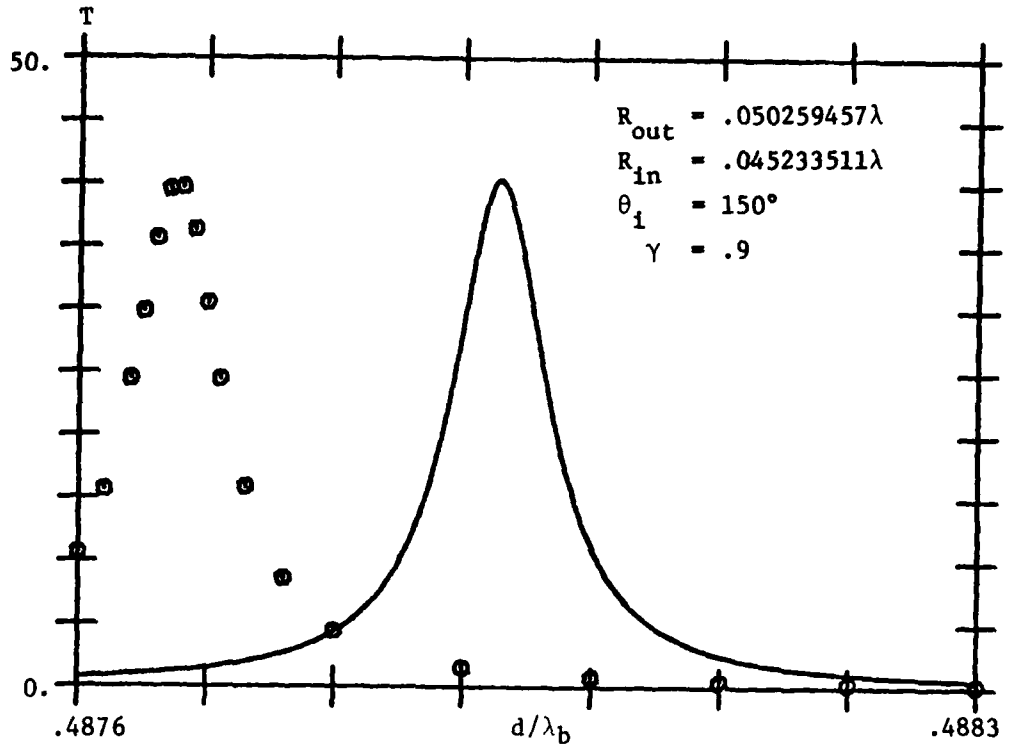

Fig. 37. Transmission coefficient of the aperture in Fig. 36(a), as a function of the screen thickness.

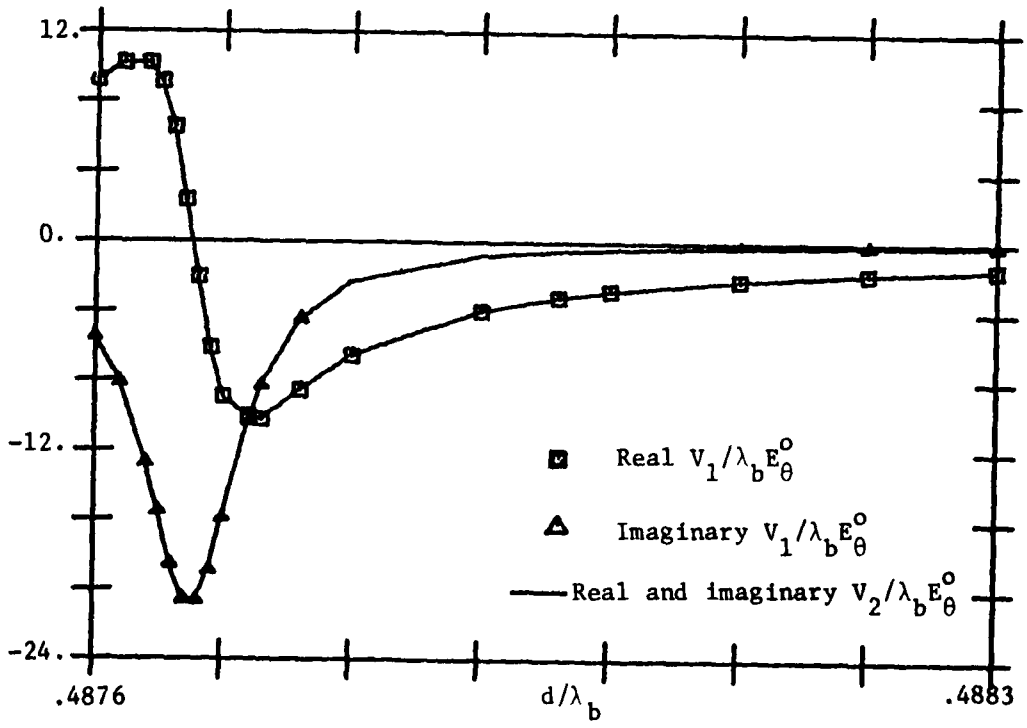

Fig. 38. V_1 and V_2, voltages of the equivalent circuit of the aperture in Fig. 36(a), normalized with respect to $\lambda_b E^o_\theta$, as functions of the screen thickness.

and imaginary parts of V_2. Note that the peak occurs where the real parts of V_1 and V_2 are zero. This is expected because resonance occurs when the imaginary part of the transfer admittance y_{12} is zero and our current source is imaginary. Also note that, since d is close to $\frac{\lambda}{2}$, V_1 and V_2 are almost exactly the same as for the case $d = \frac{\lambda}{2}$ shown in Table 1. Figures 39 and 40 show the transmission coefficient and the voltages for the case in Fig. 36(b). Again, the agreement is excellent and, this time, since $\frac{G'}{B'} \sim \frac{1}{20}$, a comparable percentage error in B' would not cause the pulses to look completely separated.

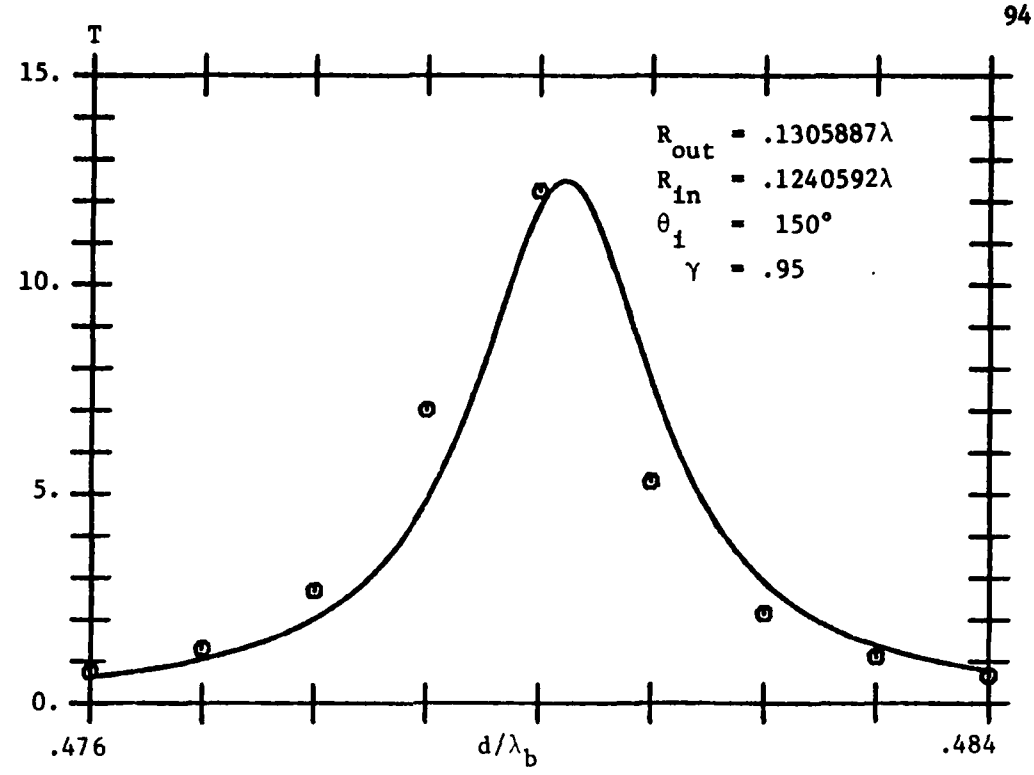

Fig. 39. Transmission coefficient of the aperture in Fig. 36(b), as a function of the screen thickness.

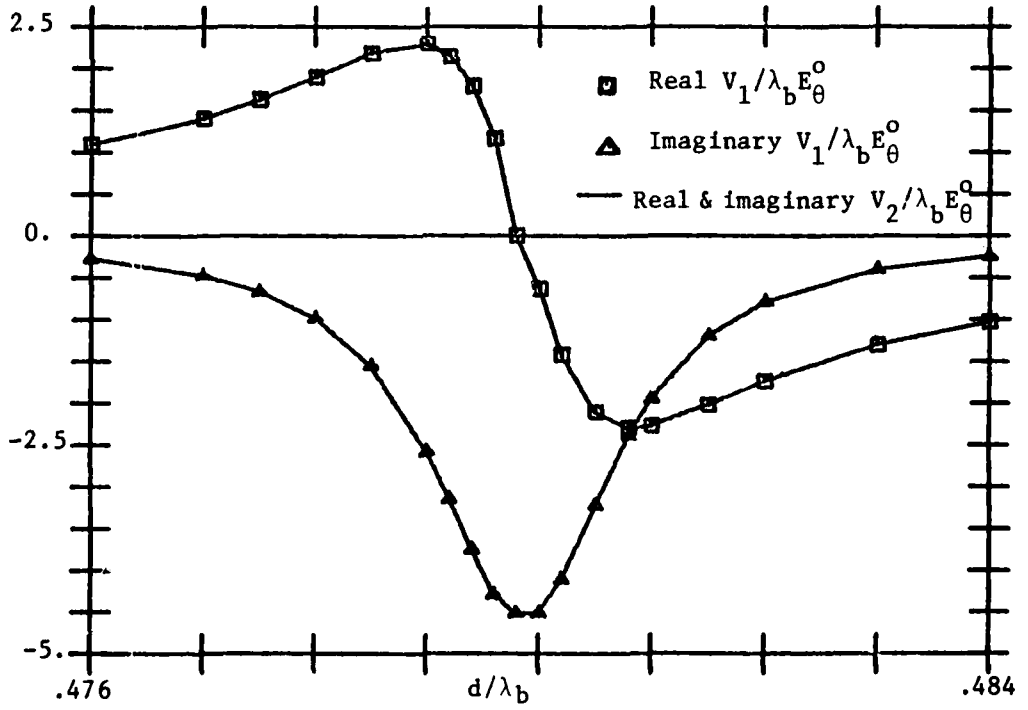

Fig. 40. V_1 and V_2, voltages of the equivalent circuit of the aperture in Fig. 36(b), normalized with respect to $\lambda_b E^o_\theta$, as functions of the screen thickness.

Chapter 6

CONCLUSION

A general formulation is developed for solving the problem of electromagnetic transmission through a rotationally symmetric aperture in a conducting screen of finite thickness. The solution obtained is in the form of the Fourier coefficients (in ϕ) of the equivalent currents on the boundary of the aperture region. All field and power characteristics can be computed from these coefficients. The number of Fourier modes needed depends on the size of the aperture and the nature of the excitation. Because of the symmetry of the problem, each mode can be solved separately. The basic formulation resembles that of [10], except that our problem is a three-dimensional one. Also, for the modal formulation, when the waveguide region is of resonant size, problems can arise in forming the field operator in this region, as observed in [7]. This problem is solved in Chapter 2 by using the proper constraints (Table 1) on the magnetic currents and introducing new unknowns. Note should be made that the case $k'_{nm} = 0$ needs to be treated carefully, as shown in Chapter 2. However, this case does not correspond to a cavity resonance. While the procedures for treating a resonant case may seem applicable to only a few special cases, the concept can be extended to a more general case because the magnetic currents on the aperture faces can always be separated into two parts, one a linear combination of waveguide modes and the other orthogonal to them. The modal solution can

also be extended to treat an aperture with region b composed of cascaded waveguide sections.

In the low frequency discussion of Chapter 4, an equivalent circuit was developed for a narrow annular slot. An effort was made to show the validity of a one term moment solution in this case, as done in [25]. Also, the assumption was made that only the TEM mode propagates. This limits the overall size of the aperture as shown by (4-6). If the mean radius of the narrow annular slot is arbitrary, then there may be a propagating mode for each n, as seen in (4-5). Further study of each of those modes is recommended to develop the corresponding equivalent circuits for such cases. Our analysis of the TEM mode remains valid as far as the power transmission associated with the particular mode is concerned.

Appendix

PROOF OF EQUATION (4-18)

In this appendix, we prove that

$$Y = \int_0^{\pi} \frac{\cos\phi\, e^{-jkR}}{R}\, d\phi$$

$$\cong -\frac{1}{R_a}\left\{\left[\ln\frac{e^2|\rho-\rho'|}{8R_a} - \frac{\pi}{2}\int_0^{2kR_a} E_2(x)dx\right] + \frac{j\pi}{2}\int_0^{2kR_a} J_2(x)dx\right\} \tag{A-1}$$

when $W \ll R_a$. R is defined as

$$R = \sqrt{\rho^2 + \rho'^2 - 2\rho\rho'\cos\phi} \tag{A-2}$$

The subscript of k in (4-18) is left out for convenience. Consider Y as a function of k, and write

$$Y(k) = Y(0) + \int_0^{k} \frac{dY(\alpha)}{d\alpha}\, d\alpha \tag{A-3}$$

From (A-1), we find

$$\frac{dY(\alpha)}{d\alpha} = -j\int_0^{\pi} \cos\phi\, e^{-j\alpha R}\, d\phi \tag{A-4}$$

and

$$Y(0) = \int_0^{\pi} \frac{\cos\phi}{R}\, d\phi \tag{A-5}$$

Since Y(0) is real, we have

$$\mathrm{Im}(Y) = -\int_0^k d\alpha \int \cos\phi \cos(\alpha R)d\phi \qquad \text{(A-6)}$$

When $w << R_a$, we can obtain, from (A-2),

$$R \cong 2R_a \sin\frac{\phi}{2} \qquad \text{(A-7)}$$

Substituting (A-7), and the new variable

$$\psi = \frac{1}{2}(\pi - \phi) \qquad \text{(A-8)}$$

into (A-6), we obtain

$$\mathrm{Im}(Y) = 2\int_0^k d\alpha \int_0^{\pi/2} \cos 2\psi \cos(2\alpha R_a \cos\psi)d\psi \qquad \text{(A-9)}$$

From 10.11.1. of [26], we obtain

$$\mathrm{Im}(Y) = -\frac{\pi}{2R_a}\int_0^{2kR_a} J_2(x)dx \qquad \text{(A-10)}$$

Now we consider the real part of Y. From (A-3) to (A-5), we obtain

$$\mathrm{Re}(Y) - Y(0) = -\int_0^k dk \int_0^{\pi} \cos\phi \sin(\alpha R)d\phi \qquad \text{(A-11)}$$

Substituting (A-7) and (A-8) into (A-11), we find

$$\mathrm{Re}(Y) - Y(0) = 2\int_0^k d\alpha \int_0^{\pi/2} \cos 2\psi \sin(2\alpha R_a \cos\psi)d\psi \qquad \text{(A-12)}$$

From 10.11.3. of [26], we obtain

$$\mathrm{Re}(Y) - Y(0) = \frac{\pi}{2R_a} \int_0^{2kR_a} E_2(x)dx \qquad \text{(A-13)}$$

Finally, we consider Y(0). Substituting (A-2) and (A-8) into (A-5), we obtain

$$Y(0) = \frac{2}{(\rho+\rho')} \int_0^{\pi/2} \left[\left(\frac{\rho^2+\rho'^2}{2\rho\rho'}\right) \frac{1}{\sqrt{1 - \beta^2\sin^2\psi}} - \frac{(\rho+\rho')^2}{2\rho\rho'} \sqrt{1 - \beta^2\sin^2\psi} \right] d\psi \qquad \text{(A-14)}$$

where

$$\beta^2 = \frac{4\rho\rho'}{(\rho + \rho')^2} \cong 1 \quad (\text{for } w << R_a) \qquad \text{(A-15)}$$

From 17.3.1, 3, 26 of [27], we find, for $w << R_a$,

$$Y(0) \cong \frac{-1}{R_a} \ln \left(\frac{e^2|\rho - \rho'|}{8R_a}\right) \qquad \text{(A-16)}$$

Combining (A-10), (A-13) and (A-16), we obtain (A-1).

REFERENCES

[1] S. C. Kashyap, et al., "Diffraction Pattern of a Slit in a Thick Conducting Screen," Journal of Applied Physics, vol. 42, No. 2, February 1971, pp. 894-895.

[2] S. C. Kashyap and M.A.K. Hamid, "Diffraction Characteristics of a Slit in a Thick Conducting Screen," IEEE Trans on Antennas and Propagation, vol. AP-19, No. 4, July 1971, pp. 499-507.

[3] N. Morita, "Diffraction of Electromagnetic Waves by a Two-Dimensional Aperture with Arbitrary Cross-Sectional Shape," Electronics and Communications in Japan, vol. 54-B, No. 5, 1971, pp. 58-61.

[4] F. L. Neerhoff and G. Mur, "Diffraction of a Plane Electromagnetic Wave by a Slit in a Thick Screen Placed Between Two Different Media," Appl. Sci. Res., vol. 28, July 1973, pp. 73-88.

[5] L. N. Litvenenko, et al., "Diffraction of a Planar, H-Polarized Electromagnetic Wave on a Slit in a Metallic Shield of Finite Thickness," Radio Engineering and Electronics Physics, vol. 22, March 1977, pp. 35-43.

[6] K. Hongo and G. Ishii, "Diffraction of an Electromagnetic Plane Wave by a Thick Slit," IEEE Trans. on Antennas and Propagation, vol. AP-26, No. 3, May 1978, pp. 494-499.

[7] D. T. Auckland and R. F. Harrington, "Electromagnetic Transmission Through a Filled Slit in a Conducting Plane of Finite Thickness, TE Case," IEEE Trans. on Microwave Theory and Techniques, vol. MTT-26, No. 7, July 1978, pp. 499-505.

[8] H. Henke, et al., "Diffraction by a Flanged Parallel-Plate Waveguide and a Slit in a Thick Screen," Radio Science, vol. 14, No. 1, January-February 1979, pp. 11-18.

[9] D. T. Auckland and R. F. Harrington, "Electromagnetic Transmission through Cascaded Rectangular Regions in a Thick Conducting Screen," AEÜ, vol. 34, No. 1, 1980, pp. 19-26.

[10] D. T. Auckland and R. F. Harrington, "A Nonmodal Formulation for Electromagnetic Transmission through a Filled Slot of Arbitrary Cross Section in a Thick Conducting Screen," IEEE Trans. on Microwave Theory and Techniques, vol. MTT-28, No. 6, June 1980, pp. 548-555.

[11] A. N. Akhiezer, "On the Inclusion of the Effect of the Thickness of the Screen in Certain Diffraction Problems," Sov. Phys.-Tech. Phys., vol. 2 (6), 1957, pp. 1190-1196.

[12] H. A. Bethe, "Theory of Diffraction by Small Holes," Physics Reviews, vol. 66, October 1950, pp. 163-182.

[13] K.H.L. Garb, et al., "Effect of Wall Thickness in Slot Problems of Electrodynamics," Radio Engineering and Electronic Physics, vol. 13, No. 12, 1968, pp. 1888-1896.

[14] K.H.L. Garb, R. S. Meyerova and R. F. Fikhmanas, "Consideration of Wall Thickness in Problems of Diffraction of Electromagnetic Waves at Small Openings," Radio Engineering and Electronic Physics, vol. 23, February 1978, pp. 10-16.

[15] N. A. McDonald, "Electric and Magnetic Coupling through Small Apertures in Shield Walls of any Thickness," IEEE Trans. on Microwave Theory and Techniques, vol. MTT-20, No. 10, October 1972, pp. 689-695.

[16] R. F. Harrington, Time-Harmonic Electromagnetic Fields, McGraw-Hill Book Company, New York, 1961.

[17] R. F. Harrington, Field Computation by Moment Methods, The Macmillan Company, New York, 1968.

[18] J. R. Mautz and R. F. Harrington, "An Improved E-field Solution for a Conducting Body of Revolution," Report RADC-TR-80-194, Rome Air Development Center, Griffiss Air Force Base, New York, June 1980.

[19] J. R. Mautz and R. F. Harrington, "An H-field Solution for a Conducting Body of Revolution," Report RADC-TR-80-362, Rome Air Development Center, Griffiss Air Force Base, New York, November 1980.

[20] J. R. Mautz and R. F. Harrington, "Electromagnetic Coupling to a Conducting Body of Revolution with a Homogeneous Material Region," Report TR-81-1, Department of Electrical and Computer Engineering, Syracuse University, Syracuse, New York, May 1981.

[21] J. R. Mautz and R. F. Harrington, "H-field, E-field and Combined Field Solutions for Bodies of Revolution," Technical Report TR-77-2, Department of Electrical and Computer Engineering, Syracuse University, Syracuse, New York, February 1977.

[22] J. McMahon, "On the Roots of the Bessel and Certain Related Functions." Annals of Mathematics, vol. 9, 1894-1895, pp. 23-30.

[23] R Truell, "Concerning the Roots of $J_n'(x)N_n'(kx) - J_n'(kx)N_n'(x) = 0$," Journal of Applied Physics, vol. 14, No. 7, July1943, pp. 350-352.

[24] C. Cha and R. F. Harrington, "Electromagnetic Transmission through an Annular Aperture in an Infinite Conducting Screen," AEÜ, vol. 35, No. 4, April 1981, pp. 167-172.

[25] R. F. Harrington and D. T. Auckland, "Electromagnetic Transmission through Narrow Slots in Thick Conducting Screen," IEEE Transactions on Antennas and Propagation, vol. AP-28, No. 5, September 1980. pp. 616-622.

[26] G. N. Watson, A Treatise on the Theory of Bessel Functions, 2nd edition, Cambridge University Press, Cambridge, England, 1958.

[27] M. Abramowitz and I. Stegun, Handbook of Mathematical Functions, Dover Publications Inc., New York, 1951.

[28] P.L.E. Uslenghi, "A Simple Model for Electromagnetic Field Penetration through Gaskets and Seams," Alta Fraquenza, vol. 45, No. 10, October 1976, pp. 616-620.

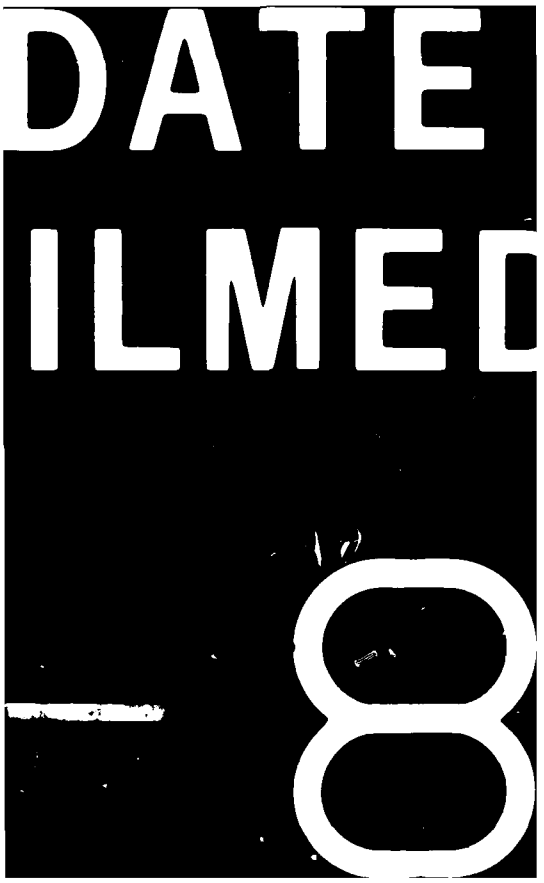
DATE
ILMED
8